

# Towards non-empirical nuclear energy functionals from low-momentum interactions

T. Duguet\*

*Centre de Saclay, IRFU/Service de Physique Nucléaire, F-91191 Gif-sur-Yvette, France*

*National Superconducting Cyclotron Laboratory,*

*Michigan State University, East Lansing, MI 48824, USA and*

*Department of Physics and Astronomy, Michigan State University, East Lansing, MI 48824, USA*

## Contents

<b>I. Introduction</b>	3
A. Generalities	3
B. Nuclear hamiltonian and renormalization group methods	6
C. A path towards non-empirical energy density functionals	9
1. Connecting the nuclear EDF method to ab-initio approaches	10
2. Connecting the nuclear DFT method to ab-initio approaches	11
D. Outline of the lectures	11
<b>II. Basics of energy density functional methods</b>	13
A. Generalities	13
B. Single-reference EDF method	13
1. Elements of formalism	13
2. Spontaneous symmetry breaking	14
3. Single-particle field	16
4. Pairing field	16
5. Eigen spectrum	17
C. Empirical energy functionals	18
1. Density matrices and local densities	20
2. Energy	20
3. Single-particle field	21
4. Pairing field	21
D. Pseudo potential and effective interaction	22
E. Multi-reference extension	23
F. Correlations	23
G. Performances and limitations	25
<b>III. Low-momentum interactions from renormalization group methods</b>	27
A. Generalities	28
B. Low-momentum interactions in the NN sector	30
C. Advantages for light-nuclei calculations	33
D. Low-momentum interactions in the 3N sector	35
E. Summary	36
<b>IV. Towards non-empirical energy density functionals</b>	37
A. Generalities	37
B. Elements of time-ordered many-body perturbation theory	38
1. Unperturbed vacuum of reference	38
2. Correlation energy and the perturbative expansion	40
3. Computation	40
C. Many-body perturbation theory calculation of nuclear systems	42
1. Infinite nuclear matter	42

---

\*Electronic address: [thomas.duguet@cea.fr](mailto:thomas.duguet@cea.fr)

2. Doubly-magic nuclei	44
D. Mapping many-body perturbation theory onto the SR-EDF method	45
1. Generalities	45
2. Comparing Skyrme-EDF and MBPT energy expressions	46
E. The density matrix expansion	48
1. Basic features	48
2. Negele and Vautherin DME	49
3. Novel DME approach based on phase-space-averaging techniques	50
4. On-going developments	51
<b>V. Summary</b>	<b>52</b>
<b>VI. Acknowledgments</b>	<b>53</b>
<b>VII. Bibliography</b>	<b>53</b>

## I. INTRODUCTION

### A. Generalities

In spite of over fifty years of theoretical and experimental studies, low-energy nuclear physics remains an open and difficult problem. While extensive progress has been made, an accurate and universal description from first principles is still beyond reach.

The first difficulty resides in the inter-particle interaction at play. Strong inter-nucleon interactions relevant to describing low-energy phenomena must be modeled within the non-perturbative regime of the gauge theory of interacting quarks and gluons, i.e. quantum chromodynamics (QCD). Within such a frame, nucleons are assigned to spin and isospin SU(2) doublets such that they are 4-component fermions interacting in various configurations stemming from invariances of the problem, e.g. they interact through central, spin-orbit, tensor, quadratic spin-orbit... couplings. As an example, Fig. 1 displays coordinate-space matrix elements the state-of-the-art local two-nucleon (NN) Argonne V18 [1] potential in the four two-body spin/isospin channels. In addition to its complex operator structure, the NN force produces a weakly-bound neutron-proton state (i.e. the deuteron) in the coupled  $^3S_1$ - $^3D_1$  channels and a virtual di-neutron state in the  $^1S_0$  channel. Associated large scattering lengths, together with the short-range repulsion between nucleons make the nuclear many-body problem highly non-perturbative. In addition to such difficulties, the treatment of three-body (3N) interactions in a theory of point-like nucleons is unavoidable. This has become clear over the last fifteen years as one was aiming at a consistent understanding of (i) differential nucleon-deuteron cross-sections [2–4], (ii) the under-estimation of triton and light-nuclei binding energies [5], (iii) the Tjon line [6], (iv) the violation of the Koltun sum rule [7], (v) the saturation of symmetric nuclear matter [8–13] and (vi) the Coester line problem [14–16].

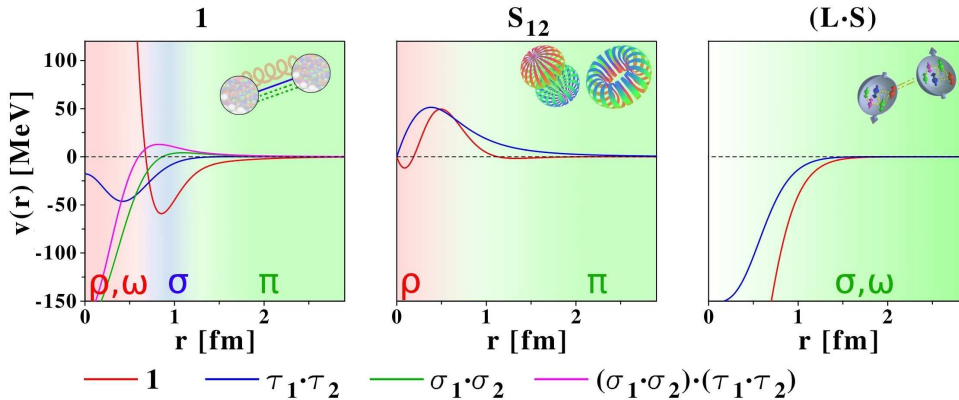


FIG. 1: (Color online) Coordinate-space matrix elements of Argonne V18 NN force in the four different spin/isospin channels, i.e. contributions that are proportional to  $1$ ,  $\tau_1 \cdot \tau_2$ ,  $\sigma_1 \cdot \sigma_2$  and  $(\tau_1 \cdot \tau_2)(\sigma_1 \cdot \sigma_2)$ , where  $\sigma_i$  ( $\tau_i$ ) denotes the one-body spin (isospin) Pauli matrix acting on nucleon number  $i$ . Each channel separates into various contributions: central  $1$ , tensor  $S_{12}$  and spin-orbit  $(\vec{L} \cdot \vec{S})$ . Centrifugal  $\vec{L}^2$  and quadratic spin-orbit  $(\vec{L} \cdot \vec{S})^2$  components are not shown. The various mesons ( $\rho$ ,  $\omega$ ,  $\sigma$ ...) that are thought to propagate the inter-nucleon interaction at various distances are also schematically represented.

The second difficulty stems from the nature of the system of interest. Most nuclei (i.e. those with masses typically between 40 and 350) are by essence intermediates between few- and many-body systems, as schematically pictured in Fig. 2. As a result (a) most nuclei are beyond theoretical and computational limits of ab-initio techniques that describe the interacting system from basic NN and 3N vacuum forces, while (b) finite-size effects play a significant role, which prevents statistical treatments. Furthermore, a unified view of low-energy nuclear physics implies a coherent description of (i) small- and large-amplitude collective motions, (ii) closed and open systems, e.g. the structure-reaction interface that is mandatory to understand spontaneous and induced fission, fusion, nucleon emission at the drip-line..., as well as (iii) the structure of exotic systems.

The treatment of the nuclear many-body problem aims at computing ground- (masses, radii, deformation and multipolar moments...) and excited- (single-particle, vibrational, shape and spin isomers, high-spin and super-deformed rotational bands...) states properties over the nuclear chart, not only for the nearly 3100 ob-

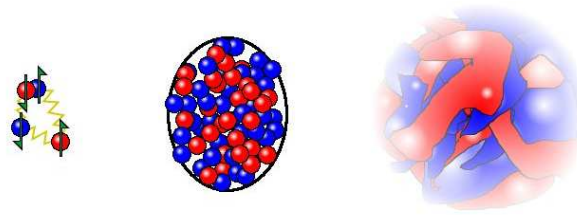


FIG. 2: (Color online) Pictorial view of a nucleus, as an intermediate between pure few-body and extended many-body systems.

served nuclei [17] but also for the thousands that are still to be discovered. In that respect, a cross-fertilization between theoretical and experimental studies is topical, with the apparition of (i) new-generation radioactive-beam (RIB) facilities producing very short-lived systems with larger yields, and (ii) high-precision detectors allowing precise measurements with low statistics and high noise-to-signal ratios. Upcoming facilities based on in-flight fragmentation, stopped and reaccelerated beams or a combination of both are going to further explore the nuclear chart towards the limits of stability against nucleon emission, the so-called nucleon drip-lines. The study of the terra incognita in the neutron-rich region will help understand the astrophysical nucleosynthesis of about half of the nuclei heavier than iron through the conjectured r-process that was recently ranked among the "Eleven science questions for the next century" by the American National Research Council [18]. The large neutron-over-proton ratio accessible through neutron-rich nuclei leads to the modification of certain cornerstones of nuclear structure, e.g. some of the "standard" magic numbers are strongly weakened while others (may) appear [19]. When adding even more neutrons, the proximity of the Fermi energy to the particle continuum gives rise to new phenomena, such as the formation of light nuclear halos, e.g.  $^{11}\text{Be}$  [20, 21] or  $^{11}\text{Li}$  [22, 23], with anomalously large extensions [24, 25] or the existence of di-proton emitters [26]. In addition to reaching out to the most exotic nuclei, experiments closer to the valley of stability still provide critical information. For instance, precise mass measurements using Penning traps [27, 28] or Schottky spectrometry [29] refine and extend mass difference formulæ, e.g. leading to a better understanding of pairing correlations. Also, the study of Wigner energy [30] associated with the over stability of  $N = Z$  elements might provide leads regarding the existence of static  $T = 0$  proton-neutron pairing, while the study of the first  $2^+$  state in even-even nuclei together with its  $B(E2)$  transition to the ground state provides key information about closing and opening of magic numbers. Of course, experiments dedicated to the study of rotational or vibrational bands [31], shape coexistence [32, 33], fission properties of actinides [34], collective modes [35] are all of primer interest. Finally, other limits of existence are of fundamental importance, e.g. the quest for superheavy elements and for the conjectured island of stability beyond the  $Z = 82$  magic number [36].

The challenge of contemporary nuclear structure theory is thus to describe this entire range of nuclei and properties as well as neutron stars and supernovae in a controlled and unified way. While bulk properties of nuclei can be roughly explained using macroscopic approaches such as the liquid drop model (LDM) [38, 39], microscopic techniques are the tool of choice for a coherent description of all static and dynamical nuclear properties. This leads to defining the class of so-called *ab-initio* methods that consists of solving the nuclear many-body problem, as exactly as possible, in terms of vacuum NN, 3N, 4N... interactions. For three- and four-nucleon systems, essentially exact solutions of the Faddeev or Yakubowski equations can be obtained using realistic vacuum forces [40–42]. Likewise, Green function Monte-Carlo (GFMC) calculations [43–45] provide a numerically exact description of nuclei up to carbon starting from local NN and 3N vacuum forces, although such a method already faces huge numerical challenges for  $^{12}\text{C}$ . Complementary *ab-initio* methods allow the treatment of nuclei up to  $A \approx 16$ , e.g. (i) the stochastic variational method (SVM) that expands the many-body wave function over gaussian wave packets [46–48], (ii) the no-core shell model (NSCM) [49–52] that projects the interacting problem on a given model space defined within a harmonic oscillator basis. Coupled-cluster (CC) theory [53–58], which constructs the correlated ground-state from a product state using an exponentiated cluster expansion, truncated to  $B$ -body operators (typ.  $B \sim 1 - 3$ ), renders possible calculations in the immediate vicinity of doubly-magic nuclei up to  $A \approx 50$ . In the same regime, the self-consistent Green's function (SCGF) approach offers an interesting alternative to CC [59–61] through the approximate computation of the dressed one-body Green's function that describes the propagation of a nucleon in the correlated medium and from which one and two-body observable can be extracted.

To go to heavier systems, an approximate treatment of both the interacting problem is needed. Part of the

Name	Short description	Variational	Scale as	Up to
Few-body (Faddeev...)	$H\Psi = E\Psi$ 	Yes	$M^A$	$A = 2-4$
Green-Function Monte-Carlo (GFMC)	$\Psi(\tau) = e^{-(H-E_0)\tau}\Psi_T$ $= [e^{-(H-E_0)\Delta\tau}]^n \Psi_T$ + auxiliary field 	Yes	$\frac{M!}{(M-A)!A!}$	$A < 12$
No-core Shell Model	$H\Psi = E\Psi$ 	Yes	$4^A$	$A < 16$
Coupled- Cluster (CC)	$ \Psi\rangle = e^S  \Psi_0\rangle$ $S = S_1 + S_2 + \dots$ 	No	$(M-A)^4 A^2$	$A < 100$ Only doubly-magic for now

M : configuration space size

FIG. 3: (Color online) Schematic illustration of Faddeev-Yakubowski, Green-Function Monte-Carlo, No-Core Shell Model and Coupled-Cluster methods (from top to bottom). In each case, the basic equation used, a logo summarizing the method, the computational cost in terms of system and configuration space sizes as well as the actual (or estimated for the CC case) range of application are shown. Taken from Ref. [37].

physics that is not treated explicitly is often accounted for through the formulation and use of so-called *in-medium interactions*. For instance, the configuration interaction (CI) model [62, 63], or shell model (SM), constructs a model space within which valence nucleons interact through an effective interaction that compensates for high-lying excitation outside that model space as well as for excitations of the core that are not treated explicitly. Even though such an effective interaction can be constructed starting explicitly from vacuum interactions, e.g. as a microscopic  $G$ -matrix complemented with perturbative core-polarization diagrams [64], certain combinations of two-body matrix elements<sup>1</sup> need to be slightly refitted on experimental data within the chosen model space (sd, pf...) to correct for the so-called monopole part of the interaction. Conjectures that wrong monopoles originate from the omission of the 3N force in the starting vacuum Hamiltonian are currently being explored [66, 67]. Eventually, unknown spectroscopic properties are described with a very high accuracy with such refitted effective interactions [62, 65]. Still, improved accuracy is needed in the shell model in order to use nuclei as laboratories for fundamental symmetries, e.g. to provide isospin-symmetry-breaking corrections to superallowed decays, study neutrinoless double-beta decay or octupole enhancement factors of electric dipole moments. Finally, the theoretical tool of choice for the microscopic and systematic description of medium- and heavy-mass nuclei is the energy density functional (EDF) method [68], often referred to as "self-consistent mean-field method"<sup>2</sup>. Based on a relativistic or a non-relativistic framework, such a method provides a unified description of nuclei over the whole nuclear chart thanks to its favorable numerical scaling with increasing  $A$ . However, state-of-the-art calculations are based on empirical energy functionals (Skyrme, Gogny...) that are adjusted on experimental data, which raises questions regarding (i) the connection with underlying vacuum NN and 3N forces, and (ii) the predictive power of extrapolated EDF results into the terra incognita, as is illustrated in Fig. 4 for a particular observable of interest related to the prediction of halo structures and the location of the neutron drip-line in medium-mass nuclei.

Consequently, the connection between currently used effective interactions or energy functionals for the approximate calculations of medium-heavy nuclei and vacuum forces is neither explicit nor qualitatively transparent. Discussing how to go beyond the present status within the frame of EDF methods is the central objective of the present lectures. However, the technical capability of doing so depends on the characteristics of the initial Hamiltonian that need now to be discussed.

<sup>1</sup> In the sd shell for example, it is necessary to (slightly) refit about 30 combinations of two-body matrix elements in order to reach about 140 keV root mean square error on nearly 600 pieces of spectroscopic data [65].

<sup>2</sup> We refer to M. Grasso's lectures in the present volume [69] as well as to Sec. II for details.

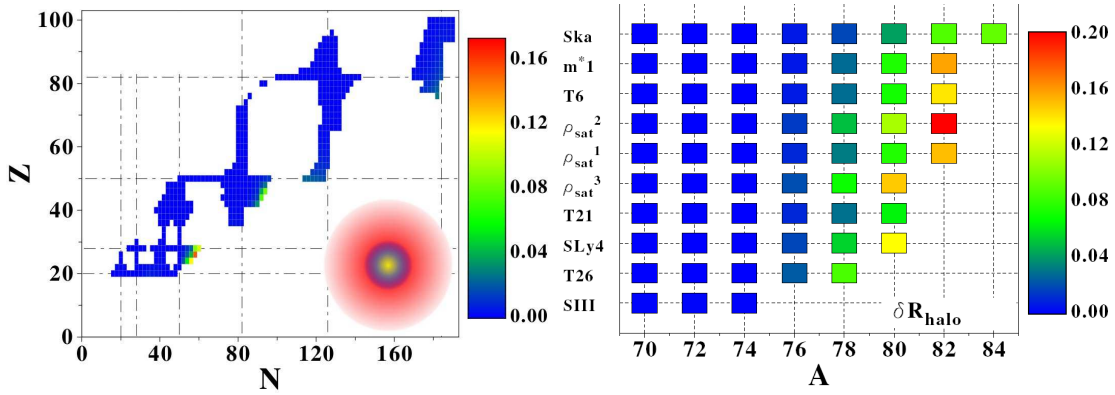


FIG. 4: (Color online) Left : halo parameter  $\delta R_{\text{halo}}$  [70] extracted for nearly five hundreds (predicted) spherical nuclei using SLy4 [71] Skyrme parameterization. Right : halo parameter  $\delta R_{\text{halo}}$  computed for drip-line chromium isotopes using different Skyrme parameterizations of the nuclear EDF; i.e. SLy4 [71],  $m^*_1$  [72],  $\rho_{\text{sat}}^i$  with  $i = 1, 2, 3$  [72], T6 [73], SKa [74], T21 [75], T26 [75] and SIII [76]. Large discrepancies in the prediction of the drip-line position and in the extracted halo parameter are obtained from the various parameterizations. Taken from Ref. [72].

## B. Nuclear hamiltonian and renormalization group methods

Establishing an interparticle Hamiltonian, which is the most basic precursor to many-body calculations, is a challenge for low-energy nuclear physics. The two-body sector has been intensively investigated such that various interactions exist that reproduce phase shifts with  $\chi^2/N_{\text{dof}} \approx 1$  in the elastic regime (up to about 300–350 MeV energy in the laboratory frame). The unsettled frontier is three- and higher-body forces.

As for the NN part, so-called *high-precision conventional models* have been available since the 1990s. Based on an operator expansion [1], a meson-exchange model [77, 78], or a simple parametrization [79], such NN models constitute phenomenological ansätze whose parameters (typically 40) are adjusted to reproduce high-precision nucleon-nucleon scattering data with an almost perfect precision. Figure 1 displays the four two-body spin/isospin channels of Argonne V18 [1] potential in coordinate space. The longest-range feature is the one-pion exchange and is common to most conventional potentials. The mid-range part, which provides a net attraction, has usually been associated with two-pion exchange and/or the exchange of a phenomenological  $\sigma$  "meson". The short-range part of the potential can be attributed to the exchange of heavier mesons ( $\rho$ ,  $\omega$ ) or simply empirically parameterized. In Fig. 1, one sees that the short-distance presents a repulsive core (often called a "hard core"). The fact that Argonne V18 potential is local leads to such a strong short-range repulsion in the S-waves when fitting elastic scattering phase-shifts. However, locality of the potential between composite particles is a feature that is only expected at long distances. As a matter of fact, the potential at short range is not an observable such that locality is only imposed for convenience, not because of physical necessity. There exists an infinite number of equally valid potentials related to each other through unitary transformations, and once one allows for non-locality, a repulsive core is no longer inevitable.

Recently, the development of chiral effective field theory <sup>3</sup> ( $\chi$ -EFT) has made possible the connection between low-energy inter-nucleon forces and QCD, whose relevant high-energy effects are renormalized through fitted low-energy contact terms [81–84]. Typically, the same precision ( $\chi^2/N_{\text{dof}} \approx 1$ ) as for conventional NN potentials is obtained at next-to-next-to-next-to-leading-order (N<sup>3</sup>LO) using about 26 parameters. Eventually, lattice QCD calculations are expected to help constraining low-energy coupling constants that are not determined precisely enough through data fitting [85, 86]. The main benefits of  $\chi$ -EFT are (i) to formulate the problem at hand in terms of relevant low-energy degrees of freedom (pions and nucleons) while retaining the (chiral) symmetry (breaking) of the underlying theory (QCD) and (ii) to naturally explain the phenomenologically-observed hierarchy that makes two-nucleon interactions more important than three-nucleons interactions, which are themselves dominant compared to four-nucleon forces etc. Such a hierarchy relates to the existence of a *power counting* that organizes the infinite number of diagrams in the  $\chi$ -EFT

<sup>3</sup> We refer to E. Epelbaum's lectures in the present volume for details [80].

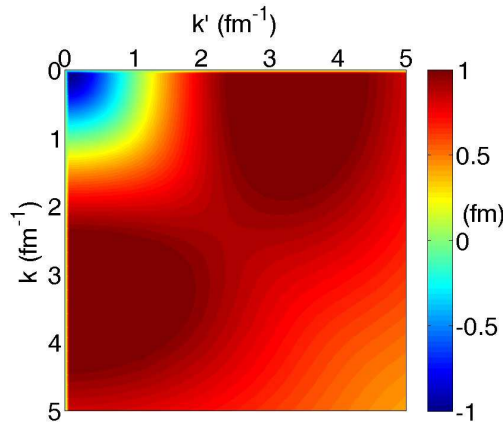


FIG. 5: (Color online) Matrix elements of the Argonne V18 NN potential in the  $^1S_0$  partial-wave. Matrix elements are given as a function of the incoming/outgoing relative momentum ( $k/k'$ ) of the two interacting nucleons. Matrix elements are measured in fm, i.e. one uses  $\hbar = c = m = 1$ , where  $m$  is the nucleon mass. Taken from Ref. [90].

Lagrangian [80].

Conventional or  $\chi$ -EFT Hamiltonians display several sources of nonperturbative behavior that complicate nuclear structure calculations. First are the virtual excitations of nucleons to high relative momenta (energy). This is made apparent by computing the matrix element of the NN potential in (relative) momentum space, as shown in Fig. 5 for the  $^1S_0$  partial wave of Argonne V18, where the strong low- to high-momentum coupling driven by the short-range repulsion is manifested by the large regions of repulsive off-diagonal matrix elements. While such virtual excitations are due to the strongly model-dependent short-range central and tensor forces in conventional potentials, they remain significant in  $\chi$ -EFT potentials that better separate the high-energy, model-dependent, physics from the low-energy sector of interest. The second source of non-perturbative behavior is due to the presence of low-energy bound and nearly-bound states in the  $^3S_1$  and  $^1S_0$  of the NN interaction, respectively. Such states correspond to poles in the scattering  $T$  matrix that render the perturbative Born series divergent at low energy.

Progress toward controlled nuclear calculations has long been hindered by the difficulty to solve the nuclear many-body problem expressed in terms of nuclear potentials that couple low- and high-momentum modes. This has historically been accepted as an unavoidable reality. Recently, EFT and RG methods [87–90] have promoted a completely different view point based on the fact that the Hamiltonian (potential) is not an observable to be fixed from experiment (there is no “true potential”), but rather that there exists an infinite number of Hamiltonians (potentials) capable of accurately describing low-energy physics [91]. In order to be predictive and systematic, an organization (“power counting”) must be present to permit a truncation of possible terms in the Hamiltonian (potential). As briefly explained above,  $\chi$ -EFT potentials indeed build on such considerations. They are based on a power counting that organizes terms in the Hamiltonian in powers of  $Q/\Lambda_{\text{EFT}}$ , where  $\Lambda_{\text{EFT}} \sim 500\text{--}600$  MeV embodies the separation of scale between the high-energy/short-distance sector that is not modeled explicitly (e.g., heavy mesons,  $\Delta$  resonances. . .) and the low-energy/long-range sector associated with explicitly treated degrees of freedom (pions and point-like nucleons) and characterized by typical momenta  $Q \sim m_\pi, k_F$ . As long as a complete Hamiltonian to some order is used (including many-body forces), all observable should be equivalent up to truncation errors, independently of the details used to model the short-distance (high-energy) physics. In that respect,  $\chi$ -EFT potentials provide a modern starting point to attack the nuclear many-body problem.

Renormalization group (RG) methods exploit EFT ideas even further. Starting from a  $\chi$ -EFT Hamiltonian, one can proceed to a (unitary) transformation to *decouple* low-momentum modes from high-momentum ones that are still present at the separation scale  $\Lambda_{\text{EFT}}$  used to build the  $\chi$ -EFT Hamiltonian to some order in the power counting. The RG transformation “changes the resolution scale  $\Lambda$ ” ( $< \Lambda_{\text{EFT}}$ ) of the Hamiltonian, while preserving the original truncation error, such that it becomes *softer* thanks to the elimination of the original non-perturbative coupling between low- and high-momentum modes. In such a context, NN, 3N, 4N. . . forces between nucleons depend on  $\Lambda$  [92–94]. Tracking the change of many-body observable with the resolution scale  $\Lambda$  of the input Hamiltonian can be used as a powerful tool to study the underlying physics scales and to evaluate the incompleteness of approximate calculations or of dropping multi-body forces in the Hamiltonian.

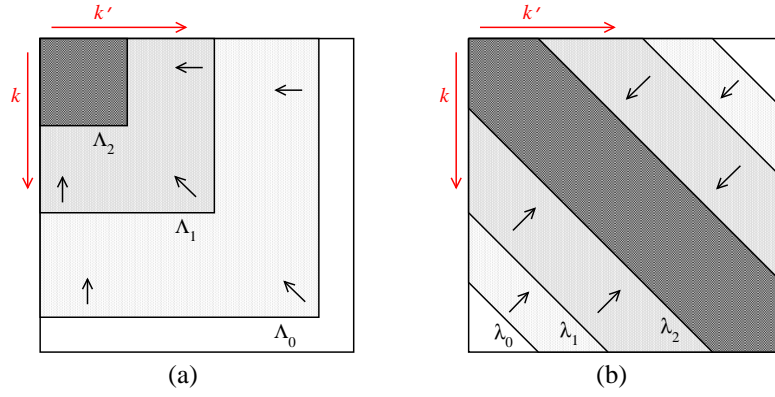


FIG. 6: (Color online) Schematic illustration of two types of RG evolution for NN potentials in momentum space : (a)  $V_{\text{low}k}$  running in  $\Lambda$ , and (b) SRG running in  $\lambda$ . At each  $\Lambda_i$  or  $\lambda_i$ , the matrix elements outside of the corresponding lines are zero, so that high- and low-momentum states are eventually decoupled. Taken from Ref. [90].

Eventually, the source of nonperturbative behavior associated with weakly and nearly bound states, which remains independent of the cutoff in the two-body sector, is also tamed down as the density of the medium increases [95]. Using such class of *low-momentum* Hamiltonians leads to interesting consequences ; i.e. the nuclear many-body becomes much more perturbative than with conventional or  $\chi$ -EFT Hamiltonians [87].

While soft potentials derived from RG methods constitute a new development in nuclear physics [93, 96], attempts to use soft potentials to compute the equation of state of infinite nuclear matter were made in the mid sixties and early seventies [97, 98]. It had long been observed that a strongly repulsive core is not resolved until eight times nuclear saturation density [99] such that saturation is not driven by it. However, soft potentials were abandoned because they seemed incapable of quantitatively reproducing nuclear matter properties, and in particular its saturation. From the EFT perspective, a failure to reproduce nuclear matter observable should not be interpreted as showing that the low-energy potential is wrong, but that it is incomplete. This misconception still persists and has led to the conclusion that low-momentum NN interactions are "wrong" because they do not give saturation in nuclear matter and finite nuclei are overbound for lower cutoffs. The missing physics that invalidates such a conclusion is many-body forces. In a low-energy effective theory, many-body forces are inevitable ; the relevant question is how large they are ? As already mentioned, it has been established beyond doubt that 3N forces are required to provide a consistent description of various low-energy nuclear phenomena. When evolving the NN part through RG methods, three-body (and higher-body) interactions evolve naturally with the resolution scale. As will be seen, 3N forces offer a natural and quantitative tool to generate saturation in conjunction with soft NN interactions.

There exists in fact two major classes of RG transformations used to construct low-momentum interactions, which are schematically illustrated in Fig. 6. In the  $V_{\text{low}k}$  approach, decoupling is achieved by lowering a momentum cutoff  $\Lambda$  above which matrix elements go to zero. In the SRG unitary approach, decoupling is achieved by lowering a momentum cutoff  $\lambda$  using flow equations that drive the potential toward a band diagonal form in momentum space. The effects can be readily seen in the series of contour plots in Figs. 7(a) and 7(b). With either approach, lowering the cutoff leaves low-energy observable unchanged by construction, but shifts contributions between the NN, 3N, 4N... interaction strengths and the sums over intermediate states in loop integrals.

We note that the RG is an integral part of any EFT. Matching of the EFT at a given truncation level (to data or to an underlying theory) but at different regulator cutoffs establishes the RG evolution (or "running") of the EFT couplings. This includes the shift of strength between loop integrals and couplings and between two and many-body interactions. However, because the EFT basis is truncated, the error at the initial cutoff is not preserved with the running, in contrast to the momentum-space RG evolution using  $V_{\text{low}k}$  or SRG techniques, which keep all orders.

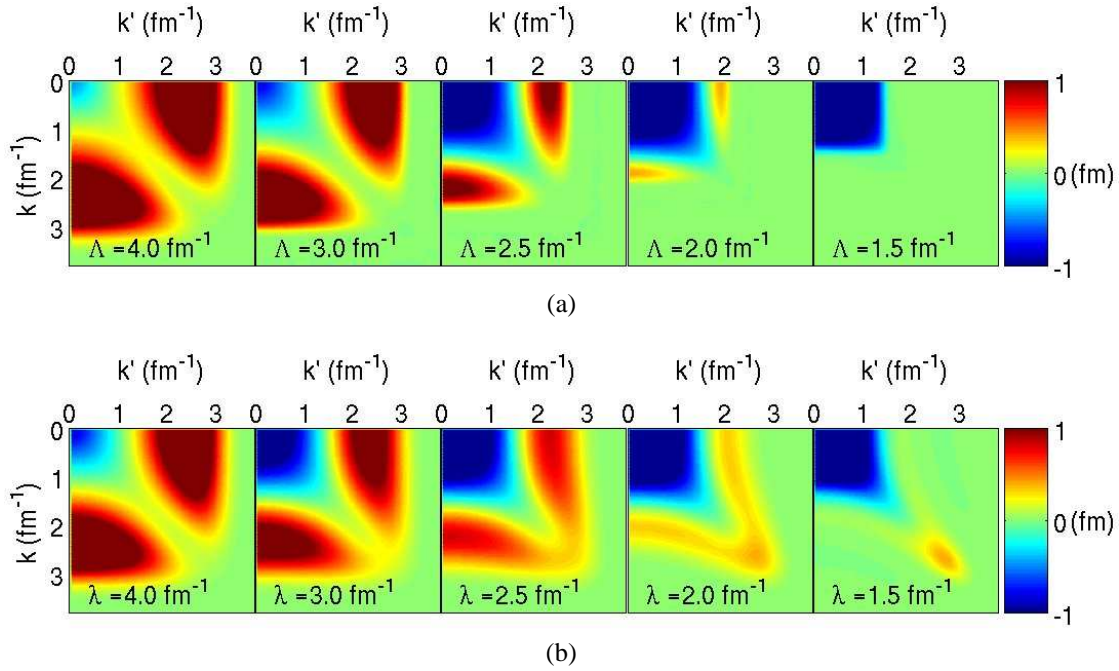


FIG. 7: (Color online) Two types of RG evolution applied to one of the chiral  $N^3\text{LO}$  NN potentials (550/600 MeV) of Ref. [100] in the  $^3S_1$  channel : (a)  $V_{\text{low}k}$  running in  $\Lambda$ , and (b) SRG running in  $\lambda$ . Taken from Ref. [90].

### C. A path towards non-empirical energy density functionals

Impressive progress has been made in extending the limits of ab-initio methods beyond the lightest nuclei [60, 61, 101–103]. Still, the nuclear EDF approach remains the only computationally-feasible method to provide a comprehensive description of medium- and heavy-mass nuclei [68]. Indeed, EDF calculations present a computational scaling that makes them amenable to systematic studies of systems with large numbers of nucleons, independently of their expected shell structure. This makes also possible to study the idealized system of *infinite nuclear matter* that is relevant to the description of compact astrophysical objects such as neutron stars. The nuclear EDF method presents formal similarities with density functional theory (DFT) [104–110] that provides a framework to compute the exact ground-state energy and one-body density of electronic many-body systems in condensed-matter physics and quantum chemistry [111]. However, and even if it is often referred to as *nuclear DFT* [112–117], the nuclear EDF method as it has been done so far has deeply rooted conceptual differences with standard DFT that relate to symmetries ; e.g. see Refs. [118–123]. We briefly come back to this point below.

Questions in astrophysics and the advent of new experimental facilities to study nuclei at the limits of existence are driving multi-pronged efforts to calculate nuclear structure and reaction properties across the full table of nuclides in a reliable manner. In that respect, modern parameterizations of the nuclear EDF, i.e. Skyrme, Gogny, or relativistic energy functionals, provide a good description of bulk properties and, to a lesser extent, of spectroscopic features of known nuclei [68]. However, such parameterizations are phenomenological as they rely on empirically-postulated functional forms whose free couplings are to be adjusted on finite-nuclei data through a chosen fitting protocol. Their lack of microscopic foundation often leads to parametrization-dependent predictions away from known data and makes it difficult to design systematic improvements. As a matter of fact, limitations of existing EDFs have been identified [75, 124–126] over the last decade and relate to (i) their (too) simple analytical representations, (ii) the biases in their adjustment procedure and (iii) the lack of a solid microscopic foundation. Fueled by interests in controlled extrapolations of nuclear properties in isospin, density, and temperature, efforts are currently being made to develop energy functionals with substantially reduced errors and improved predictive power. One possible path forward focuses on empirically improving the analytical form and the fitting procedure of existing phenomenological functionals [75, 124, 127–131].

A second path that complements the development of empirical EDFs based on trial-and-error consists

of connecting energy functionals to ab-initio nuclear structure calculations. Such a connection is meant to lead to so-called *non-empirical* energy functionals possessing a link to the microscopic nuclear Hamiltonian describing few-body scattering and bound-state observable. Given the limited reach of ab-initio schemes, such a strategy aims at benefiting from the best of both worlds, i.e. combining the predictive character of an ab-initio reference method with the gentle numerical scaling of the EDF method that can be applied to any nucleus, independently of its doubly-magic, singly-magic or doubly-open-shell character.

In practical terms, there exists multiple paths to non-empirical energy functionals and the optimal choice is not obvious at this point in time. First, various ab-initio methods can be used as starting points, the idea being to set up the connection in nuclear systems (e.g. infinite nuclear matter, doubly-magic nuclei...) accessible to that ab-initio method prior to extending the use of the microscopically-constrained energy functional to more complicated systems. Second, such a connection can be implemented at various levels of sophistication. Lastly, such a connection to ab-initio methods necessitates, in order to be rigorously formulated, to distinguish between approaches based on the standard nuclear EDF method as it has empirically been used so far and approaches that try to base the energy functional approach to nuclei on DFT.

### 1. Connecting the nuclear EDF method to ab-initio approaches

A rather indirect procedure consists of benchmarking EDF results obtained for a set of systems and observable from an empirically-postulated form with those produced through the ab-initio method of reference. Unknown couplings of the empirical EDF parametrization can be "microscopically" constrained in this way. However, the reliability of the postulated functional form can only be assessed indirectly through such a strategy. Still, constraining the employed parametrization to reproduce a large set of (independent) observable can allow one to discriminate between different functional forms [75, 124, 126]. The benefit of such an indirect approach is that any ab-initio method that can provide precise enough benchmarks for the systems/observables of interest can be used. But again, no direct/explicit connection with vacuum interactions is realized in this case such that no specific insight about the *form* of new functional terms that can capture the missing physics is easily gained in this way.

An approach that we aim at promoting in the present lecture consists of connecting more explicitly the functional *form* and the *value* of its couplings to vacuum nuclear interactions. The objective is not to replace but rather complement approaches based on empirical EDF's that already achieve an accuracy for known observable, e.g. nuclear masses, which will be difficult if not impossible to reach with purely non-empirical functionals. One is essentially looking for *microscopically-educated guesses* of new functional terms and the value of their couplings. Eventually, a fine-tuning of the couplings, within the intrinsic error bars with which they will have been produced, can be envisioned. In practice, microscopically-educated functional terms are to be complemented with yet empirical ones until the former account for enough in-medium correlations. Of course, one must prevent the added empirical terms from double counting the physics that is already included through microscopically-derived ones.

Within such a scheme, microscopically-educated functional terms are to be derived through analytical approximations of the ground-state energy computed from the ab-initio method of reference. It is a challenging task whose complexity depends on the particular many-body method and nuclear Hamiltonian one starts from. Indeed, not all ab-initio methods offer a natural matching, even through a set of controlled approximations, to energy density functionals that are close to the form of standard quasi-local (Skyrme, relativistic point coupling...) or non-local (Gogny, effective meson-exchange Lagrangian...) variants. As a matter of fact, ab-initio methods that are amenable to such a mapping must share certain key features with EDF methods, the most important of which being the concept of spontaneous symmetry breaking (and further restoration). Let us take the part of the EDF that drives superfluidity as an example, i.e. the part that is a functional of the anomalous pairing tensor  $\{\kappa_{ij}\}$ . Such a dependence exists in the EDF only because pairing correlations are grasped through the breaking of good particle-number associated with  $U(1)$  gauge symmetry. Deriving microscopically-educated terms that are explicit functional of  $\{\kappa_{ij}\}$  can only be achieved using an ab-initio method that also incorporates pairing correlations through the breaking (and restoration) of  $U(1)$  gauge symmetry<sup>4</sup>. Similarly, static quadrupole correlations contained in the energy functional can be more directly benchmarked using an ab-initio method that allows the breaking (and restoration) of angular momentum

---

<sup>4</sup> Of course, the corresponding ab-initio calculations must be doable in systems where such terms are indeed switched on, i.e. all but doubly-magic nuclei in the present example.

associated with  $SO(3)$  rotational symmetry.

## 2. Connecting the nuclear DFT method to ab-initio approaches

It has become customary in nuclear physics to assimilate the SR-EDF method, eventually including corrections *a la* Lipkin or Kamlah, with DFT, i.e. to state that the Hohenberg-Kohn (HK) theorem underlays nuclear SR-EDF calculations. This is a misconception as distinct strategies actually support both methods. Whereas the SR-EDF method minimizes the energy with respect to a symmetry-breaking trial density, DFT relies on an energy functional whose minimum must be reached for a one-body local density<sup>5</sup> that possesses *all* symmetries of the actual ground-state density, i.e. that displays fingerprints of the symmetry quantum-numbers that characterize the exact ground-state [132]. As a matter of fact, generating a symmetry-breaking solution is known to be problematic in DFT, as it lies outside the frame of the HK theorem, and is usually referred to as the *symmetry dilemma*. To by-pass the symmetry dilemma and grasp kinematical correlations associated with symmetries, several reformulations of DFT have been proposed over the years, e.g. see Refs. [133, 134], some of which are actually close in spirit to the nuclear MR-EDF method [133].

Recent efforts within the nuclear community have been devoted to formulating a HK-like theorem in terms of the internal density, i.e. the matter distribution relative to the center of mass of the self-bound system [118, 119]. Together with an appropriate Kohn-Sham scheme [119], it allows one to reinterpret the SR-EDF method as a functional of the internal density rather than as a functional of a translational-symmetry-breaking density. This constitutes an interesting route whose ultimate consequence would be to remove entirely the notion of breaking and restoration of symmetries from the energy functional approach and make the SR formulation a complete many-body method, at least in principle. To reach such a point though, the work of Refs. [118, 119] must be extended, at least, to rotational and particle-number symmetries, knowing that translational symmetry was somewhat the easy case to deal with given the explicit decoupling of internal and center of mass motions.

Within the (hopefully extended) scheme of Ref. [119], one can envision to design a so-called *ab-initio nuclear DFT* approach [135]. Although some of the techniques used to do so might be the same as for designing non-empirical nuclear EDF, we differentiate both attempts as they build on different theoretical grounds that influence strongly the way symmetries are handled and the need for a multi-reference extension. Given that the present lectures are dedicated to describing the path towards non-empirical EDFs only, we refer the reader to Ref. [135] for a discussion regarding current efforts made to design an ab-initio nuclear DFT.

For illustration purposes, we can briefly mention one way to proceed that is specific to the nuclear DFT and that does not apply to the nuclear EDF. The idea is (i) to compute through an ab-initio method of reference the (a set of) ground-state density(ies) and energy for a set of nuclei embedded in a tunable (set of) external potential(s), (ii) find for various choices of the external potential(s) the associated one-body local Kohn-Sham potential(s) from which a non-interacting system can be extracted that reproduce the correlated density(ies), (iii) use a model energy functional parametrization whose functional derivative(s) with respect to the (set of) local density(ies) map the one-body local Kohn-Sham potential(s) extracted from the previous step. The difficulties of such a scheme in the nuclear case rely in the fact that (i) the tunable external potential(s) are A-body operators rather than one-body ones as in electronic system DFT [119] and that (ii) it is not guaranteed that there exists a Kohn-Sham non-interacting system that can reproduce several correlated local densities at the same time; i.e. this has to do with the so-called non-interacting  $v$ -representability of such a set of local densities. Such an approach is currently being developed based on CC calculations of doubly-magic nuclei [136].

## D. Outline of the lectures

Following the preceding discussion, the present set of lectures discusses the route towards an explicit and quantitative connection between high-precision NN and 3N models and energy density functionals used to describe heavy nuclei, as is schematically illustrated in Fig. 8. To do so, the nuclear energy density functional method is briefly reviewed in Sec. II. The basics of the formalism are discussed and the limitations of EDFs

---

<sup>5</sup> The scheme can be extended to a set of several local densities or even to the full density matrix.

calculations employing currently available empirical parameterizations are exemplified through a limited number of cases.

The design of non-empirical energy functionals nowadays can be envisioned thanks to the new paradigm set by low-momentum vacuum interactions. Indeed, such *soft* nuclear interactions allow a quantitative treatment of infinite nuclear matter [87–89] and doubly closed-shell nuclei [137, 138] within the frame of many-body perturbation theory (MBPT) [139, 140], e.g. Hartree-Fock becomes a reasonable (if not fully quantitative) starting point. Consequently, Sec. III is dedicated to reviewing low-momentum interactions generated through renormalization group techniques.

In this context, MBPT calculations constitute our most basic ab-initio method of reference. To suit our purpose, we consider Goldstone (time-ordered) MBPT based on an unperturbed vacuum that possibly breaks particle number and rotation invariances. Works following such a strategy have been initiated recently [135, 141, 142]. Section IV B is thus dedicated to summarizing the basics of Goldstone MBPT, where the explicit breaking of particle number is however omitted for simplicity.

Although MBPT constitutes the simplest, yet quantitative, ab-initio reference method to be contemplated, systematic MBPT calculations of self-bound superfluid heavy nuclei in terms of realistic nuclear interactions, even restricted to second order, still constitute a numerical challenge as of today. Indeed, perturbative contributions to the energy involve density matrices and propagators folded with finite-range interaction vertices, and are therefore highly non-local in both space and time. It is why controlled approximations are mandatory to map such calculations onto a numerically tractable EDF that allows for non-empirical calculations of heavy open-shell nuclei. At lowest order in MBPT (i.e., Hartree-Fock), the density matrix expansion (DME) of Negele and Vautherin [143] can be unambiguously applied to approximate the spatially non-local energy expression as a generalized Skyrme functional with density-dependent couplings calculated explicitly from vacuum interactions. Section IV E is thus dedicated to discussing the basics of the DME following recent works that have revived and improved such a method [144–154]. The non-trivial density dependence of the DME couplings is a consequence of the finite-range of the underlying NN interactions, and is controlled by the longest-ranged components of the NN interaction. Consequently, the DME offers a path to incorporate physics associated with long-range one- and two-pion exchange interactions into existing Skyrme functionals. Given the rich spin and isospin structure of such interactions, it is hoped that their inclusion will improve predictive power away from known data and provide microscopic constraints on the isovector structure of nuclear EDFs. Still, and as briefly illustrated in Sec. IV D 2, the DME in its standard formulation is not amenable to approximating perturbative contributions beyond HF such that one is awaiting as of today for a generalization of such an expansion technique. This is part of the perspectives of the building and the use of non-empirical nuclear energy functionals whose first attempts are discussed in Sec. IV E 4.

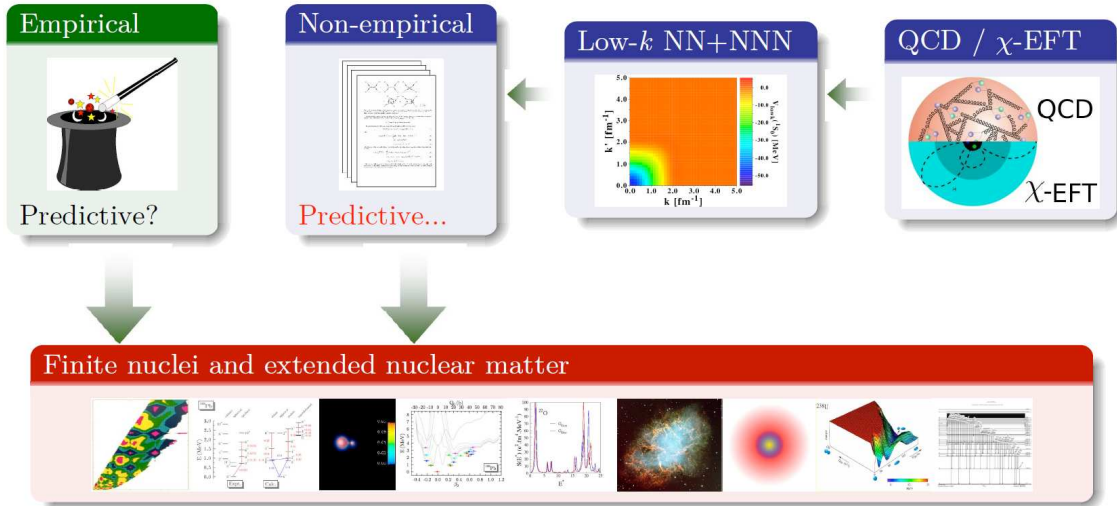


FIG. 8: (Color online) Schematic representation of the design of non-empirical energy density functional rooted into Chiral NN and 3N interactions, further softened through renormalization group methods.

## II. BASICS OF ENERGY DENSITY FUNCTIONAL METHODS

### A. Generalities

The nuclear EDF method [68] is a two-step approach *empirically adapted* from specific variational wave-function-based approaches. The first step is denoted as the single-reference EDF (SR-EDF) implementation and has originally been adapted from the symmetry-unrestricted Hartree-Fock-Bogoliubov (HFB) method using a *density-dependent* effective Hamilton "operator" [155]. Later on, the approximate energy was formulated directly as a possibly richer functional of one-body density matrices computed from a symmetry-breaking product-state of reference. The second step, carried out through the multi-reference (MR) extension of the SR-EDF approach has been adapted from the projected Hartree-Fock-Bogoliubov and generator coordinate methods. The nuclear EDF method strongly relies on the concept of spontaneous symmetry breaking and associated restoration. The MR step necessitates a prescription to extend the SR energy functional<sup>6</sup> associated to a single auxiliary state of reference, i.e. a diagonal energy kernel, to the non-diagonal energy kernel associated with a pair of reference states. This leads to difficulties [120, 121, 156–159] that will not be discussed in the present lectures.

Unlike the wave-function-based approaches it has been adapted from, the nuclear EDF method is *not* based on an attempt to approximate the correlated many-body wave-function. Rather, part of the correlations are directly built into the energy functional kernel under the form of a functional of one-body density matrices. The main advantages of the method are that (i) it uses the full space of single-particle states, (ii) although it is fully quantal, the use of densities and currents as basic variables combined with the spontaneous breaking of symmetries provides a natural description of collective behaviors, (iii) the energy functional is universal in the sense that it is meant to be applied to all nuclei (but the lightest) and that (iv) correlations varying smoothly with the filling of nuclear shells, i.e. with the number of particles are rather easily mocked up into the energy functional kernel itself. On the other hand, the main difficulties are that (a) although the EDF method is applicable to any nucleus, there exists no unique parametrization at this point in time that works satisfactorily for all nuclei and all observable, (b) the empirical character of existing parameterizations of the EDF strongly limits its predictive power, (c) certain categories of correlations that vary rapidly with the number of particles can hardly be parameterized into the EDF itself or grasped through the breaking of symmetries such that non-trivial extensions of the basic SR-EDF method, i.e. MR-EDF schemes, are often unavoidable to reach the necessary accuracy, and finally that (d) a quantitative account of spectroscopic properties also necessitates MR-EDF extensions.

In the present section, the basic SR-EDF is briefly described while Fig. 14 summarizes its key features. The MR extension is however only sketched through Fig. 15. Also, time-dependent variants of the SR- and MR-EDF methods are not discussed in the present document [160, 161].

### B. Single-reference EDF method

#### 1. Elements of formalism

The binding energy  $\mathcal{E}[\rho, \kappa^*, \kappa]$  of the many-body system is postulated to be a functional, in the mathematical sense, of the one-body density matrix and pairing tensor defined, respectively, in an arbitrary single-particle basis  $\{b_i\}$  as

$$\rho_{ji} \equiv \langle \Phi | b_i^\dagger b_j | \Phi \rangle \quad ; \quad \kappa_{ji} \equiv \langle \Phi | b_i b_j | \Phi \rangle , \quad (1)$$

where  $|\Phi\rangle$  denotes a symmetry-breaking state of reference. The latter is an *auxiliary* state in the sense that it is not meant to provide a realistic approximation of the correlated many-body wave-function but a reference to compute the density matrices  $\rho$  and  $\kappa$ . The form of  $|\Phi\rangle$  is the result of a compromise between simplicity and the need to incorporate enough physics, e.g. providing a non-zero value of  $\kappa$  requires a many-body state that spans Hilbert spaces associated with different number of particles. In practice, the SR-EDF implementation

---

<sup>6</sup> I.e., the density-dependence of the effective Hamilton operator in more standard formulations.

relies on using a product state of the Bogoliubov type

$$|\Phi\rangle \equiv \prod_i \beta_i |0\rangle \quad ; \quad \beta_i \equiv \sum_j U_{ji}^* b_j + V_{ji}^* b_j^\dagger, \quad (2)$$

which is a vacuum of the fermionic quasi-particle operators  $\{\beta_i\}$  defined through the latter Bogoliubov transformation, i.e.  $\beta_i |\Phi\rangle = 0$  for all  $i$ . The information contained in the product state  $|\Phi\rangle$  is encoded into the so-called generalized density matrix

$$\mathcal{R} \equiv \begin{pmatrix} \rho & \kappa \\ -\kappa^* & 1 - \rho^* \end{pmatrix},$$

which is idempotent, i.e.  $\mathcal{R}^2 = \mathcal{R}$ . The dependence of the EDF on  $\kappa$  allows the treatment of static pairing correlations between nucleons. Such correlations are responsible for the superfluid nature of a majority of nuclei and impacts essentially all low-energy properties of nuclei as well as certain static and dynamical features of neutron stars. Microscopically speaking, like-particle pairing in nuclei (mostly) reflects the strong attraction of the NN interaction in the  $^1S_0$  partial-wave [141, 142, 162–165].

The optimization of the vacuum state  $|\Phi\rangle$ , i.e. the determination of the amplitudes  $(U, V)$  of the unitary Bogoliubov transformation, is performed through the minimization of the energy  $\mathcal{E}[\rho, \kappa^*, \kappa]$  under the constraints that (i) the average number of particles in  $|\Phi\rangle$  remains fixed to a chosen value and (ii) the auxiliary state remains a quasi-particle vacuum, i.e. its generalized density  $\mathcal{R}$  remains idempotent. Given that  $\rho$  is hermitian and  $\kappa$  is antisymmetric, the irreducible set of independent variables selected for the variation is  $\{\rho_{ij}, \rho_{ij}^*, \kappa_{ij}, \kappa_{ij}^*\}$  for  $j < i$  and  $\rho_{ii}$  for all  $i$ . Using a Lagrange method, the constrained minimization reads

$$\delta \left( \mathcal{E}[\rho, \kappa, \kappa^*] - \frac{1}{2} \lambda (\text{Tr}\{\rho\} + \text{Tr}\{\rho^*\}) - \text{Tr}\{\Lambda(\mathcal{R}^2 - \mathcal{R})\} \right) = 0, \quad (3)$$

where the Lagrange parameters  $\{\lambda, \Lambda_{ij}\}$  are adjusted to satisfy the conditions

$$\text{Tr}\{\rho\} = \text{Tr}\{\rho^*\} = \langle \hat{N} \rangle = N \quad ; \quad \mathcal{R}^2 - \mathcal{R} = 0. \quad (4)$$

The minimization leads to solving Hartree-Fock-Bogoliubov-like equations expressed in the single-particle basis  $\{b_i\}$  as

$$\mathcal{H} \begin{pmatrix} U \\ V \end{pmatrix}_\mu \equiv \begin{pmatrix} h - \lambda & \Delta \\ -\Delta^* & -h^* + \lambda \end{pmatrix} \begin{pmatrix} U \\ V \end{pmatrix}_\mu = E_\mu \begin{pmatrix} U \\ V \end{pmatrix}_\mu, \quad (5)$$

from which the quasi-particle wave-functions  $(U, V)_\mu$  and energies  $E_\mu$  are extracted. The Bogoliubov matrix  $\mathcal{H}$  is expressed in terms of effective fields  $(h, \Delta)$  and effective vertices  $(v^{ph}, v^{pp})$  defined through

$$h_{ij} \equiv \frac{\delta \mathcal{E}}{\delta \rho_{ji}} \equiv t_{ij} + \sum_{kl} \bar{v}_{ikjl}^{ph} \rho_{lk} \quad ; \quad \Delta_{ij} \equiv \frac{\delta \mathcal{E}}{\delta \kappa_{ij}^*} \equiv \frac{1}{2} \sum_{kl} \bar{v}_{ijkl}^{pp} \kappa_{kl}. \quad (6)$$

Given that the effective fields depend on the quasi-particle amplitudes  $(U, V)$  through  $\rho = V^* V^T$  and  $\kappa = V^* U^T$ , equation of motion 5 is to be solved iteratively and self-consistently.

## 2. Spontaneous symmetry breaking

TAB. I: Categories of nuclei that tend to spontaneously break translational, rotational and particle number invariances at the SR level. Connection is also provided between the spontaneous breaking of those symmetries and excitation modes observed in nuclei.

	Nuclei	Excitation pattern
Translation in coordinate space	All	Surface vibrations
Rotation in gauge space	All but doubly-magic	Energy gap
Rotation in coordinate space	All but singly-magic	Rotational bands

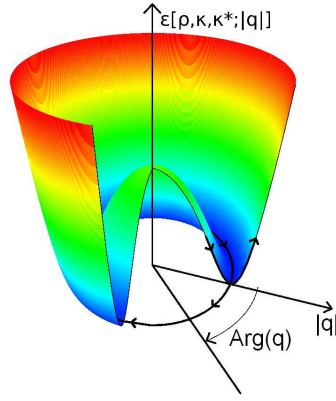


FIG. 9: (Color online) Schematic view of the SR energy as a function of the phase and magnitude of the order parameter  $q$  of a spontaneously broken symmetry.

The nuclear EDF method strongly relies on the concept of symmetry breaking, i.e. the auxiliary state  $|\Phi\rangle$  does not necessarily reflect the symmetries of the underlying Hamiltonian. In other words,  $|\Phi\rangle$  is allowed to span several irreducible representations of the symmetry group  $\mathcal{G}$  of the nuclear Hamiltonian  $H$  when minimizing the energy functional. In the nuclear case, the symmetry group  $\mathcal{G}$  is characterized by the simultaneous commutation of  $H$  with neutron number  $N$ , proton number,  $Z$ , center of mass momentum  $\vec{P}$ , total angular momentum  $J^2$  in the center of mass and its projection on a chosen axis  $J_z$ , parity  $\Pi$  and time reversal  $\mathcal{T}^2$  operators.

Given that  $|\Phi\rangle$  is allowed to span several irreducible representations of the symmetry group, the density matrices  $\rho$  and  $\kappa$  approximate those of a wave packet rather than those of an eigenstate of  $H$ . As a result, the spontaneous breaking of the symmetries carries information about the favored modes of excitation of the system, as exemplified in Tab. I.

The breaking of each symmetry is monitored by the magnitude and the phase of an order parameter  $q$ , such that the (approximate) SR energy  $\mathcal{E}[\rho, \kappa^*, \kappa; |q|]$  only depends on the magnitude of  $q$  and not on its phase, as schematically shown in Fig. 9. This corresponds to the fact that a spontaneous symmetry breaking is accompanied by the presence of a zero-energy Goldstone mode. The energy as a function of  $|q|$  provides a *potential energy curve/surface* that characterizes the restoring force of the system against the variation of  $|q|$ ; i.e. the "polarizability" of the system with respect to "deforming" it along the collective variable  $|q|$ . In practical terms, the potential energy curve can be accessed through repeated SR-EDF calculations *constrained* to various values of  $|q| = \langle \Phi | Q | \Phi \rangle$  where  $Q$  is most often taken as a one-body operator, i.e. by adding the Lagrange term  $-\lambda_{|q|} (\text{Tr}\{\rho Q\} - |q|)$  to Eq. 3.

The (breaking of) symmetries translates into the (reduced) symmetries of the fields  $h$  and  $\Delta$ , which eventually translates into the (absence of) symmetry quantum numbers carried by the solutions of Eq. 5 and by the (reduced) degeneracy of the corresponding eigen spectrum. Of course, that a certain symmetry does break spontaneously usually depends on the number of elementary constituents of the system under consideration. For example, while translational symmetry (strongly) breaks in all nuclei, particle-number symmetry tends to (weakly) break in all but doubly-magic nuclei whereas rotational symmetry remains unbroken if either the neutron number or the proton number is "magic"<sup>7</sup> as is recalled in Tab. I.

As explained in Sec. II F, the breaking of symmetries is an efficient and inescapable way of grasping essential correlations into a simple SR description of nuclear systems. The drawback is that the connection between certain computed quantities and experimental observable is not direct, until one eventually restores the broken symmetries. As a matter of fact, the breaking of symmetries can only provide an intermediate description of a finite system such that good symmetries must eventually be restored to describe properties of actual eigenstates. Doing so is one of the objective of the MR extension of the nuclear EDF method.

<sup>7</sup> The fact that the neutron or proton number is magic is not known a priori but is based on a posteriori observations and experimental facts. In particular, the fact that traditional magic numbers, i.e.  $N, Z = 2, 8, 20, 28, 50, 82, 126$ , remain as one goes to very isospin-asymmetric nuclei is the subject of intense on-going experimental and theoretical investigations [19].

### 3. Single-particle field

The role played by the single-particle field  $h$  is most easily understood in the limit where the auxiliary state  $|\Phi\rangle$  is taken as a Slater determinant, i.e. when particle-number symmetry is enforced such that pairing correlations are not explicitly incorporated through dependencies on  $\kappa$ . In such a case, the equations of motion (Eq. 5) reduce to the eigen-value problem

$$[h\varphi_i](\vec{r}) \equiv \varepsilon_i \varphi_i(\vec{r}), \quad (7)$$

whose eigen-spectrum  $\{\varepsilon_i\}$ , as schematically shown in Fig. 10, provides an approximation to the nuclear "shell structure", i.e. to one-nucleon separation energies between the ground state of the  $N$ -body system and eigen-states of the  $(N-1)$ - and  $(N+1)$ -body systems. As the EDF incorporates a large fraction of correlations, in particular through the breaking of symmetries, the field  $h$  must be seen as effectively reflecting a *correlated* single-particle motion.

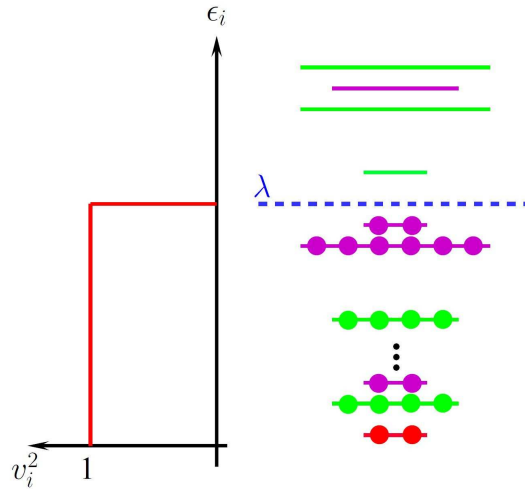


FIG. 10: (Color online) Schematic representation of the single-particle "shell structure" obtained by solving Eq. 7.

Although the SR-EDF method is *not* a Hartree-Fock approximation, a Koopmans-like theorem holds such that the single-particle energy  $\varepsilon_i$  of an occupied (unoccupied) level provides a fair approximation of the computed one-nucleon separation energies. Of course, such an internal consistency of the SR method does not guarantee that such a separation energy is itself a good approximation of the experimental observable and even that it can be straightforwardly related to it. First, the inclusion of pairing correlations will modify such a separation energy in singly- or doubly-open shell nuclei that are statically paired. Second, the loss of good angular momentum associated with the breaking of rotational invariance makes the connection to experimental states indirect in doubly-open shell nuclei. Third, and most importantly, the effect of collective fluctuations that significantly renormalize the position of the quasi-particle peak and the spreading of the single-particle strength that is not pronounced enough (although not zero as is often believed) at the SR level.

Finally, and although such a quantity is even more likely to be renormalized by collective fluctuations, energy differences  $\varepsilon_p - \varepsilon_h$  involving an occupied ( $h$ ) and an empty ( $p$ ) single-particle state close to the Fermi energy provides a first approximation of low-lying individual excitations of the  $N$ -body system.

### 4. Pairing field

As explained above, static pairing correlations are grasped within the SR-EDF through the breaking of particle number, i.e. through the use of an auxiliary state of the Bogoliubov form (Eq. 2) that is a linear superposition of Slater determinants with various numbers of particles. As is schematically shown in Fig. 11, the effective vertex  $v^{pp}$  (Eq. 6) drives the scattering of nucleonic pairs on top of the single-particle shell structure provided by  $h$ . Such a process correlates nucleons in time-reversed states and eventually results in

a non-zero pairing field  $\Delta$  whenever the pairing energy gained in this way overcomes the cost of scattering pairs to higher-energy states.

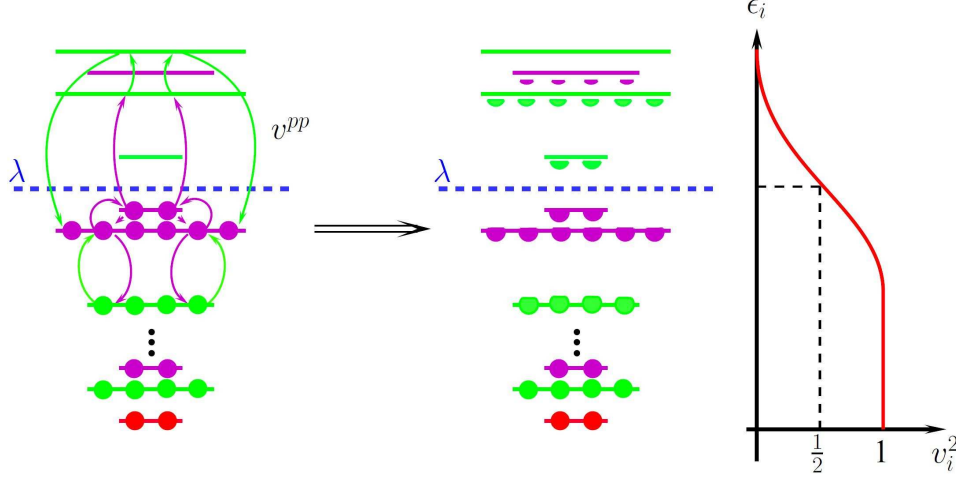


FIG. 11: (Color online) Schematic representation of the pair scattering mechanism driving by the effective vertex  $v^{pp}$  (Eq. 6) and of its resulting impact on the average occupation of canonical single-particle states (Eq. 8).

For all but magic numbers ( $\pm 1$  particle), i.e. systems ( $\pm 1$  particle) with a large gap at the Fermi energy in the  $\{\epsilon_i\}$  spectrum, the minimization of the energy does usually lead to a solution with a non-zero pairing field  $\Delta$ . At convergence, this yields smoothed-out single-particle occupations as schematically shown in Fig. 11. This can be best seen in the so-called *canonical* single-particle basis  $\{a_\nu\}$  that provides the one-body density matrix and the pairing tensor under the particular form

$$\rho_{\mu\nu} \equiv v_\mu^2 \delta_{\mu\nu} = \frac{1}{2} \left[ 1 - \frac{h_{\mu\mu} - \lambda}{\sqrt{(h_{\mu\mu} - \lambda)^2 + \Delta_{\mu\bar{\mu}}^2}} \right] \delta_{\mu\nu}, \quad (8)$$

$$\kappa_{\mu\bar{\nu}} \equiv u_\mu v_\nu \delta_{\mu\nu} = \frac{\Delta_{\mu\bar{\mu}}}{2\sqrt{(h_{\mu\mu} - \lambda)^2 + \Delta_{\mu\bar{\mu}}^2}} \delta_{\mu\nu}, \quad (9)$$

as well as the auxiliary state under a BCS-like form

$$|\Phi\rangle = \prod_{\mu>0} \left( u_\mu + v_\mu a_\mu^+ a_{\bar{\mu}}^+ \right) |0\rangle, \quad (10)$$

in which single-particle states  $(\mu, \bar{\mu})$  are two-by-two conjugated.

### 5. Eigen spectrum

The HFB eigen-spectrum of Eq. 5 is separated into two groups with opposite eigenvalues  $\{E_i : (U, V)_i\}$  and  $\{-E_i : (V^*, U^*)_i\}$ . If the chemical potential  $\lambda$  is positive, the quasi-particle spectrum is entirely continuous. If  $\lambda < 0$ , the system is bound [166] such that the quasi-particle spectrum is partly continuous ( $|E_i| > -\lambda$ ) and partly discrete ( $|E_i| < -\lambda$ ). Such a property is illustrated in Fig. 13. One observes in particular that quasi-particles associated with deep single-particle states couple to the continuum through the residual pairing interaction and acquire a width, i.e. they describe unstable elementary excitations of the systems. When the Fermi level tends to zero, the quasi-particle spectrum becomes more and more continuous as a result of the increased coupling induced by pair scattering between bound and unbound single-particle states. To build the auxiliary product state  $|\Phi\rangle$  and the density matrices associated to it, one must select only half of the solutions such that only one of the conjugated solutions (i.e.  $E_i$  and  $-E_i$ ) is picked. The lowest energy state

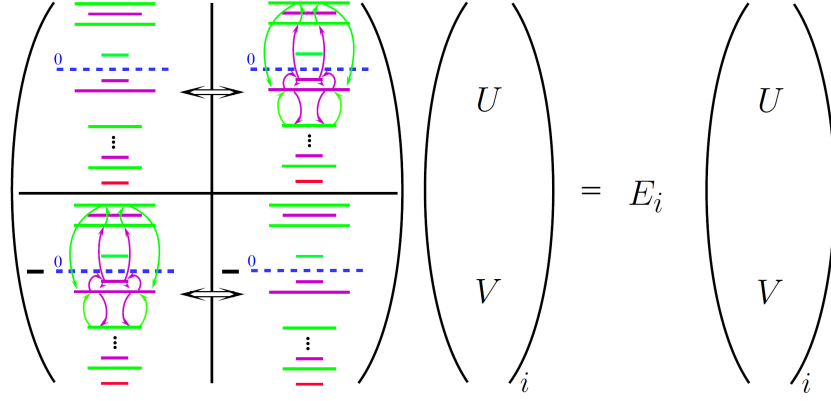


FIG. 12: (Color online) Schematic representation of the interplay between the single-particle field  $h$  and the pairing field  $\Delta$  in the HFB matrix (see text).

is obtained from selecting all quasi-particle with positive energies. Doing so, localized one-body and pairing densities are obtained as long as  $\lambda < 0$ , in spite of the fact that most of selected quasi-particles belong to the continuum [166].

Within the HFB self-consistent scheme, modified single-particle occupations associated with the non-zero field  $\Delta$  feedback onto the single-particle field  $h$  through its dependence on  $\rho$ , which then feedbacks onto the pair scattering, etc, as is schematically depicted in Fig. 12. Such a feature modifies the structure of the ground state and the nature of elementary excitations. Given that the eigen-spectrum approximately reads<sup>8</sup>

$$E_i \approx \sqrt{(\varepsilon_i - \lambda)^2 + \Delta_{ii}^2}, \quad (11)$$

elementary excitations described by auxiliary states of the form  $|\Phi_{ij}\rangle = \beta_i^\dagger \beta_j^\dagger |\Phi\rangle$  are such that

$$\mathcal{E}_{ij}^{(N)} - \mathcal{E}_0^{(N)} \approx E_i + E_j \geq 2\Delta_F, \quad (12)$$

where  $\Delta_F$  denotes the matrix element of the pairing field associated with the canonical pair  $(\mu_F, \bar{\mu}_F)$  the closest to the Fermi level. Consequently, a gap opens up in the excitation spectrum of open-shell nuclei that would be absent in the limit of zero pairing as

$$\mathcal{E}_{ij}^{(N)} - \mathcal{E}_0^{(N)} \xrightarrow{\Delta=0} |\varepsilon_p - \lambda| + |\varepsilon_h - \lambda| = \varepsilon_p - \varepsilon_h \quad (13)$$

and given that the spacing at the Fermi between single-particle states is essentially zero in open-shell nuclei. Such features can also be read off Fig. 13 that displays the modification of the quasi-particle excitation spectrum brought about by the inclusion of pairing correlations.

### C. Empirical energy functionals

The SR-EDF method outlined above can be applied as soon as a parametrization of the nuclear EDF is available. As of today, existing parameterizations have been built empirically through trial and error, i.e. using symmetry requirements to constraint the functional form and fitting to data to fix the free coupling constants. In the following, we briefly review how the formal building of the Skyrme-type local parametrization is achieved in the limit where time-reversal symmetry is enforced.

---

<sup>8</sup> Such an expression is strictly valid in the canonical basis only but, except for low-lying  $l = 0$  quasi-particle states in drip-line nuclei, the actual HFB spectrum is close to the canonical one.

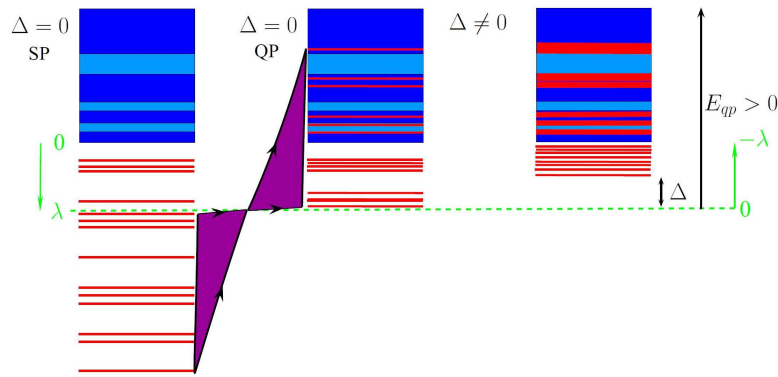


FIG. 13: (Color online) Excitation spectrum built from the eigen-spectrum of  $h$ . a) Single-particle spectrum  $\varepsilon_i$ : discrete bound states in black and continuum in red. Single-particle resonances are represented with their width on top of the continuum background. b) Associated quasi-particle energy spectrum, i.e.  $E_i = |\varepsilon_i - \lambda|$ . c) Quasi-particle spectrum  $E_i$  after switching on pairing correlations. Resonances coming from deeply-bound single-particle states acquire a finite width as a result of their coupling to the single-particle continuum through pair scattering. In b) and c), only the positive part  $\{E_i\}$  of the quasi-particle spectrum is shown, i.e. the mirror negative part at  $\{-E_i\}$  is omitted for simplicity.

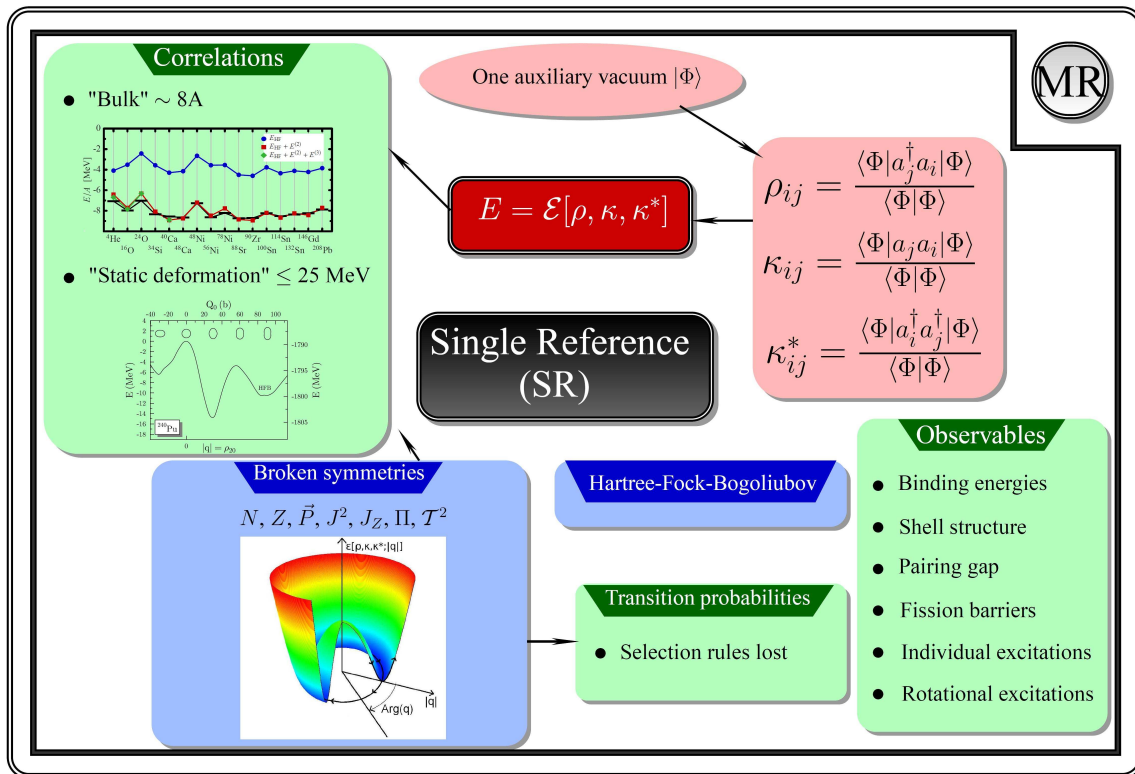


FIG. 14: Schematic representation of the single-reference implementation of the nuclear EDF method (embedded in the more general multi-reference implementation). The various ingredients of the method, e.g. the auxiliary states  $|\Phi\rangle$  from which the density matrices are computed, the importance of spontaneous symmetry breaking and the associated loss of selection rules, as well as the type of correlations that are accounted for, are indicated. Observable that are reasonably described at the SR level are also listed.

### 1. Density matrices and local densities

Starting from the density matrices expressed in the  $|\vec{r}\rangle \otimes |\sigma\rangle \otimes |q\rangle$  single-particle basis

$$\rho_{\vec{r}\sigma q\vec{r}'\sigma'q} \equiv \langle \Phi | c^\dagger(\vec{r}'\sigma'q) c(\vec{r}\sigma q) | \Phi \rangle \quad ; \quad \kappa_{\vec{r}\sigma q\vec{r}'\sigma'q} \equiv \langle \Phi | c(\vec{r}'\sigma'q) c(\vec{r}\sigma q) | \Phi \rangle , \quad (14)$$

one first extracts all time-even local densities that can be built up to second order in derivatives<sup>9</sup>

$$\rho_q(\vec{r}) \equiv \sum_{\sigma} \rho_{\vec{r}\sigma q\vec{r}\sigma q} , \quad (15)$$

$$\tau_q(\vec{r}) \equiv \sum_{\sigma} \nabla \cdot \nabla' \rho_{\vec{r}\sigma q\vec{r}'\sigma q} \Big|_{\vec{r}=\vec{r}'} , \quad (16)$$

$$J_{q,\mu\nu}(\vec{r}) \equiv \frac{i}{2} \sum_{\sigma\sigma'} (\nabla' - \nabla)_{\mu} \rho_{\vec{r}\sigma q\vec{r}'\sigma'q} \sigma_{\nu}^{\sigma'\sigma} \Big|_{\vec{r}=\vec{r}'} , \quad (17)$$

$$J_{q,\kappa}(\vec{r}) \equiv \sum_{\mu,\nu=x}^z \varepsilon_{\kappa\mu\nu} J_{q,\mu\nu}(\vec{r}) , \quad (18)$$

$$\tilde{\rho}_q(\vec{r}) \equiv \sum_{\sigma} \kappa_{\vec{r}\sigma q\vec{r}\sigma q} \sigma_z^{\sigma\sigma} , \quad (19)$$

where  $\sigma_{\nu}^{\sigma'\sigma}$  and  $\varepsilon_{\kappa\mu\nu}$  denote the matrix element of the two-by-two cartesian Pauli matrix  $\mu = x, y, z$  and the Levi-Civita symbol, respectively. In Eqs. 15-19, the so-called matter, kinetic, spin-current tensor, spin-orbit and pairing densities have been defined, respectively. Additional local densities must be considered, i.e. are different from zero, when an auxiliary state breaking time-reversal symmetry is in use [168]. For a general discussion on the properties of non-local and local densities under various set of self-consistent symmetries, we refer the reader to Ref. [169]. Local densities as defined in Eqs. 15-19 are the physical degrees of freedom at play in the SR-EDF method. While their quantal nature ensures their sensitivity to nucleonic degrees of freedom, the use of densities and currents as basic variables, combined with the spontaneous breaking of symmetries, provides a natural description of collective behaviors in heavy nuclei.

### 2. Energy

The procedure consists of building the many-body energy as a local functional of the above set of local densities, i.e. as one triple integral of a local energy-density whose various terms may contain up to two Pauli matrices  $\sigma_{\nu}$  and spatial derivatives  $\nabla$  through  $\rho_q$ ,  $\tau_q$ ,  $J_{q,\mu\nu}$  and  $\tilde{\rho}_q$ . In doing so, specific constraints must be enforced for the resulting functional to be a scalar under all transformations of the symmetry group  $\mathcal{G}$ ; i.e. under transforming  $|\Phi\rangle$  and the densities  $\rho$ ,  $\kappa$ ,  $\kappa^*$  constructed from it. For a local functional of the Skyrme type, we refer the reader to Refs. [167, 170] for the formulation of such constraints.

Focusing on a system that preserves time-reversal symmetry, e.g. the ground-state of an even-even nucleus,

---

<sup>9</sup> For the anomalous part, we restrict the discussion to terms with no derivative. In addition, no isospin mixing is presently considered. See Ref. [167] for a more general and detailed presentation.

one finally obtains the functional form, hereafter referred to as the Skyrme functional

$$\begin{aligned}
\mathcal{E}[\rho, \kappa, \kappa^*] = & \int d\vec{r} \sum_q \frac{\hbar^2}{2m} \tau_q(\vec{r}) \\
& + \sum_{qq'} \int d\vec{r} \left[ C_{qq'}^{\rho\rho} \rho_q(\vec{r}) \rho_{q'}(\vec{r}) + C_{qq'}^{\rho\Delta\rho} \rho_q(\vec{r}) \Delta\rho_{q'}(\vec{r}) + C_{qq'}^{\rho\tau} \rho_q(\vec{r}) \tau_{q'}(\vec{r}) \right. \\
& + C_{qq'}^{\rho\nabla J} \rho_q(\vec{r}) \vec{\nabla} \cdot \vec{J}_{q'}(\vec{r}) + C_{qq'}^{JJc} \sum_{\mu, \nu=x}^z J_{q, \mu\nu}(\vec{r}) J_{q', \mu\nu}(\vec{r}) \\
& \left. + C_{qq'}^{JJt} \sum_{\mu, \nu=x}^z \left[ J_{q, \mu\mu}(\vec{r}) J_{q', \nu\nu}(\vec{r}) + J_{q, \mu\nu}(\vec{r}) J_{q', \nu\mu}(\vec{r}) \right] \right] \\
& + \sum_q \int d\vec{r} C_{qq}^{\tilde{\rho}\tilde{\rho}} |\tilde{\rho}_q(\vec{r})|^2, \tag{20}
\end{aligned}$$

where all couplings  $C_{qq'}^{ff'}$  may further depend on  $\vec{r}$ , e.g. through a dependence on  $\rho_q(\vec{r})$ . The first line of Eq. 20 denotes the uncorrelated kinetic energy. Given such a functional form, the set of free parameters entering the couplings are typically fitted, depending on the protocol of choice, to infinite nuclear matter properties (e.g., saturation point, compressibility, effective masses, asymmetry energy) and a selection of finite-nuclei data (e.g., masses, charge radii, spin-orbit splittings) [71, 75, 128, 171]. Unfortunately, and as will be elaborated on below, although such a functional form can be applied to all ( $A \gtrsim 16$ ) nuclei, there does not exist as of today a parametrization that satisfactorily describes nuclei and observable in a universal manner. We refer the reader to Ref. [168] for examples of modern parameterizations.

### 3. Single-particle field

Starting from the Skyrme functional given in Eq. 20, the single-particle field  $h$  defined through Eq. 6 reads

$$h_{ij}^q \equiv \int d\vec{r} \varphi_i^\dagger(\vec{r}) h^q(\vec{r}) \varphi_j(\vec{r}), \tag{21}$$

where

$$h_q(\vec{r}) = -\nabla \cdot B_q(\vec{r}) \nabla + U_q(\vec{r}) - \frac{i}{2} \sum_{\mu, \nu=x}^z [W_{q, \mu\nu}(\vec{r}) \nabla_\mu + \nabla_\mu W_{q, \mu\nu}(\vec{r})] \sigma_\nu. \tag{22}$$

The local multiplicative potentials appearing in Eq. 22 are defined as

$$U_q(\vec{r}) \equiv \frac{\delta \mathcal{E}}{\delta \rho_q(\vec{r})} \quad ; \quad B_q(\vec{r}) \equiv \frac{\delta \mathcal{E}}{\delta \tau_q(\vec{r})} \quad ; \quad W_{q, \mu\nu}(\vec{r}) \equiv \frac{\delta \mathcal{E}}{\delta J_{q, \mu\nu}(\vec{r})}, \tag{23}$$

such that their expression can be obtained from Eq. 20 by performing a functional derivative. The potential  $B_q(\vec{r})$  provides a position-dependent effective mass whereas  $W_{q, \mu\nu}(\vec{r})$  denotes the spin-orbit potential.

### 4. Pairing field

Similarly to what was done for  $h^q$ , the pairing field  $\Delta^q$  obtained from Eq. 20 reads

$$\Delta_{ij}^q \equiv \int d\vec{r} \left[ \varphi_i^\dagger(\vec{r}q) \Delta_q(\vec{r}) \varphi_j^*(\vec{r}q) - \varphi_j^\dagger(\vec{r}q) \Delta_q(\vec{r}) \varphi_i^*(\vec{r}q) \right], \tag{24}$$

where

$$\Delta_q(\vec{r}) = -\tilde{U}_q(\vec{r}) i \sigma_y. \tag{25}$$

The local multiplicative potential appearing in Eq. 25 is defined as

$$\tilde{U}_q(\vec{r}) \equiv \frac{\delta \mathcal{E}}{\delta \tilde{\rho}_q^*(\vec{r})}, \tag{26}$$

such that its expression can be obtained from Eq. 20 by performing a functional derivative. The use of a local pairing EDF leads to an ultraviolet divergence that needs to be regularized [166, 172, 173] or renormalized [174–178]. We choose not to elaborate on this point here.

#### D. Pseudo potential and effective interaction

Historically, the Skyrme EDF (Eq. 20) has been introduced as the expectation value, in the auxiliary state  $|\Phi\rangle$ , of an effective density-dependent Skyrme "interaction" complemented by a density-dependent delta "interaction" (DDDI) to generate the pairing part of  $\mathcal{E}[\rho, \kappa, \kappa^*]$ . Such effective vertices should not be seen as genuine in-medium effective interactions but rather as convenient auxiliary operators, or *pseudo potentials*, from which a local functional can be derived. Indeed, any realistic in-medium effective interaction would necessarily be both finite-range and non-local, if not energy dependent (see Eq. 64 in Sec. IV D 2). The schematic (i.e. quasi zero-range) form of the auxiliary vertices, together with the mixed account they provide of both in-medium correlations and the effect of many-forces, make their connection to actual NN and 3N interactions extremely indirect at best.

The Skyrme pseudo-potential providing the part of the EDF that depends solely on the normal density matrix takes the typical form

$$v_{\text{cent}} = t_0(1+x_0P_\sigma)\delta(\vec{r}) + \frac{1}{2}t_1(1+x_1P_\sigma)[\delta(\vec{r}), \vec{k}^2 + \overleftarrow{k}^2\delta(\vec{r})] + t_2(1+x_2P_\sigma)\overleftarrow{k} \cdot \delta(\vec{r}) \vec{k} \quad (27)$$

$$v_{\text{cent}}^\rho = \frac{1}{6}t_3(1+x_3P_\sigma)\rho_0^\alpha(\vec{r})\delta(\vec{r}), \quad (28)$$

$$v_{\text{is}} = iW_0(\vec{\sigma}_1 + \vec{\sigma}_2)\overleftarrow{k} \wedge \delta(\vec{r}) \vec{k}, \quad (29)$$

$$v_{\text{tens}} = \frac{t_e}{2} \left\{ [3(\vec{\sigma}_1 \cdot \overleftarrow{k})(\vec{\sigma}_2 \cdot \overleftarrow{k}) - (\vec{\sigma}_1 \cdot \vec{\sigma}_2)\overleftarrow{k}^2] \delta(\vec{r}) + \delta(\vec{r}) [3(\vec{\sigma}_1 \cdot \vec{k})(\vec{\sigma}_2 \cdot \vec{k}) - (\vec{\sigma}_1 \cdot \vec{\sigma}_2)\vec{k}^2] \right\} \\ + t_o \left\{ 3(\vec{\sigma}_1 \cdot \overleftarrow{k})\delta(\vec{r})(\vec{\sigma}_2 \cdot \vec{k}) - (\vec{\sigma}_1 \cdot \vec{\sigma}_2)\overleftarrow{k} \cdot \delta(\vec{r}) \vec{k} \right\}, \quad (30)$$

where the various terms denote central, spin-orbit and tensor components, respectively. In the above expression,  $\vec{k} = -i(\nabla_1 - \nabla_2)/2$  defines the relative momentum operator of the incoming nucleonic pair and  $\overleftarrow{k}$  its complex conjugate associated with the outgoing nucleonic pair acting on the wave-functions located to its left. The operator  $P_\sigma = (1 + \vec{\sigma}_1 \cdot \vec{\sigma}_2)/2$  is the spin-exchange operator that controls the relative strength of the  $S = 0$  and  $S = 1$  two-body spin channels for a given term in the two-body effective vertex.

Computing the expectation value of the Skyrme "interaction" in the state  $|\Phi\rangle$ , a functional of the same form as the one given in the first three lines of Eq. 20 is obtained. Such an apparent similarity between the EDF approach introduced in the previous section and the historical Skyrme "interaction" approach hides two important differences. In the latter case, and although it is not an intrinsic limitation of the "interaction" approach as it can be made more general than in Eqs. 27-30, only  $C_{qq}^{\rho\rho}$  do further depend on  $\rho_q(\vec{r})$ . Such a restricted dependence of the couplings on the matter density was considered at the time as the minimal extension beyond a strictly density-*independent* Skyrme vertex that could reasonably account for nuclear saturation and single-particle properties at the same time. Most importantly, the couplings of terms depending on time-odd densities (not shown in Eq. 20) are entirely fixed by those associated with terms depending on time-even densities (shown in Eq. 20) when the EDF is derived from the Skyrme "interaction". In the more general EDF approach, about half of such relationships can be relaxed while the other half remains as the result of symmetry constraints. Historically, the density-dependent term (Eq. 28) was introduced with  $\alpha = 1$  such that it was equivalent, in time-reversal invariant systems, to a three-body contact pseudo-potential. Eventually,  $\alpha$  was taken smaller than one to account for a realistic incompressibility of symmetric nuclear matter  $K_\infty$  and to provide reasonably good single-particle energies  $\{\varepsilon_i\}$  at the same time.

As for the  $T = 1$  pairing part of the EDF, it is traditionally derived as the average value of a DDDI made of the following two terms

$$\tilde{v}_{\text{cent}} = \tilde{t}_0(1 - P_\sigma)\delta(\vec{r}), \quad (31)$$

$$\tilde{v}_{\text{cent}}^\rho = \tilde{t}_3(1 - P_\sigma)\rho_0^\gamma(\vec{r})\delta(\vec{r}), \quad (32)$$

that are purely central and of S-wave character. Doing so provides a functional form similar to the last line of Eq. 20. For  $\tilde{t}_3 = 0$ , one refers to a *volume*-type pairing given that  $C_{qq}^{\tilde{\rho}\tilde{\rho}}$  is independent of the density. For

$\tilde{t}_3 = -\tilde{t}_0/\rho_{\text{sat}}$ , where  $\rho_{\text{sat}}$  is the saturation density of nuclear matter, one refers to a *surface*-type pairing as  $C_{qq}^{\tilde{\rho}\tilde{\rho}}$  is larger at the surface of the nucleus than in its volume. In between, one refers to a *mixed*-type pairing.

As will be discussed in Sec. IV, the connection between a local EDF of the Skyrme type and underlying NN and 3N interactions can be performed at the level of the EDF itself, not at the level of the Skyrme "interaction" that has in fact no physical meaning whatsoever. At the price of dealing with a very non-local energy functional, it becomes possible to consider an intermediate finite-range, non-local, energy- and density-dependent effective vertex that possesses the physical meaning of an in-medium interaction [179].

### E. Multi-reference extension

An exhaustive discussion as to why and how the SR-EDF method is extended to a multi-reference formalism (see Fig. 15) is beyond the scope of the present lectures. Historically, the MR-EDF implementation has been adapted from the projected Hartree-Fock-Bogoliubov and generator coordinate methods. In generic terms, the aim is to allow for (collective) fluctuations of the phase and magnitude of the order parameters associated with the symmetries broken at the SR level. Doing so, correlations associated with large amplitude collective motions complement static correlations incorporated at the SR level. Beyond including further ground-state correlations, excitations of the system corresponding to treated fluctuations are accessed and selection rules are recovered, which allows the computation of transition probabilities on a safe ground. Consequently, the MR extension is not only meant to refine the description of observable reasonably accounted for by SR calculations but also to extend the reach of the method as to which observable and nucleus can be safely compared to experiment (see Fig. 15). Many variants or approximations of it are also being implemented and extensively used, e.g. the quasi-particle random phase approximation or the Bohr Hamiltonian method [68]. The energy functional at play in full MR-EDF calculations depends on so-called *transition* density matrices constructed from all possible pairs of auxiliary product-states entering the MR set. For each such pair, the SR (diagonal) energy functional kernel must be extended to a non-diagonal energy kernel. This leads in general to non-trivial difficulties and to the necessity to use functionals containing integer powers of the density matrices only [120, 121, 156–159].

### F. Correlations

Given that the nuclear EDF method is empirical, the most delicate point consists of assessing with a certain rigor what correlations are actually accounted for, especially given that the method comes into two consecutive steps that must be implemented consistently. First, it is essential to understand that the SR-EDF approach does *not* reduce to a Hartree-Fock (HF) approximation when formulating the many-body problem in terms of vacuum NN plus 3N interactions. Otherwise, SR-EDF calculations could not even qualitatively, if not quantitatively, account for the equation of state of infinite nuclear matter [87, 88] or for doubly-magic nuclei [137, 138], as they do by construction. From the outset, correlations beyond HF are effectively built into  $\mathcal{E}[\rho, \kappa, \kappa^*]$  thanks to its flexible functional form and the fitting of its parameters to data. Such a fact makes improper to refer to SR-EDF calculations as representing "mean-field" or "Hartree-Fock" calculations as is often done.

Second, it is first essential to realize that the appropriate form of the functional must be discussed within the frame of spontaneous broken symmetries. The latter provide the most efficient way of grasping static collective correlations. Figure 16 displays the correlation energy incorporated in  $^{240}\text{Pu}$  and  $^{120}\text{Sn}$  ground-states energy through the spontaneous breaking of rotational and particle-number symmetries, respectively. Such symmetry breakings may account for up to 20 MeV correlation energy out of about 2 GeV binding energy, i.e. for about 2%, which is much larger than the targeted accuracy on nuclear masses. Such correlations could hardly be re-summed into a symmetry-conserving energy kernel, i.e. there would be little chance to describe at the same time doubly-magic, singly-magic and doubly open-shell nuclei using an energy functional that enforces particle-number and rotational symmetries. Indeed, static pairing and quadrupolar correlations increase and decrease significantly across a major shell, which makes difficult to mock them up through (conventional) functional terms that do not break symmetries.

Third, and as already mentioned, it is mandatory to treat the fluctuations of the order parameter of the broken symmetries when describing a finite quantum system. As shown in Fig. 16, doing so for angular momentum and particle number adds a few MeV binding to the ground-state energy of heavy nuclei. This is significant in view of the few hundreds keV targeted accuracy on nuclear masses and tend to improve on wrong patterns that exist at the SR-EDF level [180]. As discussed in Sec. IIE, the incorporation of such

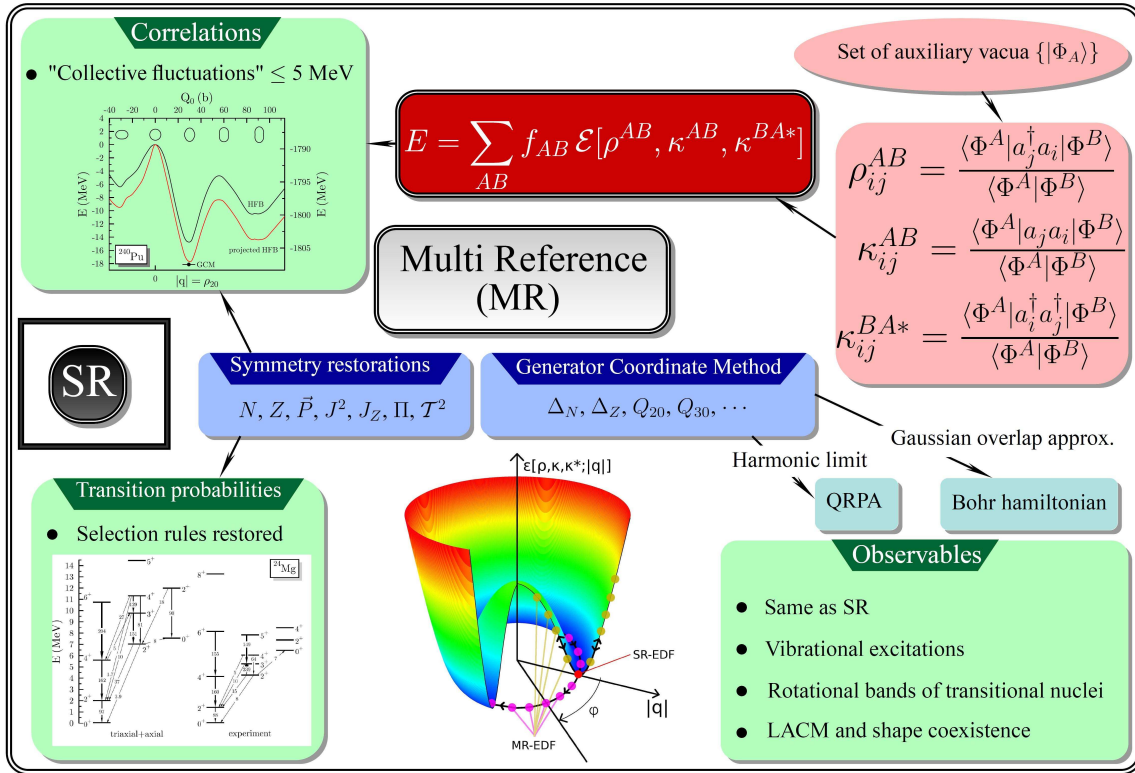


FIG. 15: (Color online) Schematic representation of the multi-reference implementation of the nuclear EDF method (encompassing the more limited single-reference implementation). The various ingredients of the method, e.g. the set of auxiliary states  $\{|\Phi_A\rangle\}$  from which the transition density matrices are computed, treated collective fluctuations, the restoration of symmetries and the associated recovering of selection rules, as well as the type of correlations that are accounted for, are indicated. Observable that are accessible at the MR level are also listed.

correlations within the MR-EDF implementation is characterized by the extension of the diagonal energy kernel  $\mathcal{E}[\rho, \kappa, \kappa^*]$  into a more general non-diagonal energy kernel that depends on transition density matrices. Still, one may ask whether or not such correlations that vary quickly with the filling of nuclear shells may be re-summed directly into the diagonal (symmetry-breaking) energy kernel  $\mathcal{E}[\rho, \kappa, \kappa^*]$  by simply using a more elaborated functional form. As a matter of fact, methods approximating correlations from symmetry restorations in this way, e.g. Lipkin [181, 182] or Kamlah [183, 184] methods, do exist. While it is likely that the strongly broken translational symmetry can be safely treated through such approximate projection methods<sup>10</sup>, whether the same is true for weakly broken symmetries, e.g. particle number symmetry in all but doubly-magic nuclei or rotational symmetry in transitional nuclei, is still unclear as of today.

In summary, the empirical EDF method relies on a qualitative decoupling of different categories of correlations at play, i.e. on the different scales that characterize them (see Tab. II), and on the fact that correlations that vary quickly with the filling of nuclear shells are explicitly accounted for through the breaking of symmetries and the quantum collective fluctuations of their associated order parameters. Until a completely non-empirical design of the SR and MR EDF implementation exists, such a decoupling can only be approximate and the separated account of various categories of correlations subject to trial and error. In that respect, it is worth noting that until very recently [130] no parametrization of the basic energy kernel  $\mathcal{E}[\rho, \kappa, \kappa^*]$  had been fitted on the basis of MR calculations, i.e. including correlations associated with quantum collective fluctuations. Such a procedure is to be systematized in the future, not only to avoid the obvious double counting of correlations that exist when employing in MR calculations an energy functional fitted on data at the SR level,

<sup>10</sup> Such a statement is to be taken with a grain of salt for rather light nuclei [185].

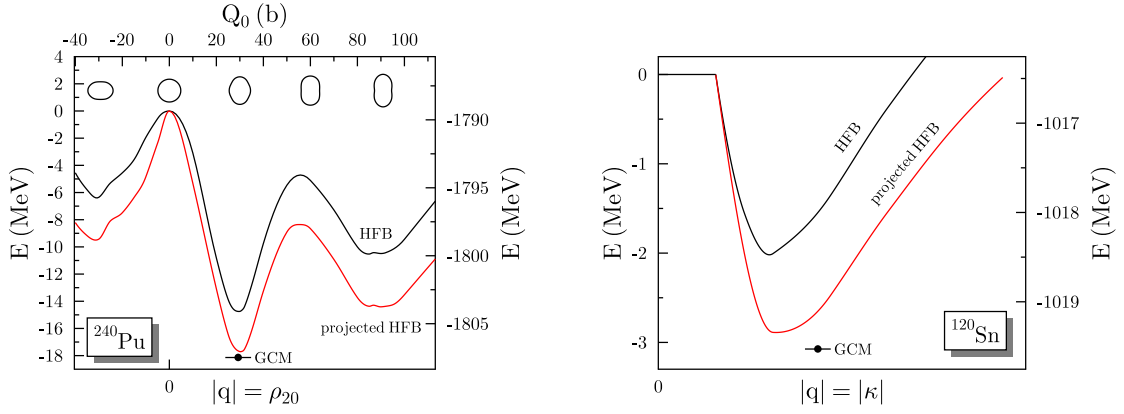


FIG. 16: (Color online) Energy gain from (i) spontaneous symmetry breaking and (ii) symmetry restoration as a function of the magnitude of the order parameter  $q$ , followed by (iii) the mixing along that collective coordinate. Left : breaking and restoration of rotational symmetry in the ground state of  $^{240}\text{Pu}$  as a function of the axial quadrupole moment of the single-nucleon density distribution, followed by the mixing along the latter collective coordinate (adapted from Ref. [186]). Right : breaking and restoration of neutron-number symmetry in the ground state of  $^{120}\text{Sn}$  as a function of the norm of the anomalous pair density, followed by the mixing along the latter collective coordinate. The right vertical axis indicate the absolute binding energy. Adapted from Ref. [187].

but also to take into account the impact of such correlations on the fitted parameters.

TAB. II: Schematic classification of correlation energies as they naturally appear in nuclear EDF methods. The quantity  $A_{\text{val}}$  denotes the number of valence nucleons while  $G_{\text{deg}}$  characterizes the degeneracy of the valence major shell.

Correlations	Treatment	Scale	Vary with
Bulk	Summed into EDF kernel	$\sim 8A$ MeV	$A$
Static collective	Non-zero order parameter $q$	$\sim 25$ MeV	$A_{\text{val}}, G_{\text{deg}}$
Dynamical collective	Fluctuations of $q$	$\sim 5$ MeV	$A_{\text{val}}, G_{\text{deg}}$

### G. Performances and limitations

It is an essential and constant effort made by practitioners to gauge performances and limitations of existing parameterizations of the nuclear EDF kernel, at both the SR and MR levels. Unfortunately, providing an exhaustive and quantitative account of such an analysis is far beyond the scope of the present lectures. Consequently, we limit ourselves to a schematic and qualitative discussion based on a few observable computed at the SR level.

Roughly speaking, modern parameterizations of existing EDFs, e.g. Skyrme or Gogny, provide a fair description of bulk properties (ground-state mass, charge radius, "deformation", various separation energies, etc), as well as of certain spectroscopic properties, of known nuclei [168]. Figure 17 displays nuclear ground-state binding energies and charge radii along three different isotopes chains. Experimental data are compared to results of SR-EDF calculations restricted to spherical symmetry and obtained using SkP [166] and SLy4 [71] parameterizations of the Skyrme EDF, complemented with a mixed-type pairing. The results for Sn and Pb isotopes provide an idea of the quality of the agreement that can be obtained with data. As a matter of fact, the best root-mean-square deviation relative to 2149 measured masses is (i) about 1.5 MeV at the SR level [188] and (ii) about 800 keV at the MR level [130]. Figure 17 also exemplifies the importance of static quadrupole correlations that are essential to obtain a fair description of doubly-open-shell nuclei. Indeed, the restriction of the calculation to spherical symmetry does not lead to the same qualitative and quantitative agreement with data for doubly-open-shell Dy nuclei than for semi-magic Sn and Pb isotopes. Given the scale used for masses in Fig. 17, it is worth noting that such a difference is very significant. When allowing for it, rotational symmetry breaks in the SR calculation of Dy isotopes, which brings the agreement with data on the same

qualitative level as the one seen for Sn and Pb isotopes in Fig. 17. Including quadrupole fluctuations further improve the agreement with data [180].

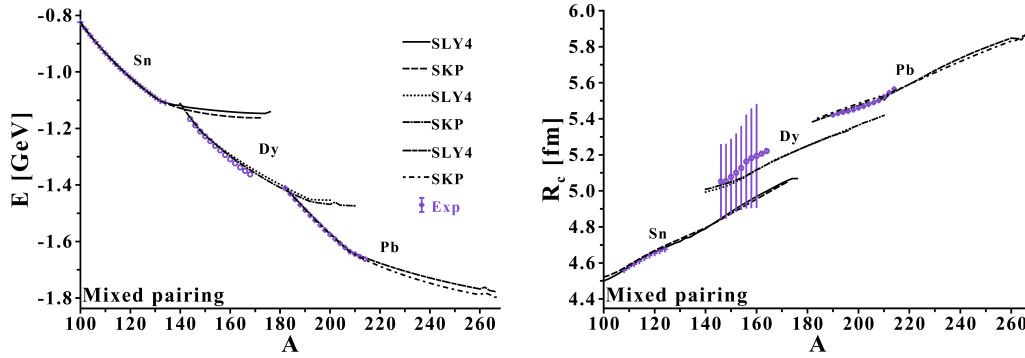


FIG. 17: (Color online) SR-EDF calculations of Sn, Dy and Pb isotopic chains in spherical symmetry using SKP [166] and SLY4 [71] parameterizations of the Skyrme EDF complemented with a mixed-type pairing. Left : absolute binding energies. Right : Charge radii. Taken from Ref. [189].

Besides the satisfactory phenomenology provided for known nuclei, existing parameterizations of the EDF lack predictive power away from available data and a true spectroscopic quality. This is first exemplify in Fig. 18 where predictions for binding energies, neutron pairing-gaps and two-neutron separation energies of tin isotopes are shown for various combinations of Skyrme and DDDI functionals, knowing that the latter is adjusted consistently with the former to reproduce the pairing gap (center plot) in  $^{120}\text{Sn}$ . While the results are consistent with each other and with existing data, predictions obtained with various parameterizations of (nearly) the same functional form display a typical "asymptotic freedom" away from known data, in particular as one crosses  $N = 82$ , i.e. as one jumps into the next major shell where the parameterizations have not been constrained. Such a behavior is seen for most observable and nuclear isotopic/isotonic chains and can thus be considered as archetypal of the situation presently encountered with nuclear EDF methods.

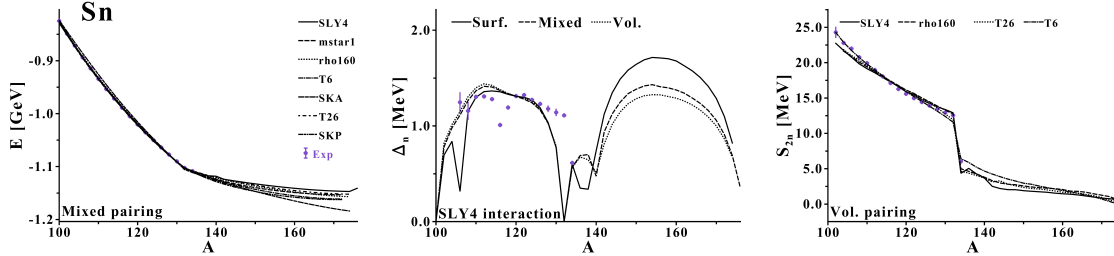


FIG. 18: (Color online) SR-EDF calculations of Sn isotopes in spherical symmetry using various combinations of SLY4 [71], mstar1 [72], rho160 [72], T6 [73], SKa [74], T26 [75], SkP [166] Skyrme parameterizations and volume-, mixed- and surface-type pairing. Left : absolute binding energies. Middle : neutron theoretical pairing gap. Right : Two-neutron separation energies. Taken from Ref. [189].

In fact, the most stringent test regarding the quality of existing EDFs relates to spectroscopic features. Although single-particle energies  $\{\varepsilon_i\}$  extracted from Eq. 7 do not provide the most advanced estimate of one-nucleon separation energies through EDF methods (see Secs. II B 3 and II B 4), any spectroscopic data is strongly influenced by such an underlying single-particle shell structure. Figure 19 provides the distribution of  $\Delta\varepsilon_i = \varepsilon_i - \varepsilon_i^{\text{exp}}$  for three different (refitted) Skyrme parameterizations, where  $\varepsilon_i^{\text{exp}}$  denotes 58 separation energies of good single-particle character around doubly-magic nuclei [125]. The results demonstrate that current Skyrme functionals poorly predict the location of known spherical shells such that existing functional forms do not allow the lowering of the root-mean-square deviation below about 1 MeV<sup>11</sup>. Given the numerous

<sup>11</sup> Such a systematic error is larger than the uncertainty related to associating  $\varepsilon_i$  from the SR-EDF calculation to separation energies.

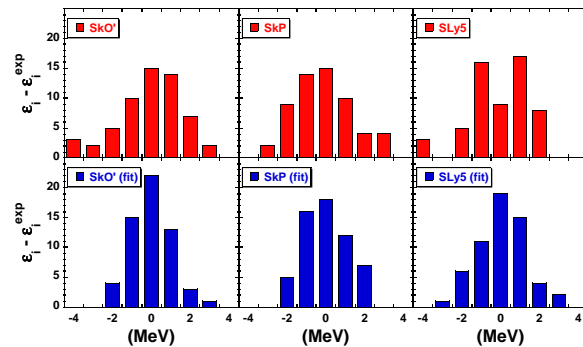


FIG. 19: (Color online) Histograms of residuals  $\Delta\varepsilon_i = \varepsilon_i - \varepsilon_i^{\text{exp}}$  for standard (upper panels) and refitted (lower panels) Skyrme parameterizations SkO' [195], SkP [166], and SLy5 [71]. Taken from Ref. [125].

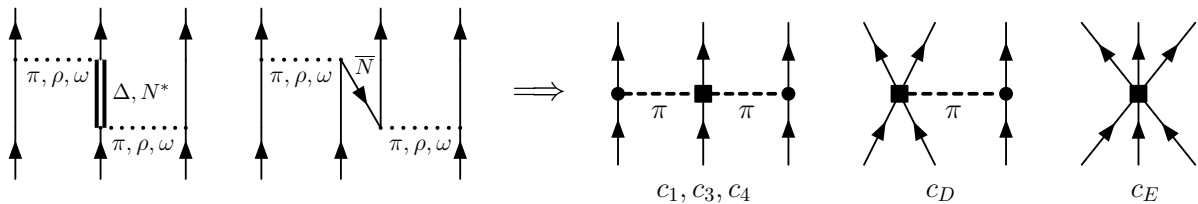


FIG. 20: Diagrams representing an amplitude between an initial (entering three lines) and a final (leaving three lines) three-body state. Time flows from bottom to top. Left : diagrams are reducible to successive two-body interactions. Right : diagrams contain an interaction involving the three nucleons at the same time. Going from the left panel to the right panel illustrates how eliminating degrees of freedom leads naturally to the existence of many-body forces ; e.g. three-body forces in the present case. Taken from Ref. [90].

on-going investigations of the evolution of nuclear shells towards neutron-rich or superheavy nuclei, such a limitation is critical. Providing results of spectroscopic quality constitutes the most immediate challenge for theorists designing parameterizations of the nuclear EDF. As a matter of fact, several groups currently work on empirically improving the analytical form and the fitting of energy functionals, e.g. see Refs. [127, 190] for recent attempts to pin down the isovector content of local pairing functionals, Refs. [75, 126, 191–194] for investigations on the role of tensors terms in the Skyrme EDF and Ref. [129] for the recent derivation of the local Skyrme-type EDF to sixth-order in derivatives.

Given that available experimental data do not constrain unambiguously all non-trivial characteristics of the nuclear EDF, it is interesting to complement the phenomenology at play with an approach that relies less on trial-and-error and fitting to data. Our ultimate objective is thus to connect  $\mathcal{E}[\rho, \kappa^*, \kappa]$ , as well as the effective vertices  $v^{ph}$  and  $v^{pp}$ , in a consistent and explicit fashion to vacuum NN and 3N interactions. It is the objective of Sec. IV to discuss the path towards non-empirical EDF parameterizations explicitly linked to such vacuum interactions. So-called *low-momentum* vacuum interactions are instrumental in that respect as will be made clear in Sec. IV B. Consequently, we first dedicate Sec. III to introducing low-momentum interactions generated from renormalization group techniques.

### III. LOW-MOMENTUM INTERACTIONS FROM RENORMALIZATION GROUP METHODS

The present section briefly outlines the ideas that found low-momentum interactions generated from renormalization group methods. For a thorough review of the subject, we refer the interested reader to Ref. [90].

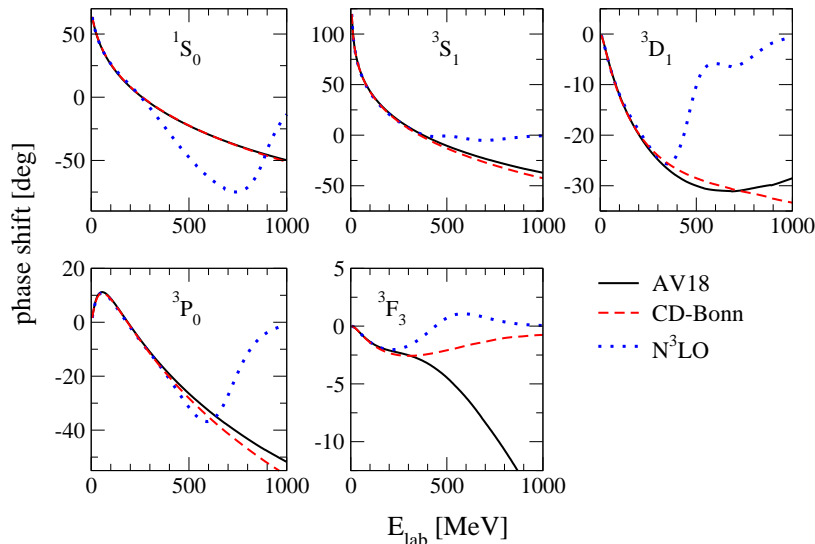


FIG. 21: (Color online) Phase shifts for the Argonne V18 [1], CD-Bonn [78] and Chiral  $N^3\text{LO}$  [196] potentials in selected channels. The phase shifts after the RG evolution from each initial potential agree for all values of the SRG scale to within the widths of the lines at all energies. Taken from Ref. [197].

### A. Generalities

The first essential observation relates to the fact that any nuclear structure<sup>12</sup> Hamiltonian  $H$  is a low-energy effective theory of QCD. It is unavoidable in such a context that certain underlying, i.e. high-energy, degrees of freedom are omitted when designing the Hamiltonian. Such an omission translates into the fact that  $H$  is characterized, even though it is often implicit, by an *intrinsic resolution scale*  $\Lambda$  that separates momenta/energies/degrees-of-freedom whose dynamics is treated explicitly from those that are included only implicitly, i.e. which are *renormalized* or *integrated out* in the modeling of  $H(\Lambda)$ .

The second important observation relates to the fact that integrating out degrees of freedom necessarily translates into the presence of multi-body forces in  $H(\Lambda)$ . This is exemplified in Fig. 20 that illustrates how the elimination of nucleonic excitations or anti-nucleon components, as well as mesons whose masses are larger than the cut-off scale  $\Lambda$ , transforms diagrams involving repeated two-body interactions into a set of irreducible three-nucleon vertices. As a matter of fact, there should/could exist up to  $A$ -body forces when applying  $H(\Lambda)$  to a  $A$ -body system. Of course, the relative importance of the various components of  $H(\Lambda)$  remains to be qualified at each given  $\Lambda$ . Eventually, any given model of the Hamiltonian governing the dynamics of point-like nucleons can be written under the generic form

$$H(\Lambda) \equiv T + V^{NN}(\Lambda) + V^{3N}(\Lambda) + \dots, \quad (33)$$

where  $\Lambda$  characterizes the high-momentum/short-distance physics whose details are not modeled explicitly and the fact that each individual component of  $H(\Lambda)$  depends on it. In a sense, there is no such thing as *the* nuclear Hamiltonian. As will become clear below, the fact that interaction vertices or the Hamiltonian itself depend on the resolution scale simply says that such quantities are intrinsically *non-observable*.

The third key observation relates to the fact that existing models of  $H(\Lambda)$ , i.e. so-called high-precision conventional potentials (e.g. AV18 [1], CD-Bonn [78]...) or chiral potentials [92, 94, 199, 200], are characterized by a rather high intrinsic resolution scale in the sense that  $\Lambda \gg \Lambda_{\text{data}}$ , where  $\Lambda_{\text{data}} \approx 2.1 \text{ fm}^{-1}$  typically corresponds to the energy  $E_{\text{lab}} \approx 350 \text{ MeV}$  up to which unambiguous scattering data are available to adjust  $V^{NN}(\Lambda)$ . Consequently, existing NN interaction models reproduce scattering phase-shifts in a similar way up to  $\Lambda_{\text{data}}$  but diverge significantly from each other above that value, as exemplified in Fig. 21. The

<sup>12</sup> We qualify in this way any Hamiltonian governing the dynamics of point-like nucleons, i.e. whose interaction vertices correspond to scattering amplitudes between incoming and outgoing nucleonic states.

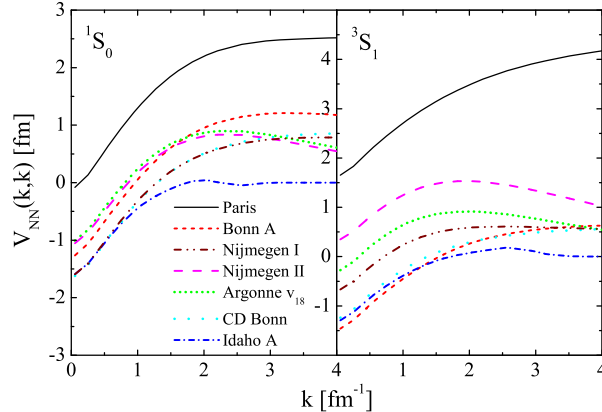


FIG. 22: (Color online) Momentum-space matrix elements of  $V^{NN}$  for various potentials in the  $^1S_0$  and  $^3S_1$  channels. Taken from Ref. [198].

lack of constrained beyond  $E_{\text{lab}} \approx 350$  MeV translates into potentials displaying different short-range/high-momentum physics as demonstrated in Fig. 22. Essentially, the short-range modeling of conventional nuclear interactions is uncontrolled and arbitrary. Such a freedom may lead in some cases to impractical features, e.g. requiring that the potential is local necessitates a strong repulsive core, which in turn implicitly relates to choosing a (very) large  $\Lambda = \Lambda_{\text{high}}$ .

One may be puzzled by the essentially arbitrary modeling of the short-range/high-momentum part of the Hamiltonian. As a matter of fact, it fits with effective field theory considerations telling us that, whenever interested in low-energy observable below a certain scale  $\Lambda_{\text{physics}}$ , the detailed modeling of high-energy virtual processes characterized by  $k \gg \Lambda_{\text{physics}}$  is irrelevant and cannot influence the result. This can in fact be used (i) to choose a practically advantageous resolution scale when building  $H(\Lambda)$  and (ii) to select the simplest model accounting for the integrated out short-distance/high-momentum physics. This is schematically illustrated in Fig. 23. Such ideas precisely underly potential models based on  $\chi$ -EFT that select pions and nucleons as dynamical degrees of freedom below  $\Lambda_\chi \approx 500$  MeV  $\lesssim m_\rho$  and model the excluded physics through contact and derivative-contact terms with scale-dependent coupling constants [92, 94, 199, 200]. Diagrams in the Lagrangian are organized in powers of  $Q/\Lambda_\chi$ . At a given order this includes contributions from one- or multi-pion exchanges and contact interactions whose couplings are fit to low-energy data for each  $\Lambda_\chi$ . There are natural sizes to many-body forces that are made manifest in the EFT power counting and which explain the phenomenological hierarchy between two-, three-, ..., A-body forces. We refer to E. Epelbaum's lectures for details on  $\chi$ -EFT and chiral potentials [80].

As just discussed, details of the high-energy physics that are *relevant* to the computation of low-energy observable can be captured by scale-dependent coupling constants in the low-energy Hamiltonian [201]. However, this does not necessarily mean that high- and low-energy physics are automatically decoupled in  $H(\Lambda)$ . One may further use the freedom offered in the modeling of the *irrelevant* high-energy physics to investigate the possibility to produce such a decoupling in view of generating *soft* Hamiltonians. Renormalization-group transformations provide an efficient tool to *evolve* nuclear Hamiltonians such that they eventually display a decoupling between high- and low-energy modes. As a rule, this must be implemented in such a way that the long-range physics encoded in the initial Hamiltonian is not distorted, e.g. in such a way that  $\pi$ -exchanges from  $\chi$ -EFT are left untouched.

In the nuclear context, two different types of RG transformations have been used to evolve interaction potentials [90], i.e. (i) the  $V_{\text{low}k}$  approach that corresponds to a *non-unitary* transformation of  $H(\Lambda)$  and (ii) the similarity renormalization group (SRG) method that corresponds to a *unitary* transformation of  $H(\Lambda)$ . We briefly discuss the  $V_{\text{low}k}$  approach to evolve  $V^{NN}$  and only display results obtained from the SRG method. Although we do sketch a few details about the SRG method when discussing the additional evolution of  $V^{3N}$ , we refer the interested reader to Ref. [90] for a thorough discussion about this particular method.

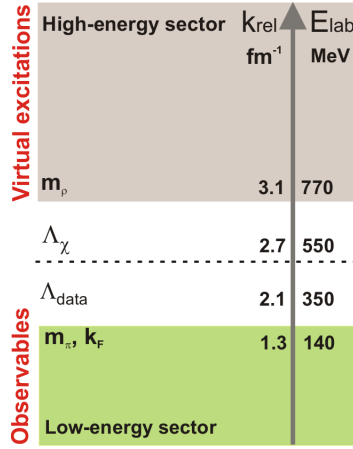


FIG. 23: (Color online) Natural separation of scales in hadron spectroscopy. From the point of view of low-energy nuclear physics, such a separation of scales leads to the definition of a low-energy sector of interest that is rather well separated from the high-energy sector whose details are irrelevant.

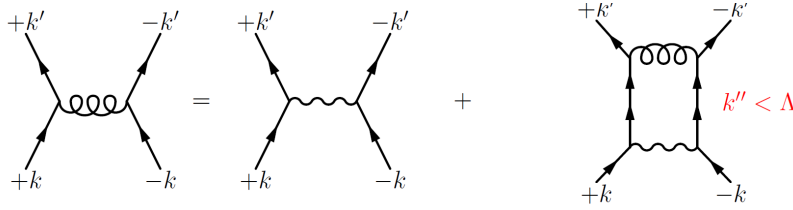


FIG. 24: (Color online) Diagrammatic representation of the regularized Lipmann-Schwinger equation (Eq. 34) from which the scattering T-matrix is obtained.

### B. Low-momentum interactions in the NN sector

Inside a nucleus, typical nucleonic momenta are  $Q \sim k_F \sim m_\pi \sim 1.3 \text{ fm}^{-1}$ . Imposing a sharp cutoff  $\Lambda$  on explicitly included relative momenta is the most direct way to limit the resolution encoded in  $V^{NN}$ . In order to incorporate the relevant details from excluded high-momentum modes, the latter must be integrated out rather than simply truncated. The idea of the  $V_{\text{low}k}$  approach is to run down the resolution scale  $\Lambda$  to about  $\Lambda_{\text{data}} \sim 2.1 \text{ fm}^{-1}$  in order to decouple unconstrained high- $k$  modes built in an input Hamiltonian  $H(\Lambda_{\text{high}})$  from low-momentum ones. Integrating out the physics associated with momentum modes  $k > \Lambda$  translates into doing so for the short-distance physics corresponding to  $r \lesssim \hbar/\Lambda$ . Such a modification of the resolution scale is a relatively small (but significant) evolution for chiral potentials and a large one for phenomenological potentials. In doing so, the truncation error, e.g. based on the  $\chi$ -EFT power counting, of the original Hamiltonian is maintained. However, and as will be seen in Sec. III D, the RG transformation necessarily generates multi-body forces, even if  $H(\Lambda_{\text{high}})$  were to contain  $V^{NN}(\Lambda_{\text{high}})$  only (which is not the case).

Within the  $V_{\text{low}k}$  approach the RG evolution proceeds by demanding that the (half-on-shell) T matrix computed from  $V^{NN}(\Lambda_{\text{high}})$  through the Lipmann-Schwinger equation (see Fig. 24)

$$T_L^{JST}(k, k'; E; \Lambda) = \frac{m}{\hbar^2} V_{LL}^{JST}(k, k'; \Lambda) + \frac{2}{\pi} \mathcal{P} \int_0^\Lambda k''^2 dk'' \frac{V_{LL}^{JST}(k, k''; \Lambda) T_L^{JST}(k'', k'; E; \Lambda)}{E - \hbar^2 k''^2/m}, \quad (34)$$

is unchanged in each partial wave as  $\Lambda$  is lowered for  $k, k' \leq \Lambda$ , i.e.

$$\frac{dT_L^{JST}(k, k'; \hbar^2 k^2/m; \Lambda)}{d\Lambda} = 0 \quad \text{for } k, k' \leq \Lambda. \quad (35)$$

Such a condition provides the RG flow equation for the NN potential  $V_{LL}^{JST}(k, k'; \Lambda)$  which, for an uncoupled partial-wave, reads as

$$\frac{d}{d\Lambda} V_{LL}^{JST}(k', k; \Lambda) = \frac{2}{\pi} \frac{V_{LL}^{JST}(k', k; \Lambda) T_{LL}^{JST}(\Lambda, k; \hbar^2 \Lambda^2/2m; \Lambda)}{1 - (k/\Lambda)^2}, \quad (36)$$

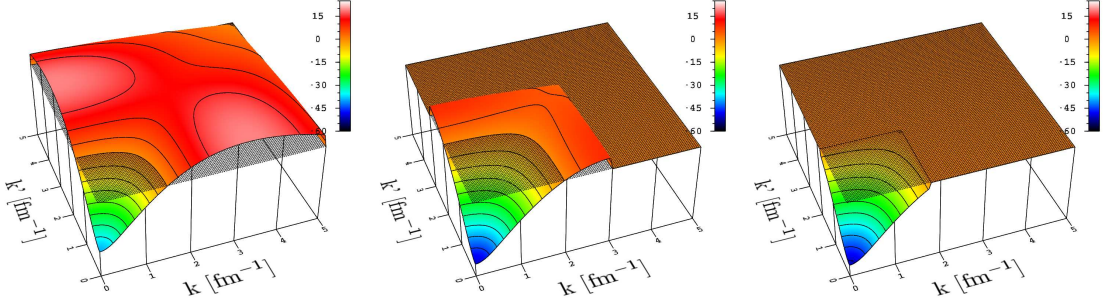


FIG. 25: (Color online) Momentum-space matrix elements of  $V^{NN}(\Lambda)$  in the  $^1S_0$  partial-wave computed from the initial Argonne V18 [1] potential at  $\Lambda = 5.0 \text{ fm}^{-1}$  (left),  $3.0 \text{ fm}^{-1}$  (middle) and  $1.8 \text{ fm}^{-1}$  (right).

for  $k, k' \leq \Lambda$  and is to be solved with the initial condition that  $V_{LL}^{JST}(k, k'; \Lambda_{\text{init}}) \equiv V_{LL}^{JST}(k, k'; \Lambda_{\text{high}})$ . Such a flow does not correspond to a naive cut of the matrix elements beyond  $\Lambda$ . Still, it is a non-unitary transformation over the two-body Hilbert space such that non-zero matrix elements only persist for  $k, k' \leq \Lambda$  where the physics is preserved.

Given that scattering phase-shifts are obtained (uncoupled partial-wave) from the "fully-on-shell" T-matrix

$$\tan \delta_L^{JST}(k; \Lambda) \equiv -k T_L^{JST}(k, k; \hbar^2 k^2 / m; \Lambda), \quad (37)$$

it is clear that such phase shifts are left invariant by the flow equation, just as the deuteron binding energy  $E_{\text{deut.}}$ . Note that keeping  $\delta_L^{JST}(k; \Lambda)$  independent of  $\Lambda$  necessarily implies that the interaction is not, i.e.  $dV^{NN}(k, k'; \Lambda)/d\Lambda \neq 0$ . It is not a problem given that, while the former quantity is observable, the latter is not.

Figure 25 exemplifies such a lowering of the resolution scale  $\Lambda$  in the  $^1S_0$  partial-wave of the NN interaction, starting from the Argonne V18 potential as an initial condition. In practice, the evolution is not done by solving the differential equation 36 but rather by performing a Lee-Suzuki transformation [202, 203]. Both approaches are equivalent. It is clear from Fig. 25 that  $V^{NN}(k', k; \Lambda)$  changes as  $\Lambda$  is lowered. This is not at all problematic given that, while  $\langle \Psi(\Lambda) | H(\Lambda) | \Psi(\Lambda) \rangle$  is typically observable,  $H(\Lambda)$  and  $|\Psi(\Lambda)\rangle$  are not. The two main modifications observed as  $\Lambda$  is decreased are that (i) strong off-diagonal matrix elements associated with the short-range repulsive core of the initial potential are tamed down, i.e. low- and high- $k$  modes are being decoupled and that (ii) the relevant features of the initial matrix elements beyond  $\Lambda$  are renormalized onto those located at  $k, k' \leq \Lambda$  that become more attractive. Eventually, one evolves towards a so-called *soft low-momentum* NN interaction  $V_{\text{low}k}$ . Notice that such low-momentum interactions are sometimes mistakenly said to be phenomenological interactions or regarded as an alternative to EFT interactions. Rather they constitute an entire class of potentials associated with an initial Hamiltonian.

Although the NN potential changes with  $\Lambda$ , NN observable are invariant by construction. As discussed in connection with Eq. 37 and as exemplifies by Fig. 26 in the case of the CD Bonn potential [205], phase shifts  $\delta_L^{JST}(k)$  below  $\Lambda$  are preserved by the RG evolution in all partial waves. Complementarily, the energy of the only bound two-nucleon state, i.e. the deuteron, remains invariant as  $\Lambda$  is lowered as illustrated in Tab. III.

TAB. III: Deuteron binding energy computed from AV18 and the low-momentum interaction evolved from it. Taken from Ref. [206].

$V^{NN}$	$E_{\text{deut.}} [\text{MeV}]$
AV18	-2.2247
$V_{\text{low}k}(2.1)$	-2.2247

An interesting question relates to the dependence of low-momentum interactions on the initial condition of the flow  $V^{NN}(\Lambda_{\text{init}})$ . As illustrated by Fig. 27 for  $^3S_1$  partial-wave,  $V_{\text{low}k}$  interactions generated from different potentials  $V^{NN}(\Lambda_{\text{high}})$  are found to be quantitatively similar for  $\Lambda \approx 2.1 \text{ fm}^{-1}$ . One talks about the *universality* of  $V_{\text{low}k}$  in the sense that the resulting low-momentum characteristics are largely independent on the high-momentum details encoded in the initial potentials; i.e. the model dependence of the latter has been *screened out*. Such a collapse to universal low-momentum interactions is attributed to the long-range pion physics common to all initial potentials and to their similar description of low-energy NN observable up to the resolution scale.

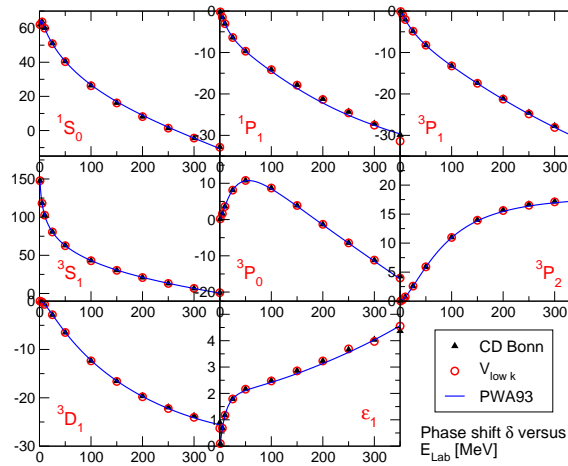


FIG. 26: (Color online) S-wave (singlet and triplet with mixing parameter) and P-wave phase shifts of  $V_{\text{low}k}$  for a cutoff  $\Lambda = 2.1 \text{ fm}^{-1}$  compared to the input CD Bonn potential [78]. Results of the multi-energy phase shift analysis (PWA93) of the Nijmegen group are also shown [204]. Taken from Ref. [198].

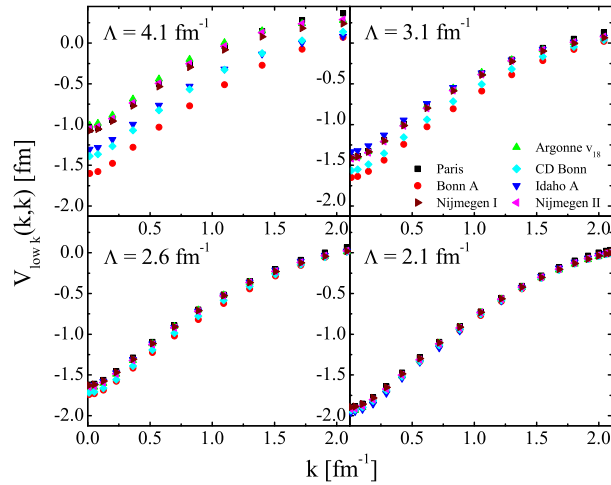


FIG. 27: (Color online) The collapse of the diagonal momentum-space matrix elements of  $V_{\text{low}k}$  as the cutoff is lowered to  $\Lambda = 2.1 \text{ fm}^{-1}$  in the  $^1S_0$  partial wave. Taken from Ref. [206]

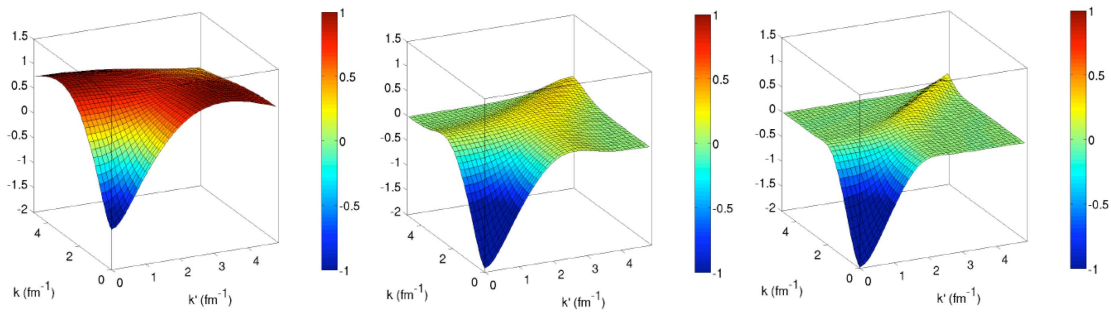


FIG. 28: (Color online) Momentum-space matrix elements of  $V^{NN}(\Lambda)$  in the  $^1S_0$  partial-wave obtained from the SRG evolution of the initial  $N^3\text{LO}$  (500) Chiral potential [196] down to  $\Lambda = 10.0 \text{ fm}^{-1}$  (left),  $3.0 \text{ fm}^{-1}$  (middle) and  $2.0 \text{ fm}^{-1}$  (right). Taken from Ref. [207].

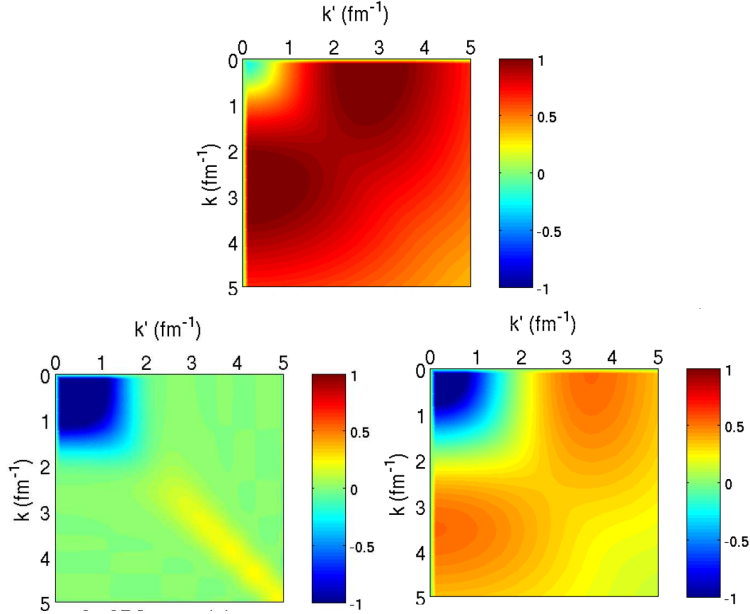


FIG. 29: (Color online) Momentum-space matrix elements in the  $^3S_1$  partial-wave. Top : Argonne V18 [1] potential. Bottom left : potential evolved from Argonne V18 through SRG down to the resolution scale of  $2.0 \text{ fm}^{-1}$ . Bottom right : G-matrix computed from Argonne V18. The qualitative features of the G matrix do not depend on the particular choice of starting energy at which it is computed. Adapted from Ref. [90].

A similar universal behavior and decoupling is found for the low-momentum part of interactions evolved through the *unitary* SRG method rather than through the non-unitary  $V_{\text{low}k}$  approach. The result of such a SRG evolution is displayed in Fig. 28 for the  $^1S_0$  partial-wave of the initial  $N^3\text{LO}$  (500) Chiral potential [196]. The low-momentum part of the resulting potential is essentially identical to  $V_{\text{low}k}$ . The only difference with the latter resides in the appearance of a diagonal band of non-zero matrix elements at high  $k \approx k'$  that is necessary to maintain unitarity over the original two-body Hilbert space, e.g. to keep phase-shifts  $\delta_L^{JST}(k)$  unchanged at *all*  $k$ . Most importantly, the decoupling of high- and low- $k$  modes is also achieved with the SRG approach as is clearly seen in Fig. 28.

To terminate the brief introduction of low-momentum interactions, let us mention that RG methods discussed here to renormalize the short-range/high-momentum physics are *not* to be confused with the Brueckner G-matrix approach [139, 208]. While  $V_{\text{low}k}$  denotes a class of *energy-independent vacuum* interactions, the G-matrix corresponds to an *energy-dependent in-medium* vertex. Most importantly, and as shown in Fig. 29, while  $V_{\text{low}k}$  achieves a decoupling between high- and low- $k$  modes, the G-matrix does not as it still displays large positive off-diagonal matrix elements that couple such modes. As a matter of fact, the G-matrix remains "hard" enough that the many-body energy cannot be expanded in powers of it, i.e. one must rely on the non-perturbative hole-line expansion [209–211].

### C. Advantages for light-nuclei calculations

Given that observable like  $\delta_L^{JST}(k)$  and  $E_{\text{deut.}}$  remain invariant under the RG flow, one may wonder about the utility of such a procedure. Beside providing a deeper understanding of the (non-absolute) nature of the nuclear Hamiltonian, RG methods exploit the scale dependence of non-observable quantities, e.g. correlations in the wave function, to provide technically simpler many-body calculations of *scale-independent* observable. This is achieved by working with a convenient/physically-sound resolution scale  $\Lambda_{\text{low}}$ . Although the introduction of RG transformations may seem formal at first, their primer interest is actually of very practical nature.

More specifically, the evolution of phenomenological or chiral EFT interactions to lower resolution and the associated decoupling of high- and low- $k$  modes are beneficial as they weaken or largely eliminate sources of non-perturbative behavior coming from the strong short-range central repulsion and the strong short-range tensor force. Eventually, lower cutoffs require smaller bases in many-body calculations, leading to improved

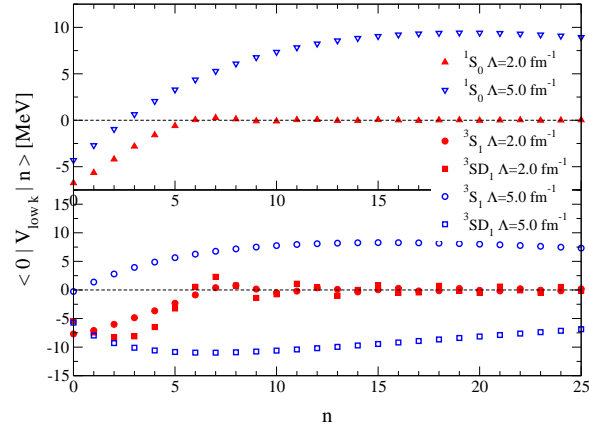


FIG. 30: (Color online) Relative harmonic-oscillator matrix elements  $\langle n' = 0 | V_{\text{low}k} | n \rangle$  versus radial quantum number  $n$  for RG scales  $\Lambda = 2.0 \text{ fm}^{-1}$  and  $\Lambda = 5.0 \text{ fm}^{-1}$ . Results are shown for the S-wave matrix elements. In both cases  $V_{\text{low}k}$  is obtained from the Argonne V18 potential [1] and  $\hbar\omega = 14 \text{ MeV}$ . Taken

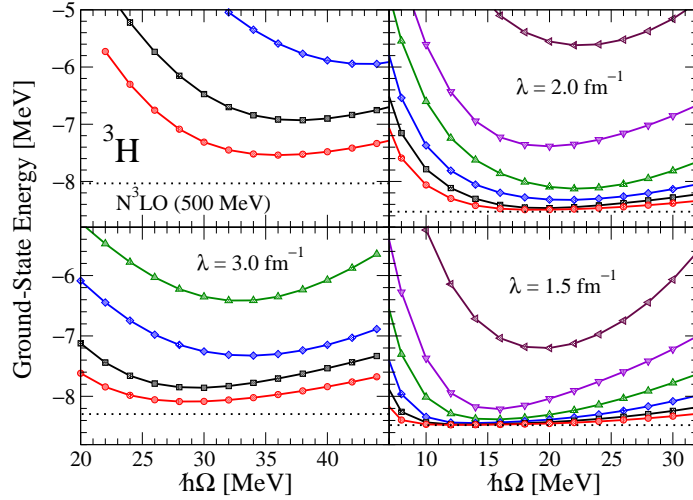


FIG. 31: (Color online) Ground-state energy of the triton as a function of  $\hbar\Omega$  at four different values of the SRG scale ( $\infty, 3, 2, 1.5 \text{ fm}^{-1}$ ). The initial potential is the 500 MeV  $N^3\text{LO}$  NN-only potential from Ref. [196]. The different lines correspond to results obtained using various (many-body) basis sizes, i.e. from  $N_{\text{max}} = 2$  to  $N_{\text{max}} = 12$ . The dotted lines show fully converged energies from independent  $N_{\text{max}} = 48$  calculations using a code from Ref. [213]. Taken from Ref. [214].

convergence for finite-nuclei investigations. Given that the plane-wave basis is not the most convenient basis to work with when computing finite-nuclei properties, Fig. 30 demonstrates for two different partial-waves that lowering the resolution scale from 5 to  $2 \text{ fm}^{-1}$  does also eliminate the coupling between low-lying and high-lying configurations of a harmonic oscillator basis.

The above statements are now exemplified through no-core shell model calculations of the triton  ${}^3\text{H}$ . Figure 31 provides the convergence of the triton binding energy computed from a  $N^3\text{LO}$  chiral potential and the SRG interaction evolved from it at various  $\lambda$  values. The binding energy is displayed as a function of the harmonic oscillator parameter  $\hbar\Omega$  for different (many-body) basis sizes ( $N_{\text{max}}$ ). One sees that the calculation is converged for a much smaller basis when  $\lambda$  is decreased. Eventually, this leads to the promise of computing heavier nuclei more easily. Looking closer at Fig. 31 though, one notices that converged values of  $E_{3\text{H}}$  are actually different in the various calculations. One may wonder whether this contradicts the fact that physical observable should be scale dependent? We address this question in the following subsection.

### D. Low-momentum interactions in the 3N sector

The key point is that an observable such as  $\langle \Psi^A(\Lambda) | H(\Lambda) | \Psi^A(\Lambda) \rangle$  of the A-body system is scale independent only if (i) many-body forces  $V^{3N}, \dots, V^{AN}$  that are originally present or generated through the RG evolution are kept in the A-body calculation and if (ii) the A-body problem is solved exactly. In other words, any scale dependence of an observable, e.g.  $\partial_\Lambda \langle \Psi(\Lambda) | H(\Lambda) | \Psi(\Lambda) \rangle \neq 0$ , signals the omission of non-negligible many-body forces and/or an incomplete many-body calculation.

In the previous example, the convergence of the NSCM calculation can be considered as achieved such that the origin of the scale dependence of  $E_{3\text{H}}$  can be traced back to the omission of  $V^{3N}$  induced by the RG evolution<sup>13</sup>. Indeed, it is essential to understand that any RG transformation necessarily generates many-body forces, even though one starts from a Hamiltonian  $H(\Lambda_{\text{init}})$  that contains a NN interaction only. Such a fact is well known from Lee-Suzuki effective-interaction theory. Whenever the system of interest contains a finite number of A bodies, up to A-body forces are picked out through the evolution while higher-body forces project out to zero.

The fact that a RG evolution induces many-body forces is most easily seen from the SRG method [215]. The SRG performs a pre-diagonalization of the Hamiltonian in a chosen basis, i.e. the plane-wave basis, by means of a series of infinitesimal unitary evolutions of  $H$  parameterized by  $\Lambda$  that takes the form of a double commutator

$$\begin{aligned} \frac{dH(\Lambda)}{d\Lambda} &= -\frac{4}{\Lambda^5} \left[ [T, H(\Lambda)], H(\Lambda) \right] \\ &\propto \left[ \left[ \sum c^\dagger c, \sum c^\dagger c^\dagger c c \right], \sum c^\dagger c^\dagger c c \right] \\ &\propto \dots + \sum c^\dagger c^\dagger c^\dagger c c c + \dots, \end{aligned} \quad (38)$$

such that many-body forces are naturally induced from an initial NN interaction. One may wonder if the generation of a whole series of many-body forces is problematic as handling them is likely to make the many-body problem untractable and requires to track them explicitly through the RG evolution. To answer such a question, one must first remember that up to A-body forces are a priori present in  $H(\Lambda_{\text{init}})$  anyway such that one might as well develop the (S)RG machinery to make them soft. Of course, one aims in practice at dropping as many of such (induced) many-body forces as possible, i.e. keep only those that are not negligible in the regime of  $\Lambda$  values one is interested in. Eventually, the problem posed by induced many-body forces will be tractable as long as (i) they remain of "natural size", e.g. they follow  $\chi$ -EFT power counting built in the initial Chiral Hamiltonian, such that only up to a-body forces with  $a \leq A$  need to be kept and (ii) tracking the RG evolution of those a-body forces is computationally feasible. Eventually, the  $\Lambda$ -dependence of computed observable can be used to assess the effect of omitted many-body forces (given that the many-body calculation is sufficiently converged).

As shown below, the current situation is that 3N interactions cannot be avoided at any  $\Lambda$  while 4N interactions (and beyond) are likely to be negligible. Given that the machinery to evolve the 3N interaction along with the NN one through SRG method has recently been developed [216], the prospect to use low momentum interactions in finite-nuclei calculations look promising at this point. Let us now illustrate the situation in three- and four-body systems.

Figure 32 displays  $E_{3\text{H}}$  versus  $E_{4\text{He}}$  obtained for different  $\Lambda$  values through NCSM calculations when omitting multi-body forces beyond  $V^{NN}(\Lambda)$ . Both binding energies depend on  $\Lambda$  and correlates along the so-called Tjon line. Such a feature suggests that 3N and possibly 4N interactions cannot be omitted. To confirm this, Fig. 33 isolates  $E_{3\text{H}}$  as a function of  $\Lambda$ . The observed variation is  $\Delta E_{3\text{H}} \sim 0.6$  MeV over the interval  $\Lambda \in [2, \infty]$ . This is non negligible but remains much smaller than the potential energy contribution from  $V^{NN}(\Lambda)$  such that the omitted many-forces seem to remain of natural size over such an interval of  $\Lambda$ .

Thus, the next step consists of evolving the induced 3N interaction along with  $V^{NN}(\Lambda)$  and including it in the NCSM calculation of  ${}^3\text{H}$  [216]. Figure 33 demonstrates that the inclusion of the induced 3N interaction makes  $E_{3\text{H}}$  scale independent as expected, whether the 3N interaction present initially in  $H(\Lambda_{\text{init}})$  is included along with the induced one or not. Incorporating the former only changes the overall result by a constant such that it moves closer to experiment. This is due to the fact the 3N part of  $H(\Lambda_{\text{init}})$  was fitted to provide a good

<sup>13</sup> As discussed below, the initial NN interaction should itself be accompanied by a 3N interaction. However, since the present calculation starts from the NN part of the Chiral Hamiltonian only, the observed scale dependence relates only to the *induced* 3N interaction.

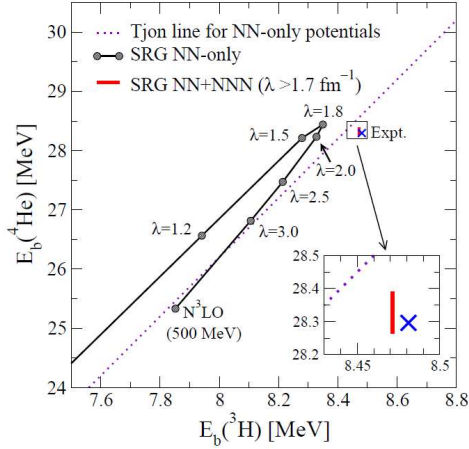


FIG. 32: (Color online) Binding energy of the alpha particle vs. the binding energy of the triton. The Tjon line from phenomenological NN potentials (dotted) is compared with the trajectory of SRG energies when only the NN interaction is kept (circles). When the initial and induced 3N interactions are included, the trajectory lies close to experiment for a SRG scale greater than  $1.7 \text{ fm}^{-1}$  (see inset). Taken from Ref. [216].

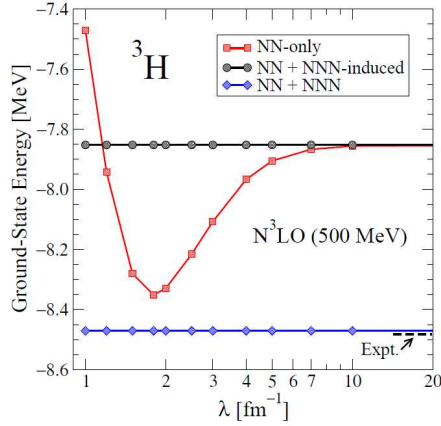


FIG. 33: (Color online) NCSM calculation of the ground-state energy of  ${}^3\text{H}$  as a function of the SRG evolution parameter. Taken from Ref. [216].

account of  $E_{3\text{H}}$ . Comparing the two sets of calculations demonstrates that the potential energy contribution of the induced 3N force is not unnaturally large compared to the one of the 3N interaction originally tailored in  $H(\Lambda_{\text{init}})$ . Eventually, the huge benefit of evolving the Hamiltonian to lower scale is that the net resulting 3N interaction is much softer than the initial one such that the NCSM calculation converges faster.

Figure 32 shows that the inclusion of  $V^{3N}(\Lambda)$  allows the result to break away from the Tjon line and move closer to experiment. The remaining scale dependence of  $E_{4\text{He}}$  due to the omission of  $V^{4N}(\Lambda)$  seems to be small as the inset shows. To confirm the last point,  $E_{4\text{He}}$  is displayed in Fig. 34 as a function of the RG scale. Although the induced 4N interaction is omitted, one sees that the energy is nearly scale independent. The slight variation of  $E_{4\text{He}}$  at low cut-off together with the difference with experiment indicate that the induced  $V^{4N}(\Lambda)$  could be responsible for about 200 keV at most. Before declaring that  $V^{4N}(\Lambda)$  can be safely neglected, it must however be monitored in heavier nuclei.

## E. Summary

To close the section on low-momentum interactions, we now list some of the key points we have encountered and learnt from RG and EFT ideas. In addition, we briefly outline the strategy that can be followed next

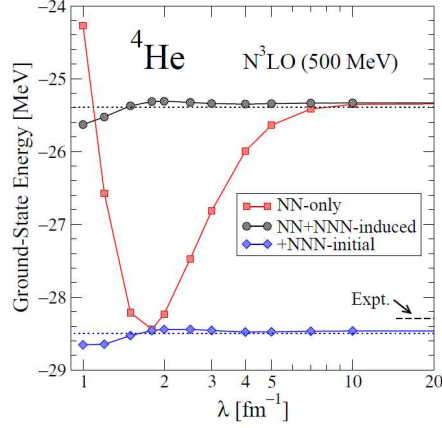


FIG. 34: (Color online) NCSM calculation of the ground-state energy of  ${}^4\text{He}$  as a function of the SRG evolution parameter. Taken from Ref. [216].

to build non-empirical parameterizations of the nuclear EDF.

1. Low-momentum interactions provide a new paradigm for realistic nuclear interactions
  - (a) The "hard core" is not an absolute feature of  $H(\Lambda)$  but a scale-dependent one
  - (b)  $H(\Lambda_{\text{high}})$  contains highly non-perturbative vertices
  - (c) Lowering the resolution  $\Lambda$  through RG transformations suppresses the main sources of non-perturbativeness
  - (d) RG transformations necessarily induce many-body forces
2. Use of  $H(\Lambda_{\text{low}})$  for low-energy studies
  - (a) One must keep  $m_\pi, k_F < \Lambda_{\text{low}} \leq \Lambda_{\text{data}}$  to leave the encoded long-range physics untouched
  - (b) The convergence of ab-initio calculations of light-nuclei is greatly improved
  - (c) The  $\Lambda$ -dependence of *observable* signals missing many-body forces and/or incomplete calculations
  - (d) Induced  $V^{3N}(\Lambda)$  must be tracked but 3N interactions are unavoidable anyway
  - (e)  $V^{4N}(\Lambda)$  seems to be negligible in  ${}^4\text{He}$  but must be monitored in heavier nuclei
3. What about the link to nuclear EDF calculations ?
  - (a) Investigate perturbative calculations of infinite nuclear matter from low-momentum interactions
  - (b) Investigate perturbative calculations of doubly-magic nuclei from low-momentum interactions
  - (c) Build the energy functional from many-body perturbation theory
  - (d) Approximate the still-too-complicated resulting EDF to constrain Skyrme- or Gogny-like energy functionals

## IV. TOWARDS NON-EMPIRICAL ENERGY DENSITY FUNCTIONALS

### A. Generalities

In Sec. II, we have outlined key features of nuclear EDF methods and elaborated on some of the challenges they currently face. In particular, the possibility to explicitly link the EDF kernel to underlying vacuum NN and 3N interactions was envisioned. Within such a context, microscopically-educated energy functionals are to be derived through analytical approximations of the ground-state energy computed from an ab-initio method of reference. As summarized in Fig. 35, the complexity of such a task depends on the nuclear Hamiltonian model and the ab-initio many-body method one starts from. Indeed, not all ab-initio methods offer a natural matching, even through a set of controlled approximations, to energy density functionals that are

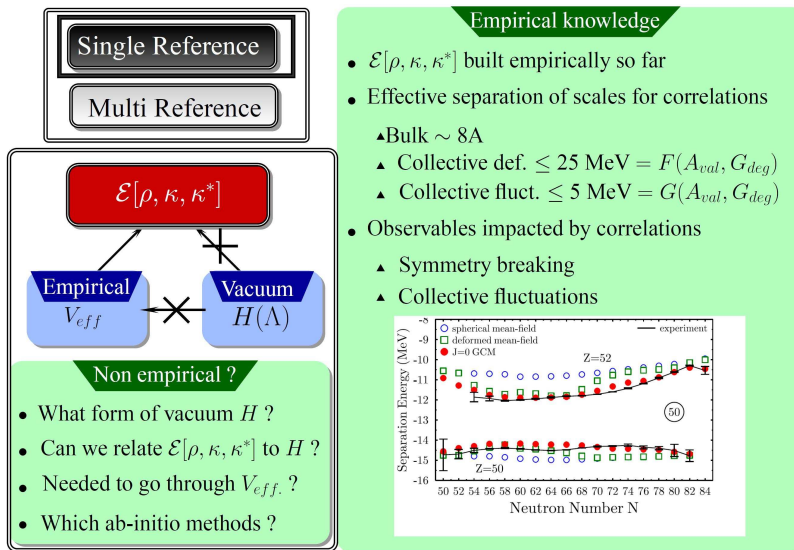


FIG. 35: (Color online) Route towards non-empirical energy functionals. Right : knowledge acquired from phenomenology. Left : questions relevant to this endeavor.

close to the form of standard quasi-local (Skyrme, relativistic point coupling. . .) or non-local (Gogny, effective meson-exchange Lagrangian. . .) variants. As discussed in the introduction, ab-initio methods that are amenable to such a mapping must share certain key features with EDF methods, the most important of which being the concept of spontaneous symmetry breaking (and further restoration).

An ab-initio method that fulfills such requirements is provided by many-body perturbation theory (MBPT) performed on top of a (potentially) symmetry-breaking vacuum. Although it is possible to consider an elaborate Dyson (Gorkov) self-consistent green's function theory [59, 217], we restrict presently ourselves to Goldstone many-body perturbation theory for simplicity [140, 209]. An interesting point is that any conventional list of available nuclear ab-initio methods<sup>14</sup> will miss out on a perturbative approach. The reason relates to the conventional wisdom that the non-perturbative short-range central repulsion and tensor force are absolute features of the NN interaction. As discussed in Sec. III, the new paradigm set by low-momentum interactions is modifying such a picture. In particular, the in-medium Weinberg eigenvalue analysis [95] indicates that the nuclear many-body problem may become perturbative when solved in terms of a low resolution-scale Hamiltonian.

As a matter of fact, recent calculations discussed below in Secs. IV C 1 and IV C 2 confirm the (essentially) perturbative nature of infinite nuclear matter and doubly-magic nuclei when expressed in terms of low-momentum NN and 3N interactions. Many-body perturbation theory becoming a reliable, if not totally quantitative, starting point to compute nuclear systems and derive microscopically-educated energy functionals through analytical approximations of the (itself approximate) ab-initio ground-state energy. Doing so requires specific approximation methods that are presented in Secs. IV D 2 and IV E, where it is explained that available methods are incomplete as of today. Before coming to that, we first introduce basic elements of Goldstone MBPT.

## B. Elements of time-ordered many-body perturbation theory

### 1. Unperturbed vacuum of reference

Although it was argued in the introduction that the ab-initio method of reference must be formulated within a symmetry-breaking framework, we restrict ourselves for simplicity to a MBPT that preserves particle

<sup>14</sup> Refer to the Denis Lacroix's introductory lecture [37].

number, i.e. which does not explicitly incorporate pairing correlations through the breaking of gauge invariance. Consequently, the MBPT presented below is not general enough to eventually constrain all parts of the nuclear EDF. In addition, formulae are written for  $V^{NN}(\Lambda)$  only although it is to be understood that  $V^{3N}(\Lambda)$  must be taken into account as well.

The unperturbed vacuum of reference takes the form of a Slater determinant

$$|\Phi(\Lambda)\rangle \equiv \prod_{i=1}^N a_i^+(\Lambda) |0\rangle, \quad (39)$$

whose one-body density matrix in the associated basis is  $\rho_{\alpha\beta}(\Lambda) = \delta_{\alpha i} \delta_{\beta i}$ . As a convention, greek indices  $\{\alpha, \beta, \dots\}$  denote arbitrary single-particle basis states while roman indices  $\{i, j, \dots\}/\{a, b, \dots\}$  denote occupied/empty ("hole/particle") single-particle basis states in the unperturbed vacuum. Next are defined Slater determinants  $|\Phi_{ij\dots}^{ab\dots}(\Lambda)\rangle$  obtained through particle-hole excitations on top of the unperturbed vacuum, e.g. 2p-2h states of the form

$$|\Phi_{ij}^{ab}(\Lambda)\rangle \equiv a_a^+(\Lambda) a_b^+(\Lambda) a_j(\Lambda) a_i(\Lambda) |\Phi(\Lambda)\rangle. \quad (40)$$

The vacuum is actually defined once the single-particle basis  $\{a_\alpha^+/\psi_\alpha\}$  has been specified. The present choice is to use the Hartree-Fock basis whose elements are solutions of the eigenvalue problem  $h^{HF}(\Lambda) \psi_\alpha = \varepsilon_\alpha(\Lambda) \psi_\alpha$ , where the Hartree-Fock field is expressed in an arbitrary basis as

$$h_{\alpha\gamma}^{HF}(\Lambda) \equiv t_{\alpha\gamma} + \sum_{\beta\delta} \bar{V}_{\alpha\beta\gamma\delta}^{NN}(\Lambda) \rho_{\delta\beta}(\Lambda). \quad (41)$$

Antisymmetrized matrix elements of  $V^{NN}(\Lambda)$  are defined through  $V_{\alpha\beta\gamma\delta}^{NN}(\Lambda) \equiv \langle 1 : \alpha ; 2 : \beta | V^{NN}(\Lambda) | 1 : \gamma ; 2 : \delta \rangle$  and  $\bar{V}_{\alpha\beta\gamma\delta}^{NN}(\Lambda) \equiv V_{\alpha\beta\gamma\delta}^{NN}(\Lambda) - V_{\alpha\beta\delta\gamma}^{NN}(\Lambda)$ .

Using Wick's theorem with respect to  $|\Phi(\Lambda)\rangle$ , the Hamiltonian  $H(\Lambda)$  is put under normal-ordered form

$$H(\Lambda) = E^{HF}(\Lambda) + \sum_{\alpha} \varepsilon_{\alpha}(\Lambda) : a_{\alpha}^{+} a_{\alpha} : + \frac{1}{4} \sum_{\alpha\beta\gamma\delta} \bar{V}_{\alpha\beta\gamma\delta}^{NN}(\Lambda) : a_{\alpha}^{+} a_{\beta}^{+} a_{\delta} a_{\gamma} : , \quad (42)$$

from which the Hartree-Fock energy

$$E^{HF}(\Lambda) \equiv \langle \Phi(\Lambda) | H(\Lambda) | \Phi(\Lambda) \rangle = \sum_i t_{ii} + \frac{1}{2} \sum_{ij} \bar{V}_{ijij}^{NN}(\Lambda), \quad (43)$$

the unperturbed Hamiltonian

$$H_0(\Lambda) \equiv E^{HF}(\Lambda) + \sum_{\alpha} \varepsilon_{\alpha}(\Lambda) : a_{\alpha}^{+} a_{\alpha} : , \quad (44)$$

and the residual interaction

$$V_{\text{res}}(\Lambda) \equiv \frac{1}{4} \sum_{\alpha\beta\gamma\delta} \bar{V}_{\alpha\beta\gamma\delta}^{NN}(\Lambda) : a_{\alpha}^{+} a_{\beta}^{+} a_{\delta} a_{\gamma} : , \quad (45)$$

can be defined. In the above set of equations, all quantities expected to depend on the resolution scale  $\Lambda$  have been labeled by it. In particular, and even if the complete Hamiltonian  $H(\Lambda)$  were used, quantities associated with an *approximate* many-body calculation, e.g.  $|\Phi(\Lambda)\rangle$ ,  $E^{HF}(\Lambda)$  or  $h_{\alpha\gamma}^{HF}(\Lambda)$ , are expected to be scale dependent. Only fully converged observable such as the actual ground state energy  $E$  are scale independent. Having said that, the label  $\Lambda$  is omitted in the following for simplicity, unless stated otherwise. Using the above definitions, it is straightforward to demonstrate that

$$H_0 |\Phi_{ij\dots}^{ab\dots}\rangle = E_{ij\dots}^{ab\dots} |\Phi_{ij\dots}^{ab\dots}\rangle, \quad (46)$$

with  $E_{ij\dots}^{ab\dots} \equiv E^{HF} + (\varepsilon_a + \varepsilon_b + \dots - \varepsilon_i - \varepsilon_j - \dots)$  and that  $\langle \Phi | V_{\text{res}} | \Phi \rangle = \langle \Phi | V_{\text{res}} | \Phi_i^a \rangle = 0$ , which shows that the residual interaction does not couple the unperturbed vacuum to itself or to unperturbed 1p-1h configurations when using Eq. 44 as a definition of  $H_0$ .

## 2. Correlation energy and the perturbative expansion

Given the unperturbed reference state and energy, one defines the correlation energy  $\Delta E^{HF}(\Lambda)$  through  $E \equiv E^{HF}(\Lambda) + \Delta E^{HF}(\Lambda)$ . The correlation energy obviously depends on the chosen unperturbed state of reference and one aspect of MBPT consists of minimizing  $\Delta E^{HF}$  through an a priori optimal choice of the unperturbed vacuum, e.g. by exploiting symmetry breaking in the spirit of the SR-EDF method. Still, it is usually not sufficient and part, if not all, of the correlation energy beyond HF must be computed explicitly. The idea of time-ordered (Goldstone) MBPT is to expand  $\Delta E^{HF}$  in powers of  $V_{\text{res}}$ . Starting from Gell-Man-Low's theorem [218], Goldstone demonstrated [140] that

$$\Delta E^{HF} = \sum_{n=0} \langle \Phi | V_{\text{res}} \left( \frac{1}{E^{HF} - H_0} V_{\text{res}} \right)^n | \Phi \rangle_{\text{connected}}, \quad (47)$$

where "connected" means that  $|\Phi\rangle$  cannot appear as an intermediate state (see below).

Summing all terms in Eq. 47 provides the exact many-body ground-state energy. However, the practical use of the perturbative expansion resides in the possibility to truncate it, i.e. in the fact that a meaningful and accurate enough result can be obtained from a finite number of terms, which usually requires that contributions decrease as  $n$  increases. In order to speed up the convergence of the perturbative series, it might be necessary to optimize the unperturbed Hamiltonian/vacuum  $H_0/|\Phi\rangle$  by modifying the content of the one-body field  $h$  that defines the single-particle basis  $\{a_\alpha^\pm/\psi_\alpha\}$  (see Sec. IV D 2). Sometimes however, modifying the content of  $h$  in a perturbative manner is not sufficient such that expansion 47 breaks down. It is precisely the case when forcing the unperturbed vacuum to fulfill a symmetry when it would choose to spontaneously break it if offered to do so. For instance, the Cooper pair instability associated with strong pairing correlations necessitates to expand around a Bogoliubov vacuum rather than a Slater determinant. As mentioned above, we do not consider this possibility here for simplicity although most of nuclear systems encounter such an instability<sup>15</sup>. Another source of non-perturbative character arises whenever one chooses to work with  $H(\Lambda_{\text{high}})$  that contains a strong coupling between low- and high-momentum modes. As demonstrated by Brueckner [139, 208, 219], such a coupling necessitates to reorganize expansion 47 by summing up so-called particle-particle ladder diagrams *prior* to truncating it. This leads to introducing the Brueckner G-matrix as a basic two-nucleon kernel. Still, the many-body energy cannot be expanded in powers of the G-matrix such that one relies on the non-perturbative hole-line expansion in this case [209–211].

The main benefit of starting from  $H(\Lambda_{\text{low}})$  rather than from  $H(\Lambda_{\text{high}})$  is precisely that the purely perturbative expansion 47 is meaningful, as exemplified in Secs. IV C 1 and IV C 2, which tremendously simplifies our view on the nuclear many-body problem.

## 3. Computation

We briefly present the method to compute contributions to Eq. 47 up to the truncation order  $n_{\text{max}}$ . We use a pedestrian approach, which is only convenient to compute low orders and only mention at the end the more practical diagrammatic approach. We exemplify the method by computing the simplest, i.e. the second order contribution ( $n = 1$ ).

The procedure consists of first inserting the (quasi) completeness relationship on the N-body Hilbert space  $\mathcal{H}_N$

$$1_N - |\Phi\rangle\langle\Phi| = \sum_i^a |\Phi_i^a\rangle\langle\Phi_i^a| + \left(\frac{1}{2!}\right)^2 \sum_{i,j}^{a,b} |\Phi_{ij}^{ab}\rangle\langle\Phi_{ij}^{ab}| + \left(\frac{1}{3!}\right)^2 \sum_{i,j,k}^{a,b,c} |\Phi_{ijk}^{abc}\rangle\langle\Phi_{ijk}^{abc}| + \dots \quad (48)$$

in between each pair of operators appearing in Eq. 47. The fact that the vacuum contribution has been subtracted from the completeness relationship in Eq. 48 relates to the fact that only "connected" terms must appear in Eq. 47 [140]. In all contributions thus generated, each resolvent operator  $(E^{HF} - H_0)^{-1}$  can be trivially applied onto unperturbed Slater determinants  $|\Phi_{ij,\dots}^{ab,\dots}\rangle$ . According to Eq. 46, it results into the energy denominator  $(\varepsilon_a + \varepsilon_b + \dots - \varepsilon_i - \varepsilon_j - \dots)^{-1}$  times the state  $|\Phi_{ij,\dots}^{ab,\dots}\rangle$ , which eventually selects the same Slater

<sup>15</sup> Only doubly-magic nuclei do not encounter the Cooper pair instability.

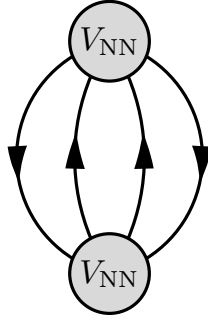


FIG. 36: (Color online) Hugenholtz diagram for the second-order contribution to the ground-state binding energy from the NN interaction.

determinant from the (quasi) completeness relationship inserted to the left of the resolvent operator as a result of the scalar product on  $\mathcal{H}_N$ . At that point, one is left with computing matrix elements  $\langle \Phi_{i'j'k'...}^{a'b'c'...} | V_{\text{res}} | \Phi_{ijk...}^{abc...} \rangle$  between a variety of unperturbed multi-particle multi-hole Slater determinants.

Let us exemplify the above procedure by calculating the second-order contribution ( $n = 1$ )

$$\Delta E_2^{HF} = \langle \Phi | V_{\text{res}} \frac{1}{E^{HF} - H_0} V_{\text{res}} | \Phi \rangle_{\text{connected}} . \quad (49)$$

We first insert the (quasi) completeness relationship 48 to the left and the right of the resolvent operator in Eq. 49. Before proceeding further, we note that the two-body residual interaction  $V_{\text{res}}$  can only couple the unperturbed vacuum to 2p-2h states, i.e. in addition to having  $\langle \Phi | V_{\text{res}} | \Phi \rangle = \langle \Phi | V_{\text{res}} | \Phi_i^a \rangle = 0$ , one can use Wick's theorem to prove that  $\langle \Phi | V_{\text{res}} | \Phi_{ij}^{ab} \rangle = \bar{V}_{ijab}^{NN}$  and that  $\langle \Phi | V_{\text{res}} | \Phi_{ijk...}^{abc...} \rangle = 0$  for 3p-3h, 4h-4h... This reduces tremendously the number of non-zero terms resulting from the above insertion of the (quasi) completeness relationship. As a result, and following the steps outlined above, the second-order contribution finally reads

$$\begin{aligned} \Delta E_2^{HF} &= \frac{1}{4} \sum_{ijab} \frac{|\langle \Phi | V_{\text{res}} | \Phi_{ij}^{ab} \rangle|^2}{E^{HF} - E_{ij}^{ab}} \\ &= \frac{1}{4} \sum_{ijab} \frac{|\bar{V}_{ijab}^{NN}|^2}{\varepsilon_i + \varepsilon_j - \varepsilon_a - \varepsilon_b} , \end{aligned} \quad (50)$$

which is necessarily negative, i.e. it lowers the ground-state energy compared to  $E^{HF}$ . Anticipating the discussion of Sec. IV D 2, it is worth noting that restricted sums over hole and particle states in Eq. 50 can be replaced by unrestricted sums over the complete single-particle basis at the price of inserting a factor  $\rho_{\alpha\alpha}$  for hole states and a factor  $1 - \rho_{\alpha\alpha}$  for particle states ; i.e. Eq. 50 can be rewritten as

$$\Delta E_2^{HF} = \frac{1}{4} \sum_{\alpha\beta\gamma\delta} \frac{|\bar{V}_{\alpha\beta\gamma\delta}^{NN}|^2}{\varepsilon_\alpha + \varepsilon_\beta - \varepsilon_\gamma - \varepsilon_\delta} \rho_{\alpha\alpha} \rho_{\beta\beta} (1 - \rho_{\gamma\gamma})(1 - \rho_{\delta\delta}) . \quad (51)$$

The computation of  $\Delta E_2^{HF}$  is instructive but hides the rising algebraic complexity as the order  $n$  increases. Many more terms are non-zero and necessitate the evaluation of matrix elements of the form  $\langle \Phi_{i'j'k'...}^{a'b'c'...} | V_{\text{res}} | \Phi_{ijk...}^{abc...} \rangle$  that are cumbersome to compute. Analyzing the outcome of the pedestrian procedure presented above, a more systematic approach can be designed to compute contributions to Eq. 47. This constitutes the so-called diagrammatic technique [220] that relies on a set of rules to draw and compute diagrams representing all possible contributions to a given order  $\Delta E_n^{HF}$ . For example, the second order contribution is represented in Fig. 36 using so-called Hugenholtz diagrams. Expression 50 can be easily recovered from such a drawing by applying the set of diagrammatic rules. Although we do not discuss such rules here, they can be found in many textbooks dealing with the quantum many-body problem, e.g. in Ref. [220].

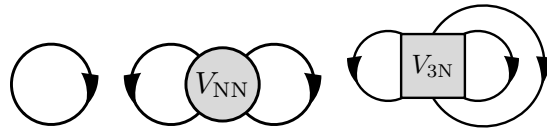


FIG. 37: (Color online) Hugenholtz diagrams for the unperturbed kinetic energy and the first-order contributions to the ground-state binding energy from NN and 3N interactions.

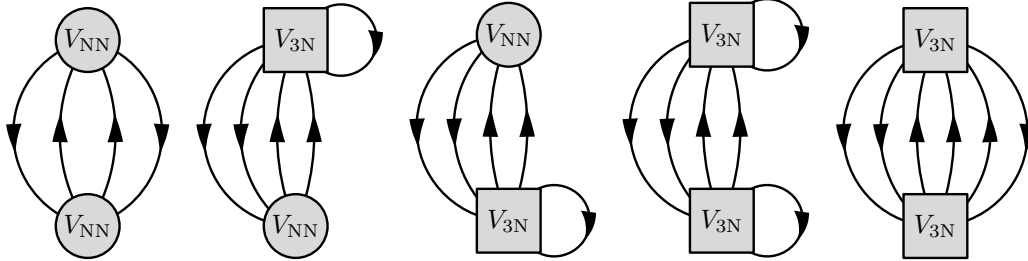


FIG. 38: (Color online) Complete set of second-order Hugenholtz diagrams from NN and 3N interactions.

### C. Many-body perturbation theory calculation of nuclear systems

#### 1. Infinite nuclear matter

The present section briefly discusses recent computations of the equation of state (EOS) of infinite nuclear matter (INM) through MBPT [87, 88]. In that respect, some ( $\Lambda$ -dependent) questions of interest are

1. Is infinite nuclear matter perturbative ?
2. What is the role of  $V^{3N}$  ?
3. What is the saturation mechanism ?
4. Can phenomenology be accounted for ?

To answer such questions, the computation is performed at first and second order in MBPT. First-order diagrams, together with the unperturbed kinetic-energy diagram, are displayed in Fig. 37 while the complete set of second-order diagrams are shown in Fig. 38. The calculation uses  $V^{NN}(\Lambda)$  from RG methods together with the Chiral 3N interaction at  $N^2\text{LO}$ . The two unknown low-energy constants ( $c_D, c_E$ ) entering the Chiral 3N interaction at  $N^2\text{LO}$  are fitted, consistently with  $V^{NN}(\Lambda)$ , on  $E_{3\text{H}}$  and the charge radius of  ${}^4\text{He}$  [88]. In other words,  $V_{3N}$  is not evolved through the similarity RG as done in Ref. [216] and discussed in Sec. III D but ( $c_D, c_E$ ) are rather adjusted for each  $\Lambda$  on light-nuclei data along with  $V^{NN}(\Lambda)$ . Still, the 3N interaction thus produced is not used as such in MBPT calculations of INM. Instead, an averaging over the third particle is performed to approximate  $V_{3N}$  by a density-dependent NN vertex  $V_{NN(N)}$ . Such a procedure relates in particular to omitting the last diagram among all second-order ones displayed in Fig. 38. Last but not least, single-particle energies entering energy denominators are computed from the HF (i.e. first-order self-energy) field including both NN and 3N contributions.

Traditionally, i.e. using conventional potentials, nuclear matter is believed to be non perturbative. This is visible in Fig. 39 displaying the EOS of symmetric matter to first, second and third order using AV18 or  $V_{\text{low } k}(2.1)$  but omitting any 3N force. With AV18, the first-, second- and third-order<sup>16</sup> contributions to the EOS are large, of alternative sign and do not display any sign of convergence. The Hartree-Fock energy in particular is large and positive due to the strongly repulsive character of AV18's S-waves such that symmetric nuclear matter is not bound at first order. Such patterns are typical of a non-perturbative problem and require that the energy is expanded in a different fashion as explained in Sec. IV B. Contrarily with  $V_{\text{low } k}(2.1)$  symmetric nuclear matter is bound at first order and higher-order contributions are quickly decreasing in absolute

<sup>16</sup> Only the third-order ladder diagram is computed here.

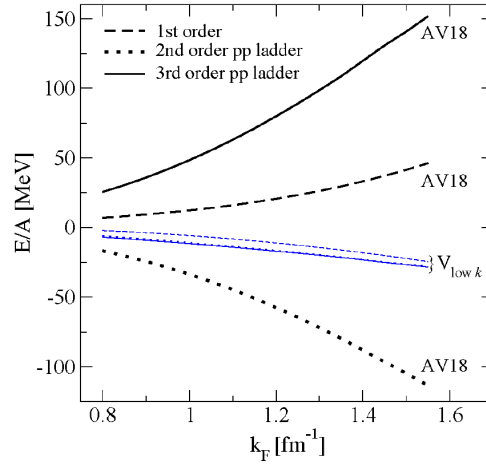


FIG. 39: (Color online) Particle-particle contributions to the EOS of symmetric nuclear matter for Argonne AV18 potential [1] (thick lines) and the low-momentum interaction  $V_{\text{low}k}$  evolved from it down to  $\Lambda = 2.1 \text{ fm}^{-1}$  (thin lines). Taken from Ref. [87].

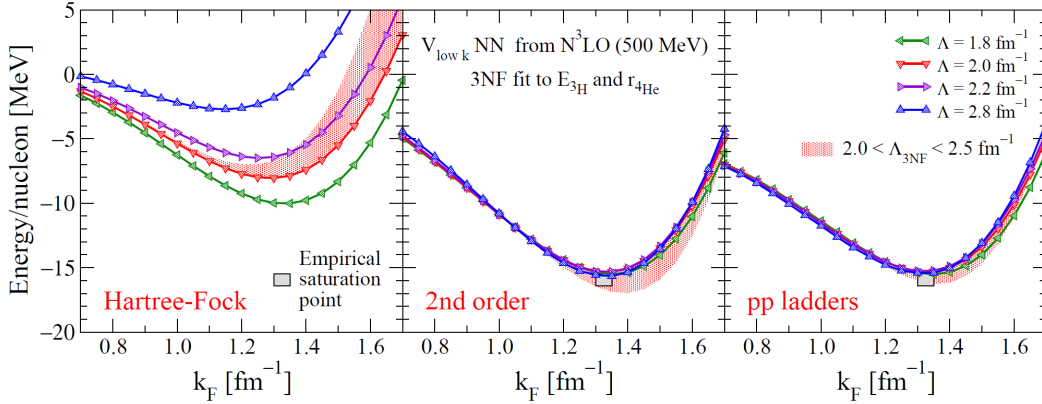


FIG. 40: (Color online) Symmetric nuclear matter energy-per-particle as a function of Fermi momentum  $k_F$ . The computation is based on evolved  $N^3\text{LO}$  NN potentials and 3N forces fit  $E_{3\text{H}}$  and the charge radius of  ${}^4\text{He}$  [88]. Results are shown at the HF level (left), including second-order contribution (middle) or particle-particle-ladder contributions to all orders (right). Taken from Ref. [88].

value such that the expansion seems to display a gentle converging character. Such patterns are typical of a perturbative problem. The present results shed a new light of the nuclear many-body problem by showing that its perturbative or non-perturbative nature depends on the resolution scale used, although the result of the complete calculation does not. This constitutes a new paradigm of nuclear theory that can be used to reduce the intrinsic difficulty to solve the associated many-body problem.

Although the expansion in terms of  $H(\Lambda_{\text{low}})$  seems to be perturbative, the EOS shown in Fig. 39 does not saturate. To reach a satisfactory description, one must take the 3N interaction into account as is visible from Fig. 40. From the left panel, one sees that symmetric nuclear matter already saturates at first order when doing so, although away from the empirical point. In addition, a significant residual  $\Lambda$  dependence is observed. As visible from the central panel of Fig. 40, the second-order contribution brings additional binding such that the EOS saturates very close to the empirical point and presents a reasonable, though slightly too low, compressibility. The various curves in each panel correspond to calculations performed for different values of NN RG scale  $\Lambda_{\text{NN}}$ . In addition, the 3N scale is allowed to vary independently of the NN one. The shaded regions in Fig. 40 show the range of results for  $2.0 \text{ fm}^{-1} < \Lambda_{3\text{N}} < 2.5 \text{ fm}^{-1}$  at fixed  $\Lambda_{\text{NN}} = 2.0 \text{ fm}^{-1}$ . Overall, the significant dependence on the RG scales at the HF level is largely suppressed at second-order, which is an indication that convergence might be reached. This is further confirmed in the right panel where,

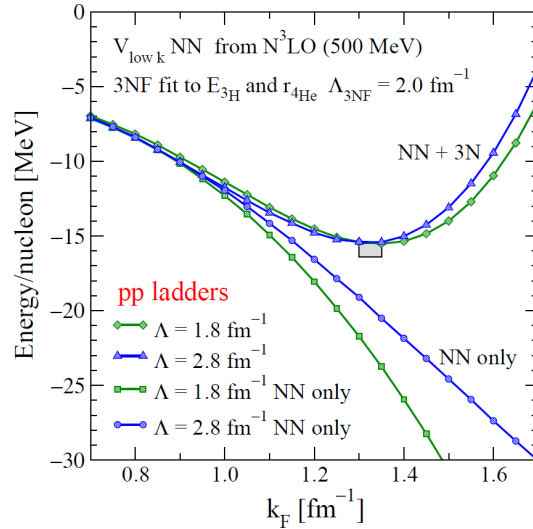


FIG. 41: (Color online) Nuclear matter energy per particle displayed in Fig. 40 at the particle-particle-ladders level compared to NN-only results for two representative NN cutoffs and a fixed 3N cutoff. Taken from Ref. [88].

except for rather low density, the summation of particle-particle ladders to all orders is not modifying the EOS. Still, the convergence pattern in the particle-hole channel has not been investigated so far.

As further illustrated by Fig. 41, the saturation of symmetric nuclear matter is driven by the 3N force when using a resolution scale in the perturbative regime from 1.8 to 3  $\text{fm}^{-1}$ . At the same time, the Coester line problem is solved by the inclusion of the 3N force such that the empirical saturation point is satisfactorily reproduced. For similar EOS calculations of pure neutron matter, we refer the reader to Ref. [89].

## 2. Doubly-magic nuclei

The present section briefly discusses recent computations of doubly-magic nuclei through MBPT [138, 221]. In that respect, some ( $\Lambda$ -dependent) questions of interest are

1. Are bulk properties of doubly-magic nuclei perturbative ?
2. What is the role of  $V^{3N}$  ?
3. Is phenomenology accounted for ?

Besides their numerical tractability, MBPT calculations of doubly-magic nuclei allows one to disentangle bulk correlations from those brought in through the spontaneous breaking of  $N, Z$  and  $J$  and the associated collective fluctuations (see discussion in Sec. II F). The results provided in Fig. 42 have been obtained through first and second-order MBPT calculations. They are only indicative given that (i) the NN interaction S-UCOM(SRG) is only renormalized in the S waves, (ii) the 3N interaction used is a schematic (regularized) contact force and (iii) second-order calculations are not converged as a function of the single-particle harmonic oscillator basis size, especially for heavy nuclei [138]. Still, such results provide valuable information on the interplay between realistic two-body and phenomenological three-body interactions as well as on how well systematics of masses and charge radii systematics of doubly-closed shell nuclei can be reproduced at this level of calculations.

The strength of the 3N contact interaction has been fixed to reproduce the systematics of charge radii at the HF level. Indeed, it is possible to track such a systematics as seen in Fig. 42, which is a non trivial result by itself. Perturbative corrections to charge radii are very small [221] and will not affect the general agreement. As for binding energies, HF provides the correct trend with  $A$  but underbinds significantly. It is to be reminded however that nuclei are not even be bound at the HF level with conventional  $H(\Lambda_{\text{high}})$  Hamiltonians. The 3N interaction is responsible for a repulsive contribution that ranges from 1.5 MeV/A in light nuclei to 3 MeV/A in  $^{208}\text{Pb}$ .

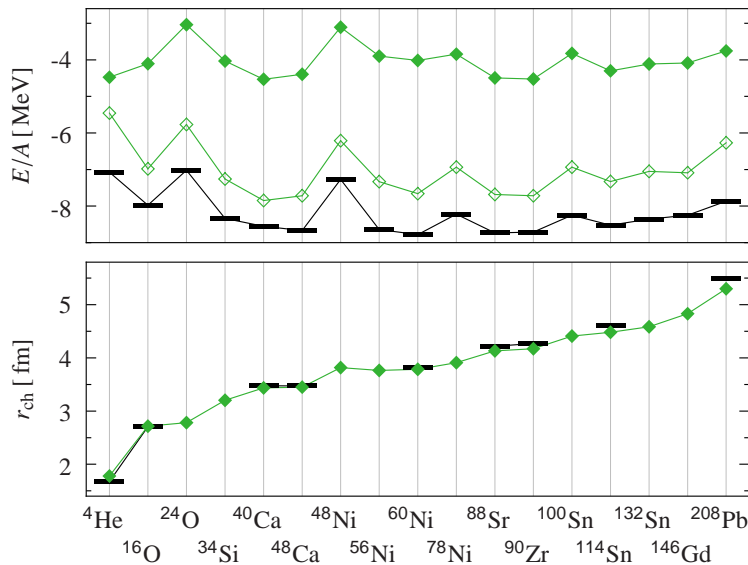


FIG. 42: (color online) Binding energies per nucleon and charge radii of selected closed-shell nuclei resulting from HF (filled symbols) and second-order MBPT (open symbols) calculations. The S-UCOM(SRG) NN interaction with  $\alpha = 0.16 \text{ fm}^4$  is used together with a 3N contact interaction characterized by the coupling  $C_{3N} = 2200 \text{ MeV fm}^6$ . The basis size is  $e_{\max} = 14$ ,  $l_{\max} = 10$ . Adapted from [138].

As shown in Fig. 42, low-order MBPT, i.e. second order, provides a good account of missing bulk correlations such that binding energy systematics are correctly accounted for. The extrapolation of the present results with the basis size  $e_{\max} \rightarrow \infty$  shows that the agreement with data is qualitatively and semi-quantitatively good. Except for light nuclei, the second-order contribution from the 3N interaction is negligible [138] such that it is omitted from the results shown in Fig. 42. Although it is not shown in Fig. 42, the second-order contribution reduces, although not completely, in particular for heavy systems, the scale dependence of the results [138].

#### D. Mapping many-body perturbation theory onto the SR-EDF method

##### 1. Generalities

As discussed in the previous section, first MBPT calculations with low-momentum interactions have demonstrated that the 3N interaction plays an important role and that second-order contributions provide the correct systematics of bulk correlations  $\approx -8 \text{ MeV/A}$  in doubly-magic nuclei. Still, results are quoted in energy per particle and can only be viewed as indicative given the much higher accuracy that is eventually needed. Such calculations pave the way towards more quantitative ab-initio studies of doubly-magic nuclei that must employ realistic 3N interactions and more advanced many-body schemes, i.e. that re-sum correlations in a non-perturbative fashion with an explicit inclusion of collective fluctuations, e.g. through MR-like methods.

The ab-initio description of singly and doubly open-shell nuclei is even more challenging. Correlations that vary rapidly with the filling of a major shell are harder to grasp and require MR techniques, if not the explicit breaking of particle number (singly open-shell nuclei) and angular momentum (doubly open-shell nuclei). In the latter case in particular, MBPT must be performed with respect to a deformed unperturbed vacuum that ultimately corresponds to handling much larger single-particle bases than for doubly-closed shell nuclei. Given that second-order MBPT scales as  $N_{\text{basis}}^5$ , this becomes quickly prohibitive computationally as  $A$  increases.

Despite such numerical difficulties, ab-initio calculations of heavier and more challenging nuclei must be pursued in order to provide theoretical benchmarks. In parallel, one must identify shortcuts to profit by the best of both low-order MBPT, i.e. its explicit link to vacuum low-momentum interactions, and of the SR-EDF method, i.e. the breaking of various symmetries, in such way that one can address doubly open-shell nuclei in a systematic fashion while avoiding the prohibitive computational scaling. In other words, one

wishes to design controlled approximations allowing the mapping of (second-order) MBPT onto a (generalized) Skyrme-like EDF. Such a program is meant to provide (i) an a posteriori understanding of the success of phenomenological energy functionals, (ii) an educated guess for extended functional forms and (iii) an estimate of the couplings of such a generalized EDF, including uncertainties associated with their RG scale dependence. Eventually, the needed accuracy could be obtained through a controlled refit of the "educated" couplings within their uncertainties, together with the addition for MR correlations associated with collective fluctuations.

## 2. Comparing Skyrme-EDF and MBPT energy expressions

Mapping MBPT onto SR-EDF does not strike as an natural and easy task at first. As already mentioned, MBPT fulfills the first basic requirement for such a mapping, i.e it naturally incorporates the symmetry-breaking concept by allowing the unperturbed vacuum of reference to break them. Still, it remains to be seen how various MBPT contributions can be approximated under the form of a quasi-local Skyrme-like EDF. To simplify the discussion, we omit the possibility to break particle number and thus to address the corresponding part of the nuclear EDF, i.e. its dependence on the anomalous tensor  $\kappa$ . Doing so requires to extend standard MBPT introduced in Sec. IV B to incorporate anomalous propagators, which is beyond the scope of the present lectures.

To simplify the discussion further, we consider the Skyrme parametrization defined in Eq. 20 in the limit where spin is omitted and where the coupling constant  $C_{qq'}^{\rho\rho}$  depends linearly on the local density such that it generates the simplest possible trilinear contribution. Eventually, the coordinate-space expression of such a simplified Skyrme EDF reads

$$\mathcal{E}[\rho] = \int d\vec{r} \sum_q \frac{\hbar^2}{2m} \tau_q(\vec{r}) + \sum_{qq'} \left[ C_{qq'}^{\rho\rho} \rho_q(\vec{r}) \rho_{q'}(\vec{r}) + C_{qq'}^{\rho\Delta\rho} \rho_q(\vec{r}) \Delta\rho_{q'}(\vec{r}) + C_{qq'}^{\rho\tau} \rho_q(\vec{r}) \tau_{q'}(\vec{r}) + C_{qq'}^{\rho\rho\rho} \rho_q^2(\vec{r}) \rho_{q'}(\vec{r}) \right]. \quad (52)$$

In the canonical basis where  $\rho_{\alpha\beta} = \rho_{\alpha\alpha} \delta_{\alpha\beta}$ , all local densities at play can be expressed under the form

$$f_q(\vec{r}) \equiv \sum_{\alpha} W_{\alpha\alpha}^f(\vec{r}q) \rho_{\alpha\alpha}. \quad (53)$$

with  $f \in \{\rho, \tau, \Delta\rho\}$  and

$$W_{\alpha\alpha}^{\rho}(\vec{r}q) \equiv \psi_{\alpha}^{\dagger}(\vec{r}q) \psi_{\alpha}(\vec{r}q), \quad (54)$$

$$W_{\alpha\alpha}^{\tau}(\vec{r}q) \equiv \nabla \psi_{\alpha}^{\dagger}(\vec{r}q) \cdot \nabla \psi_{\alpha}(\vec{r}q), \quad (55)$$

$$W_{\alpha\alpha}^{\Delta\rho}(\vec{r}q) \equiv \Delta [\psi_{\alpha}^{\dagger}(\vec{r}q) \psi_{\alpha}(\vec{r}q)], \quad (56)$$

such that the trilinear Skyrme EDF given in Eq. 52 can be re-written as [158]

$$\mathcal{E}[\rho] = \sum_{\alpha} t_{\alpha\alpha} \rho_{\alpha\alpha} + \frac{1}{2} \sum_{\alpha\beta} \bar{v}_{\alpha\beta}^{\rho\rho} \rho_{\alpha\alpha} \rho_{\beta\beta} + \frac{1}{6} \sum_{\alpha\beta\gamma} \bar{v}_{\alpha\beta\gamma}^{\rho\rho\rho} \rho_{\alpha\alpha} \rho_{\beta\beta} \rho_{\gamma\gamma}, \quad (57)$$

where matrix elements of the effective vertices are defined through

$$t_{\alpha\alpha} \equiv \int d\vec{r} \frac{\hbar^2}{2m} W_{\alpha\alpha}^{\tau}(\vec{r}q), \quad (58)$$

$$v_{\alpha\beta}^{\rho\rho} \equiv \int d\vec{r} 2 \sum_{f f'} C_{qq'}^{f f'} W_{\alpha\alpha}^f(\vec{r}q) W_{\beta\beta}^{f'}(\vec{r}q'), \quad (59)$$

$$v_{\alpha\beta\gamma}^{\rho\rho\rho} \equiv \int d\vec{r} 6 C_{qqq'}^{\rho\rho\rho} W_{\alpha\alpha}^{\rho}(\vec{r}q) W_{\beta\beta}^{\rho}(\vec{r}q) W_{\gamma\gamma}^{\rho}(\vec{r}q'). \quad (60)$$

Expression 57 demonstrates that any quasi-local Skyrme EDF can be seen as a particular functional of the density matrix  $\rho_{\alpha\beta}$ . This makes the connection with MBPT easier. Indeed, and omitting  $V^{3N}$  second-order contribution for simplicity<sup>17</sup>, the second-order MBPT energy reads in the canonical basis of the unperturbed

<sup>17</sup> As discussed in Ref. [138], such a contribution is small, at least for schematic 3N forces.

state

$$E^{HF} = \sum_{\alpha} t_{\alpha\alpha} \rho_{\alpha\alpha} + \frac{1}{2} \sum_{\alpha\beta} \bar{V}_{\alpha\beta\alpha\beta}^{NN} \rho_{\alpha\alpha} \rho_{\beta\beta} + \frac{1}{6} \sum_{\alpha\beta\gamma} \bar{V}_{\alpha\beta\gamma\alpha\beta\gamma}^{3N} \rho_{\alpha\alpha} \rho_{\beta\beta} \rho_{\gamma\gamma}, \quad (61)$$

$$\Delta E_2^{HF} = \frac{1}{4} \sum_{\alpha\beta\gamma\delta} \frac{|\bar{V}_{\alpha\beta\gamma\delta}^{NN}|^2}{\varepsilon_{\alpha} + \varepsilon_{\beta} - \varepsilon_{\gamma} - \varepsilon_{\delta}} \rho_{\alpha\alpha} \rho_{\beta\beta} (1 - \rho_{\gamma\gamma})(1 - \rho_{\delta\delta}), \quad (62)$$

which defines a non-empirical, generalized, nuclear EDF. Before stressing the differences with the Skyrme EDF, one can formally rewrite Eqs. 61 and 62 to make their resemblance with Eq. 57 even more apparent. Doing so, the second-order MBPT ground-state energy reads

$$E_2[\rho; \{\varepsilon_{\alpha}\}] = \sum_{\alpha} t_{\alpha\alpha} \rho_{\alpha\alpha} + \frac{1}{2} \sum_{\alpha\beta} \bar{w}_{\alpha\beta\alpha\beta}^{\rho\rho} \rho_{\alpha\alpha} \rho_{\beta\beta} + \frac{1}{6} \sum_{\alpha\beta\gamma} \bar{w}_{\alpha\beta\gamma\alpha\beta\gamma}^{\rho\rho\rho} \rho_{\alpha\alpha} \rho_{\beta\beta} \rho_{\gamma\gamma} + \frac{1}{24} \sum_{\alpha\beta\gamma\delta} \bar{w}_{\alpha\beta\gamma\delta\alpha\beta\gamma\delta}^{\rho\rho\rho\rho} \rho_{\alpha\alpha} \rho_{\beta\beta} \rho_{\gamma\gamma} \rho_{\delta\delta} \quad (63)$$

with up to four-body effective vertices defined as

$$\bar{w}_{\alpha\beta\gamma\delta\alpha\beta\gamma\delta}^{\rho\rho\rho\rho} \equiv 6 \frac{|\bar{V}_{\alpha\beta\gamma\delta}^{NN}|^2}{\varepsilon_{\alpha} + \varepsilon_{\beta} - \varepsilon_{\gamma} - \varepsilon_{\delta}}; \quad \bar{w}_{\alpha\beta\gamma\alpha\beta\gamma}^{\rho\rho\rho} \equiv \bar{V}_{\alpha\beta\gamma\alpha\beta\gamma}^{3N} - \frac{1}{2} \sum_l \bar{w}_{\alpha\beta\gamma\delta\alpha\beta\gamma\delta}^{\rho\rho\rho\rho}; \quad \bar{w}_{\alpha\beta\alpha\beta}^{\rho\rho} \equiv \bar{V}_{\alpha\beta\alpha\beta}^{NN} + \frac{1}{12} \sum_{\gamma\delta} \bar{w}_{\alpha\beta\gamma\delta\alpha\beta\gamma\delta}^{\rho\rho\rho\rho} \quad (64)$$

The functional  $E_2[\rho; \{\varepsilon_{\alpha}\}]$  thus obtained generalizes the Skyrme EDF in several respects, i.e. (i) it is of fourth order in the density matrix, (ii) it is not only a functional of the density matrix but also of single-particle energies and, as extensively discussed below, (iii) its coordinate-space expression is significantly more involved. The first of these extensions would be further enhanced by including  $\bar{V}^{3N}$  second-order contribution or by going to higher orders in MBPT. In itself though, it does not lie outside the frame of existing quasi-local Skyrme parameterizations that could handle higher-order dependencies on the density matrix. Contrarily, the explicit functional dependence on single-particle energies  $\{\varepsilon_{\alpha}\}$  lies outside the frame of existing nuclear EDF parameterizations. It is worth noting that such functionals are however known as *orbital-dependent energy functionals* [222] within the frame of electronic systems' density functional theory (DFT). The dependence on single-particle energies relates to the time non-locality associated with nucleonic in-medium propagations. It remains to be seen in the future whether an explicit dependence on single-particle energies is necessary and tractable in the nuclear context or whether it can be safely and consistently recast into a simpler form, e.g. an effective dependence on the density matrix.

The EDF form of Eq. 63 may naively suggest, just as Eq. 57, that it results from the average value, in the unperturbed vacuum  $|\Phi\rangle$ , of an (hypothetical) effective Hamilton operator containing two-body (second term), three-body (third term), four-body (fourth term) . . . pieces. However, Eq. 64, that provides microscopic expressions for the matrix elements of  $\bar{v}^{\rho\rho}$ ,  $\bar{v}^{\rho\rho\rho}$  . . . , demonstrates that re-extracting an (effective) Hamilton operator from the energy density has no foundation<sup>18</sup> and can at best be the result of approximations.

One further possible difference between the SR-EDF method introduced in Sec. II and MBPT described in Sec. IV B relates to the choice of self-energy  $\Sigma_{\alpha\beta}$  from which single-particle energies  $\{\varepsilon_{\alpha}\}$  are extracted. Indeed, the freedom exist in MBPT as to how  $h_{\alpha\beta} \equiv t_{\alpha\beta} + \Sigma_{\alpha\beta}$ , i.e.  $H_0$  and the unperturbed vacuum  $|\Phi\rangle$ , is chosen. Let us discuss three possible choices

1. In Sec. IV B, the HF self-energy

$$\begin{aligned} \Sigma_{\alpha\beta}^{HF} &= \sum_{\gamma} \left[ \bar{V}_{\alpha\gamma\beta\gamma}^{NN} + \frac{1}{2} \sum_{\gamma\delta} \bar{V}_{\alpha\gamma\delta\beta\gamma\delta}^{3N} \rho_{\delta\delta} \right] \rho_{\gamma\gamma} \\ &\equiv \sum_{\gamma} \bar{v}_{\alpha\gamma\beta\gamma}^{\rho h} \rho_{\gamma\gamma}, \end{aligned} \quad (65)$$

was used independently on the order  $n_{\max}$  of the ground-state energy expansion. In such a case, single-particle energies  $\{\varepsilon_{\alpha}\}$  have no particular meaning. Equation 65 provides the effective vertex  $\bar{v}^{\rho h}$  to first order.

<sup>18</sup> Note for instance that symmetry properties of  $\bar{v}_{ijkl}^{\rho\rho}$ ,  $\bar{v}_{ijklmn}^{\rho\rho\rho}$  and  $\bar{v}_{ijklijkl}^{\rho\rho\rho\rho}$  under the exchange of fermionic indices are *not* as expected from two-, three- and four-body operators.

2. A choice made to design non-empirical DFT consists of extracting the local and multiplicative optimized effective potential (OEP) from the correlated many-body energy

$$\Sigma^{OEP}(\vec{r}) \equiv \frac{\delta[E - T]}{\delta\rho(\vec{r})}, \quad (66)$$

where  $T$  is the unperturbed kinetic energy. In such a case, the energy  $\varepsilon_F$  of the last occupied orbital approximates the one-nucleon separation energy with the ground state of the neighboring system.

3. The choice leading to a natural mapping with the nuclear SR-EDF method, as it is traditionally implemented, consists of computing the energy-dependent self-energy

$$\Sigma_{\alpha\beta}^{EDF} \equiv \frac{\delta[E - T]}{\delta\rho_{\beta\alpha}}, \quad (67)$$

from the correlated binding energy and of extracting its on-shell quasi-particle part to define  $h_{\alpha\beta}$ . Consequently, and similarly to Eq. 65, the on-shell part of  $\Sigma_{\alpha\beta}^{EDF}$  provides the *dressed* effective vertex  $\bar{v}^{ph}$  (similarly to Eq. 6). In such a case, single-particle energies  $\{\varepsilon_\alpha\}$  approximate the quasi-particle component of one-nucleon separation energies with the neighboring systems.

Let us finally discuss the coordinate-space representation of the first and second-order contributions to the many-body ground-state energy. In order to make it transparent, we further simplify the analysis (i) by neglecting entirely the 3N force, (ii) by choosing  $V^{NN}$  as purely central and local, as well as (iii) by omitting spin and isospin degrees of freedom. For a more complete discussion, we refer the interested reader to Refs. [149, 152, 223]

The second term of Eq. 61 contains two contributions, i.e. the Hartree (direct) and the Fock (exchange) terms. By inserting two completeness relationships on the two-body Hilbert space  $\mathcal{H}_2$ , the Fock contribution reads

$$E^F \propto \iint d\vec{r}_1 d\vec{r}_2 V^{NN}(|\vec{r}_1 - \vec{r}_2|) \rho_{\vec{r}_1\vec{r}_2} \rho_{\vec{r}_2\vec{r}_1}, \quad (68)$$

which is a non-local functional of the *non-local* density matrix  $\rho_{\vec{r}_1\vec{r}_2}$ . Conversely, the Hartree contribution obtained from a local interaction is a non-local functional of the *local* part  $\rho_{\vec{r}_1\vec{r}_1}$  of the density matrix. Eventually, the first-order HF contribution displays a more involved coordinate-space expression than the local Skyrme functional. However, and as discussed in the next section, the fact that it is an *explicit* functional of the coordinate-space density matrix makes it amenable to the density matrix expansion.

Inserting four completeness relationships on  $\mathcal{H}_2$ , one typical second-order energy contribution reads

$$\begin{aligned} \Delta E_2^{HF} \subset & \iiint d\vec{r}_{1234} \left[ \sum_{\alpha\beta\gamma\delta} \psi_\alpha^*(\vec{r}_1) \psi_\beta^*(\vec{r}_2) V^{NN}(|\vec{r}_1 - \vec{r}_2|) \psi_\gamma(\vec{r}_1) \psi_\delta(\vec{r}_2) \right. \\ & \left. \times \psi_\gamma^*(\vec{r}_3) \psi_\delta^*(\vec{r}_4) V^{NN}(|\vec{r}_3 - \vec{r}_4|) \psi_\alpha(\vec{r}_3) \psi_\beta(\vec{r}_4) \right] \frac{\rho_{\alpha\alpha} \rho_{\beta\beta} (1 - \rho_{\gamma\gamma}) (1 - \rho_{\delta\delta})}{\varepsilon_\alpha + \varepsilon_\beta - \varepsilon_\gamma - \varepsilon_\delta}, \end{aligned}$$

and thus contains four triple integrals. The energy becomes a highly non-local functional that will be even more so when (i) starting from a non-local NN interaction, (ii) including the contribution from  $V^{3N}$  and/or (iii) going beyond second order, i.e. to larger  $n_{\max}$ . An additional key difference with  $E^{HF}$  is that  $\Delta E_2^{HF}$  is *not* an explicit functional of the coordinate-space density matrix and static potentials.

## E. The density matrix expansion

### 1. Basic features

Let us first present the basic idea of the density matrix expansion. The objective is to map finite-range physics associated with vacuum NN and 3N interactions into the form of a Skyrme-like EDF with density-dependent couplings. To do so, the studied contribution must take the form of an explicit functional of the one-body density matrix of the auxiliary state  $|\Phi\rangle$ . As discussed in the previous section, this is indeed the case of the HF contribution to the binding energy. Contrarily, the fact that  $\Delta E_2^{HF}$  is not an explicit functional of the coordinate-space density matrix makes it unamenable to the DME in its standard formulation. As a

matter of fact, one is still missing as of today a generalization of such an expansion technique to approximate contributions beyond the HF ones under a Skyrme-like form [224]. It is a challenge for the future to formulate such an extension. For now, we thus focus on approximating the HF contribution to the binding energy. The present discussion is again simplified by omitting  $V^{3N}$  as well as spin and isospin degrees of freedom, unless stated otherwise.

The DME technique comes back to Negele and Vautherin [143, 225]. Given that the energy is an explicit functional of the non-local density matrix, the central idea is to expand the latter into a finite sum of terms that are separable in relative  $\vec{r} \equiv \vec{r}_1 - \vec{r}_2$  and center of mass  $\vec{R} \equiv (\vec{r}_1 + \vec{r}_2)/2$  coordinates

$$\rho_{\vec{r}_1 \vec{r}_2} \approx \sum_f \Pi_f^\rho(kr) f(\vec{R}), \quad (69)$$

where  $f(\vec{R})$  represents a set of local one-body densities. Typically, one has  $f \in \{\rho, \tau, \Delta\rho\}$ , which corresponds to expanding the HF density matrix with up to two derivatives. The arbitrary parameter  $k$  in Eq. 69 has the dimension of the inverse of a distance and is to be equated to the local Fermi momentum<sup>19</sup>  $k \equiv k_F(\vec{R})$ , or to a similar function. Inserting expansion 69 back into Eq. 68, the Fock contribution to the energy reads

$$E^F \propto \int d\vec{R} \left[ C^{\rho\rho}(\vec{R}) \rho(\vec{R}) \rho(\vec{R}) + C^{\rho\Delta\rho}(\vec{R}) \rho(\vec{R}) \Delta\rho(\vec{R}) + C^{\rho\tau}(\vec{R}) \rho(\vec{R}) \tau(\vec{R}) \right], \quad (70)$$

which is nothing but a generalized local Skyrme-EDF expressed in terms of non-empirical, position/density dependent couplings  $C^{ff'}(\vec{R})$ , e.g.

$$C^{\rho\rho}(\vec{R}) \equiv 4\pi \int r^2 dr V^{NN}(r) \Pi_\rho^\rho(k_F(\vec{R})r) \Pi_\rho^\rho(k_F(\vec{R})r). \quad (71)$$

Equation 71 makes clear that the density/position dependence of the couplings is a direct consequence of the finite-range of the NN interaction. Given that *all* couplings acquire a density dependence through the DME, Eq. 70 is indeed more general than any existing empirical Skyrme EDF. Starting from a realistic vacuum Hamiltonian containing a 3N force, as one should, a richer EDF including a wealth of trilinear terms is obtained [223] that generalize the single trilinear term included for illustration purposes in Eq. 52. We note in passing that it is important to differentiate *genuine* density dependencies associated with original dependencies on the density matrix, as discussed in Sec. IV D 2 in connection with MBPT, from those resulting from the application of the DME. Indeed, both types of density dependencies do not carry the same physics. Last but not least, treating explicitly spin and isospin degrees of freedom also leads to a richer functional than the one displayed in Eq. 70. Including all those terms is eventually essential to any realistic application of the DME [152, 223].

Equation 70 is to be complemented with the Hartree contribution that can either be put under the form of a Skyrme-like EDF [153] or treated exactly. Regardless, the EDF thus obtained only contains the HF physics such that correlations associated with higher-order contributions must be added to produce any reasonable description of nuclei. Such a point is further discussed in Sec. IV E 4.

## 2. Negele and Vautherin DME

So far, Eq. 69 provides a formal expansion of the one-body density matrix. It remains to be seen how such an expansion can actually be obtained in practice, i.e. how quantitative  $\Pi_f^\rho$  functions are determined. Several DME variants applicable to the HF energy have been developed in the past [143, 226–228]. They mainly differ regarding (i) the choice made to fix the momentum scale  $k$ , (ii) the path followed to obtain actual expressions of the  $\Pi_f^\rho$  functions (see below) and (iii) the set of local densities that occur in the expansion.

The original DME expansion of Negele and Vautherin [143] relies on a truncated Bessel expansion of the non-locality operator  $e^{\frac{1}{2}\vec{r} \cdot (\vec{\nabla}_1 - \vec{\nabla}_2)}$  that leads to analytically-derived  $\Pi_f^\rho$  functions. The expansion presents the advantage to be exact in symmetric nuclear matter; i.e. it reduces to one term that provides the exact HF density matrix and energy. However, Negele and Vautherin's non-trivial DME is only formulated for spin-saturated nuclei where the spin degree can essentially be omitted. We refer the reader to Ref. [143] for details concerning the original DME approach.

<sup>19</sup> The local Fermi momentum relates to the isoscalar density through  $k_F(\vec{R}) = (6\pi^2 \rho_0(\vec{R})/st)^{1/3}$ , where  $s=2$  (1) and  $t=2$  (1) when spin and isospin degrees of freedom are (not) taken into account.

### 3. Novel DME approach based on phase-space-averaging techniques

Given that the overwhelming majority of nuclei are spin-unsaturated, an extension of the original DME is necessary. Recently, such a task was taken up and a new approach based on so-called *phase-space averaging techniques* was proposed to design an analytical DME in the general case of spin-unsaturated nuclei [149, 152]. After accuracy tests were performed in Ref. [149], the new expansion method was applied to realistic chiral NN and 3N potentials in Refs. [152] and [223], respectively.

Let us thus present this novel phase-space-averaging DME (PSA-DME) in some details. To do so, we re-introduce the spin degree of freedom but still omit the isospin one for simplicity. For a more complete discussion, we refer the reader to Ref. [152]. The approach aims at approximating both the scalar part  $\rho(\vec{r}_1, \vec{r}_2)$  and the vector part  $\vec{s}(\vec{r}, \vec{r}_2)$  of the one-body density matrix defined in an arbitrary single-particle basis through

$$\rho(\vec{r}_1, \vec{r}_2) \equiv \sum_{\sigma_1 \sigma_2} \rho(\vec{r}_1 \sigma_1, \vec{r}_2 \sigma_2) \langle \sigma_2 | \mathbb{1} | \sigma_1 \rangle = \sum_{\sigma_1} \sum_{ij} \varphi_i^*(\vec{r}_2 \sigma_1) \varphi_j(\vec{r}_1 \sigma_1) \rho_{ji}, \quad (72)$$

$$\vec{s}(\vec{r}, \vec{r}_2) \equiv \sum_{\sigma_1 \sigma_2} \rho(\vec{r}_1 \sigma_1, \vec{r}_2 \sigma_2) \langle \sigma_2 | \vec{\sigma} | \sigma_1 \rangle = \sum_{\sigma_1 \sigma_2} \sum_{ij} \varphi_i^*(\vec{r}_2 \sigma_2) \langle \sigma_2 | \vec{\sigma} | \sigma_1 \rangle \varphi_j(\vec{r}_1 \sigma_1) \rho_{ji}, \quad (73)$$

where the former is nothing but  $\rho_{\vec{r}_1 \vec{r}_2}$  used previously when omitting the spin degree of freedom. In the approximation that the single-particle wave-functions of spin-orbit partners are identical, it can be shown that  $\vec{s}(\vec{r}_1, \vec{r}_2)$  is zero in spin-saturated nuclei.

Considering  $\rho(\vec{r}_1, \vec{r}_2)$  and  $\vec{s}(\vec{r}_1, \vec{r}_2)$  as the first and last three components of a four-vector  $\rho_\mu(\vec{r}_1, \vec{r}_2)$ , respectively, one starts with the formal identity

$$\begin{aligned} \rho_\mu(\vec{r}_1, \vec{r}_2) &= e^{i\vec{r} \cdot \vec{k}} e^{\vec{r} \cdot \left[ \frac{\vec{\nabla}_1 - \vec{\nabla}_2}{2} - i\vec{k} \right]} \sum_{i=1}^A \varphi_i^*(\vec{r}_2 \vec{\sigma}_2) \varphi_i(\vec{r}_1 \vec{\sigma}_1) \langle \vec{\sigma}_2 | \sigma_\mu | \vec{\sigma}_1 \rangle \Big|_{\vec{r}_1 = \vec{r}_2 = \vec{R}} \\ &\approx e^{i\vec{r} \cdot \vec{k}} \left[ 1 + \vec{r} \cdot \left( \frac{\vec{\nabla}_1 - \vec{\nabla}_2}{2} - i\vec{k} \right) + \frac{1}{2} \left( \vec{r} \cdot \left( \frac{\vec{\nabla}_1 - \vec{\nabla}_2}{2} - i\vec{k} \right) \right)^2 \right] \sum_{i=1}^A \varphi_i^*(\vec{r}_2 \vec{\sigma}_2 \vec{\tau}_2) \varphi_i(\vec{r}_1 \vec{\sigma}_1 \vec{\tau}_1) \langle \vec{\sigma}_2 | \sigma_\mu | \vec{\sigma}_1 \rangle \Big|_{\vec{r}_1 = \vec{r}_2 = \vec{R}} \end{aligned} \quad (74)$$

with  $\mu \in \{0, 1, 2, 3\}$ , while  $\sigma_0$  corresponds to the two-by-two identity matrix and  $\sigma_{1,2,3} \equiv \sigma_{x,y,z}$ . The vector  $\vec{k}$  is a yet-to-be-determined momentum scale whose choice must be driven by the optimization of the truncated expansion in Eq. 74. Physically,  $\vec{k}$  typically represents an averaged relative momentum in the nucleus. Assuming a model local momentum distribution  $g(\vec{R}, \vec{k})$  and defining

$$\Pi_n(\vec{r}, \vec{R}) \equiv \frac{\int d\vec{k} e^{i\vec{r} \cdot \vec{k}} (\vec{r} \cdot \vec{k})^n g(\vec{R}, \vec{k})}{\int d\vec{k} g(\vec{R}, \vec{k})}, \quad (75)$$

$$j_{a,\mu}(\vec{R}) \equiv -\frac{i}{2} (\vec{\nabla}_a^{(1)} - \vec{\nabla}_a^{(2)}) \rho_\mu(\vec{r}_1, \vec{r}_2) \Big|_{\vec{r}_1 = \vec{r}_2 = \vec{R}}, \quad (76)$$

$$\tau_{ab,\mu}(\vec{R}) \equiv \nabla_a^{(1)} \nabla_b^{(2)} \rho_\mu(\vec{r}_1, \vec{r}_2) \Big|_{\vec{r}_1 = \vec{r}_2 = \vec{R}}, \quad (77)$$

with  $a, b \in \{x, y, z\}$ , the phase-space averaging of Eq. (74) is performed over the model space defined by  $g(\vec{R}, \vec{k})$  to obtain

$$\begin{aligned} \rho_\mu(\vec{r}_1, \vec{r}_2) &\approx \left[ \Pi_0 + \Pi_0 \vec{r} \cdot \frac{\vec{\nabla}_1 - \vec{\nabla}_2}{2} - i\Pi_1 + \frac{\Pi_0}{2} \left( \vec{r} \cdot \frac{\vec{\nabla}_1 - \vec{\nabla}_2}{2} \right)^2 - \frac{\Pi_2}{2} - i\Pi_1 \left( \vec{r} \cdot \frac{\vec{\nabla}_1 - \vec{\nabla}_2}{2} \right) \right] \\ &\quad \times \sum_{i=1}^A \varphi_i^*(\vec{r}_2 \vec{\sigma}_2 \vec{\tau}_2) \varphi_i(\vec{r}_1 \vec{\sigma}_1 \vec{\tau}_1) \langle \vec{\sigma}_2 | \hat{\sigma}_\mu | \vec{\sigma}_1 \rangle \Big|_{\vec{r}_1 = \vec{r}_2 = \vec{R}}, \\ &\approx \left[ \Pi_0 - i\Pi_1 - \frac{\Pi_2}{2} \right] \rho_\mu(\vec{R}) + i \left[ \Pi_0 - i\Pi_1 \right] \sum_a r_a j_{a,\mu}(\vec{R}) + \frac{\Pi_0}{2} \sum_{ab} r_a r_b \left[ \frac{1}{4} \nabla_a \nabla_b \rho_\mu(\vec{R}) - \tau_{ab,\mu}(\vec{R}) \right] \end{aligned} \quad (78)$$

where local densities are as defined previously. Among those, we note that, while  $j_{a,0}(\vec{R})$  denotes the so-far unspecified current density  $j_a(\vec{R})$ , densities  $\sum_a \tau_{aa,0}(\vec{R})$  and  $j_{a,i}(\vec{R})$  match, at the price of adding an isospin index, the kinetic density  $\tau(\vec{R})$  and the spin-current tensor  $J_{ai}(\vec{R})$  defined in Eqs. 16 and 17, respectively. Even without specifying the chosen model momentum distribution, it is clear that the PSA-DME of the scalar and

vector parts are treated on equal footing. In other words, the PSA leads to a channel-independent DME with identical  $\Pi_f^p$  and  $\Pi_f^v$  functions for the scalar part and the vector part of the density matrix, respectively.

As discussed in Ref. [149], the PSA-DME is well-suited to incorporate effects of the diffuseness and the anisotropy of the local momentum distribution at the surface of finite nuclei. Presently, we take a simplified approach that consists of using the phase space of symmetric nuclear matter to perform the averaging, i.e.  $g(\vec{R}, \vec{k}) = \Theta(k_F - \vec{k})$ . As a result, one obtains in Eq. 78

$$\Pi_0(k_F r) = 3 \frac{j_1(k_F r)}{k_F r} \approx 1 + \mathcal{O}(k_F r)^2, \quad (79)$$

$$\Pi_1(k_F r) = -i3 j_0(k_F r) + i9 \frac{j_1(k_F r)}{k_F r} \approx i \frac{(k_F r)^2}{5} + i \mathcal{O}(k_F r)^4, \quad (80)$$

$$\Pi_2(k_F r) = 15 j_0(k_F r) - 36 \frac{j_1(k_F r)}{k_F r} - 3 \cos(k_F r) \approx \frac{(k_F r)^2}{5} + \mathcal{O}(k_F r)^4. \quad (81)$$

While  $\Pi_0$  starts with 1,  $\Pi_1$  and  $\Pi_2$  start with  $\mathcal{O}(k_F r)^2$ . Using a weak ordering that counts  $k_F$  and a gradient on the same ground, Eq. (78) can be rearranged as

$$\rho_\mu(\vec{r}_1, \vec{r}_2) \approx \Pi_0 \rho_\mu(\vec{R}) + i \Pi_0 \sum_{ab} r_a j_{a,\mu}(\vec{R}) + \frac{\Pi_0}{2} \sum_{ab} r_a r_b \left[ \frac{1}{4} \nabla_a \nabla_b \rho_\mu(\vec{R}) - \tau_{ab,\mu}(\vec{R}) + \frac{\delta_{ab} \Lambda(k_F r) k_F^2}{5} \rho_\mu(\vec{R}) \right] \quad (82)$$

where  $i \Pi_1 \sum_a r_a j_{a,\mu}(\vec{R})$  was neglected as it turns out to be a third-order correction. The function  $\Lambda(k_F r)$  appearing in Eq. 82 is defined as

$$\Lambda(k_F r) \equiv -5 \frac{i2 \Pi_1(k_F r) + \Pi_2(k_F r)}{k_F^2 r^2 \Pi_0(k_F r)} \approx 1 + \mathcal{O}(k_F r)^2, \quad (83)$$

such that, approximating it by its leading term, one finds

$$\rho_\mu(\vec{r}_1, \vec{r}_2) \approx \Pi_0 \rho_\mu(\vec{R}) + i \Pi_0 \sum_a r_a j_{a,\mu}(\vec{R}) + \frac{\Pi_0}{2} \sum_{a,b} r_a r_b \left[ \frac{1}{4} \nabla_a \nabla_b \rho_\mu(\vec{R}) - \tau_{ab,\mu}(\vec{R}) + \delta_{ab} \frac{k_F^2}{5} \rho_\mu(\vec{R}) \right] \quad (84)$$

The last step consists of performing an angle averaging over the orientation of  $\vec{r}$ . Using the identity

$$\frac{1}{4\pi} \int d\vec{e}_r (\vec{r} \cdot \vec{A})(\vec{r} \cdot \vec{B}) = \frac{r^2}{3} \vec{A} \cdot \vec{B}, \quad (85)$$

and noting that the current density  $\vec{j}(\vec{R})$  vanishes in time-reversal invariant systems, one finally obtains

$$\rho(\vec{r}_1, \vec{r}_2) \simeq \Pi_0(k_F r) \rho(\vec{R}) + \frac{r^2}{6} \Pi_0(k_F r) \left[ \frac{1}{4} \Delta \rho(\vec{R}) - \tau(\vec{R}) + \frac{3}{5} k_F^2 \rho(\vec{R}) \right], \quad (86)$$

and

$$s_v(\vec{r}_1, \vec{r}_2) \simeq i \Pi_0(k_F r) \sum_{\mu=x}^z r_\mu J_{\mu v}(\vec{R}). \quad (87)$$

It is then trivial to reorder terms in order to generate the expansion in the form of Eq. 69, i.e. obtaining  $\Pi_\rho$ ,  $\Pi_{\Delta\rho}$  and  $\Pi_\tau$  in terms of  $\Pi_0$ . It is worth noting that, just like the original Negele and Vautherin's DME, the PSA-DME is exact in the symmetric nuclear matter limit. In Ref. [154], it was shown that the PSA-DME is the most accurate DME to second order in gradients. In the same study, a DME approach based on a (phenomenologically) damped Taylor expansion was proposed and shown to display the most optimal accuracy among existing variants when expanding the one-body density matrix up to sixth order in derivatives.

#### 4. On-going developments

In Refs. [152] and [223], the PSA-DME was applied to the non-local Fock energy obtained from chiral EFT NN and 3N interactions at N<sup>2</sup>LO. The input chiral interaction separates into finite-range pion-exchange interactions and scale-dependent contact terms, e.g. the NN piece can be decomposed according to

$$V_{EFT}^{NN} \equiv V_\pi^{NN} + V_{ct}^{NN}(\Lambda). \quad (88)$$

As a result, DME couplings  $C_{qq'}^{ff'}$  (from NN) and  $C_{qq'q''}^{ff'f''}$  (from 3N) appearing in the local EDF decompose into a cutoff-dependent coupling constant arising from zero-range contact interactions and a cutoff-independent coupling function of the density arising from universal long-range pion exchanges, e.g.

$$C_{qq'}^{\rho\tau} \equiv C_{qq'}^{\rho\tau}(\Lambda; V_{ct}^{\text{NN}}) + C_{qq'}^{\rho\tau}(\vec{R}; V_{\pi}^{\text{NN}}). \quad (89)$$

This implies that (i) the part of the resulting EDF associated with  $C_{qq'}^{ff'}(\Lambda; V_{ct}^{\text{NN}})$  and  $C_{qq'q''}^{ff'f''}(\Lambda; V_{ct}^{\text{3N}})$  is of the same form as the one obtained from a density-independent Skyrme vertex and that (ii) the novel density-dependencies entering  $C_{qq'}^{ff'}(\vec{R}; V_{\pi}^{\text{NN}})$  and  $C_{qq'q''}^{ff'f''}(\vec{R}; V_{\pi}^{\text{3N}})$  come from the best-understood parts of the underlying nuclear interactions. Restricting to time-reversal invariant systems, analytical expressions of all DME couplings were derived. The corresponding expressions are too lengthy to be reported here and we refer the reader to Refs. [152] and [223]. Still, all couplings can be written in a systematic way using a ‘‘skeleton form’’. For example, each coupling coming from the NN interaction is given by the sum of the LO ( $n = 0$ ), NLO ( $n = 1$ ), and N<sup>2</sup>LO ( $n = 2$ ) contributions

$$C_{qq'}^{ff'}(u) = \sum_{n=0}^2 C_{qq',n}^{ff'}(u), \quad (90)$$

with  $u \equiv k_F/m_{\pi}$  and the generic expressions

$$\begin{aligned} C_{qq',0}^{ff'}(u) &= \alpha_0^{ff'}(qq', u) + \alpha_1^{ff'}(qq', u) \log(1 + 4u^2) + \alpha_2^{ff'}(qq', u) \arctan(2u), \\ C_{qq',1}^{ff'}(u) &= \beta_0^{ff'}(qq', u) + \beta_1^{ff'}(qq', u) \left[ \log(1 + 2u^2 + 2u\sqrt{1+u^2}) \right]^2 + \beta_2^{ff'}(qq', u) \sqrt{1+u^2} \log(1 + 2u^2 + 2u\sqrt{1+u^2}), \\ C_{qq',2}^{ff'}(u) &= \gamma_0^{ff'}(qq', u) + \gamma_1^{ff'}(qq', u) \log(1 + u^2) + \gamma_2^{ff'}(qq', u) \arctan(u), \end{aligned}$$

where (lengthy) rational polynomials in  $u$ , i.e.  $\alpha_j^{ff'}(qq', u)$ ,  $\beta_j^{ff'}(qq', u)$  and  $\gamma_j^{ff'}(qq', u)$ , factorize functions exhibiting non-analytic behavior in  $u$  originating from the finite-range of the NN interaction.

The resulting dependence of the couplings on the isoscalar density is rather significant over the interval of interest for all couplings, which is at variance with standard phenomenological Skyrme parameterizations, whose only density-dependent couplings are  $C_{qq'}^{\rho\rho}$ . Without going into details, such a feature is visible in Fig. 43 that compares the density dependence of two particular couplings with those obtained from standard Skyrme parameterizations. We refer the reader to Refs. [152] and [223] for a more extensive analysis.

In the long term, investigating the impact of such non-trivial in-medium dependencies generated by pion exchanges is one key objective. For such a study to be based on an entirely non-empirical EDF, a generalized DME method applicable to perturbative contributions beyond HF remains to be invented [224]. In the meantime, one can use a semi-empirical approach based on a microscopically-guided Skyrme phenomenology [229] where the density-dependent couplings associated with pion-exchanges from NN and 3N interactions at the HF level are added to density-independent Skyrme parameters subsequently refit to data. This semi-phenomenological approach is motivated by the observation that the EFT contact terms can in principle be fixed to any low-energy quantities.

Even within such a semi-empirical approach, the inclusion of chiral EFT one- and two-pion-exchange interactions are expected, through their rich spin and isospin dependence, to provide valuable microscopic constraints on the poorly-understood isovector properties of the EDF. Dramatic changes of bulk nuclear properties are not envisioned compared to simpler empirical parameterizations due to the tendency of pions to average out in spin and isospin sums. However, interesting consequences can be expected for single-particle properties (which phenomenology tells us are sensitive probes of the tensor force) and systematics along long isotopic chains. In particular, two very different microscopic origins of spin-orbit properties (i.e., short-range NN and long-range 3N spin-orbit interactions) are treated on equal footing and can thus be investigated. This is in contrast to empirical Skyrme and Gogny functionals, where the zero-range spin-orbit interaction has no obvious connection with the sub-leading (but quantitatively significant) 3N sources of spin-orbit splittings. Overall, probing the impact of microscopic 3N forces on the structure of medium- and heavy-mass nuclei is one current frontier of low-energy nuclear theory.

## V. SUMMARY

The present lectures outline the starting efforts that are currently being made towards the building of so-called *non-empirical* energy density functionals that are explicitly rooted into low-momentum interactions

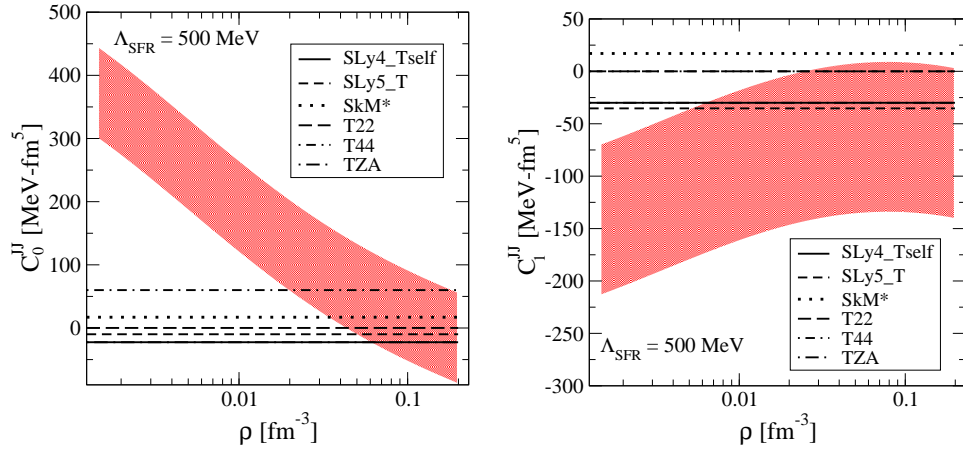


FIG. 43: (Color online) Density dependence of the Fock DME isoscalar  $C_0^{JJ}$  and isovector  $C_1^{JJ}$  couplings augmented with a "natural" Skyrme-like contribution (see Ref. [152]) and compared to the corresponding couplings obtained from a representative set of Skyrme parameterizations. Taken from Ref. [152].

generated from renormalization group methods. The goal of such an endeavor is two (re)connect two sub-fields of low-energy nuclear theory, i.e. so-called ab-initio and energy density functional approaches, which have been rather disconnect over the last three decades. Eventually, the objective is to gain predictive power in the computation of heavy-nuclei properties, in particular in view of studying the unknown territory of very neutron-rich nuclei.

## VI. ACKNOWLEDGMENTS

It is a pleasure to thank the organizers of the 2009 Joliot-Curie School 2009 which was very fulfilling, both workwise and leisurewise. I also wish to thank M. Bender, K. Bennaceur, S. K. Bogner, B. A. Brown, R. J. Furnstahl, B. Gebremariam, K. Hebeler, P.-H. Heenen, D. Lacroix, T. Lesinski, J. Meyer, V. Rotival, J. Sadoudi and A. Schwenk for fruitful collaborations on various matters related to the subject of the present lectures. Special thanks are due to V. Soma and D. Lacroix for a careful reading of the manuscript as well as to J. Sadoudi and K. Hebeler for preparing several of the figures used the present document. Last but not least, I would like to thank A. Gunther, R. Roth, H. Hergert and S. Reinhardt for adapting a figure from Ref. [138].

## VII. BIBLIOGRAPHY

- [1] R. B. Wiringa, V. G. J. Stoks, and R. Schiavilla, *Phys. Rev. C* **51**, 38 (1995).
- [2] H. Witała, W. Glöckle, D. Hüber, J. Golak, and H. Kamada, *Phys. Rev. Lett.* **81**, 1183 (1998).
- [3] S. Nemoto, K. Chmielewski, S. Oryu, and P. U. Sauer, *Phys. Rev. C* **58**, 2599 (1998).
- [4] S. Kistryn, E. Stephan, A. Biegun, K. Bodek, A. Deltuva, E. Epelbaum, K. Ermisch, W. Glöckle, J. Golak, N. Kalantar-Nayestanaki, et al., *Phys. Rev. C* **72**, 044006 (2005).
- [5] A. Nogga, H. Kamada, and W. Glöckle, *Phys. Rev. Lett.* **85**, 944 (2000).
- [6] A. Nogga, S. K. Bogner, and A. Schwenk, *Phys. Rev. C* **70**, 061002 (2004).
- [7] A. Faessler, S. Krewald, and G. J. Wagner, *Phys. Rev. C* **11**, 2069 (1975).
- [8] J. Fujita and H. Miyazawa, *Prog. Theor. Phys.* **17**, 360 (1957).
- [9] B. Loiseau and Y. Nogami, *Nucl. Phys.* **B2**, 470 (1967).
- [10] W. Zuo, I. Bombaci, and U. Lombardo, *Phys. Rev. C* **60**, 024605 (1999).
- [11] A. Lejeune, U. Lombardo, and W. Zuo, *Phys. Lett.* **B477**, 45 (2000).
- [12] W. Zuo, A. Lejeune, U. Lombardo, and J. Mathiot, *Nucl. Phys.* **A706**, 418 (2002).
- [13] W. Zuo, A. Lejeune, U. Lombardo, and J. Mathiot, *Eur. Phys. J.* **A14**, 469 (2002).

- [14] F. Coester, S. Cohen, B. Day, and C. M. Vincent, *Phys. Rev. C* **1**, 769 (1970).
- [15] R. Brockmann and R. Machleidt, *Phys. Rev. C* **42**, 1965 (1990).
- [16] R. Brockmann and R. Machleidt, *Phys. Rev. C* **42**, 1981 (1990).
- [17] A. Sonzogni (2007), URL <http://www.nndc.bnl.gov/chart/>.
- [18] Committee on the Physics of the Universe, *Connecting Quarks with the Cosmos : Eleven Science Questions for the New Century* (The National Academies Press, Washington D.C., 2003).
- [19] O. Sorlin and M.-G. Porquet, *Prog. Part. Nucl. Phys.* **61**, 602 (2008).
- [20] I. Tanihata, T. Kobayashi, O. Yamakawa, S. Shimoura, K. Ekuni, K. Sugimoto, N. Takahashi, T. Shimoda, and H. Sato, *Phys. Lett.* **B160**, 380 (1985).
- [21] M. Fukuda, T. Ichihara, N. Inabe, T. Kubo, H. Kumagai, T. Nakagawa, Y. Yano, I. Tanihata, M. Adachi, K. Asahi, et al., *Phys. Lett.* **B268**, 339 (1991).
- [22] I. Tanihata, H. Hamagaki, O. Hashimoto, Y. Shida, N. Yoshikawa, K. Sugimoto, O. Yamakawa, T. Kobayashi, and N. Takahashi, *Phys. Rev. Lett.* **55**, 2676 (1985).
- [23] I. Tanihata, H. Hamagaki, O. Hashimoto, S. Nagamiya, Y. Shida, N. Yoshikawa, O. Yamakawa, K. Sugimoto, T. Kobayashi, D. Greiner, et al., *Phys. Lett.* **B160**, 380 (1985).
- [24] P. Hansen and B. Jonson, *Europhys. Lett.* **4**, 409 (1987).
- [25] A. S. Jensen, K. Riisager, D. V. Fedorov, and E. Garrido, *Rev. Mod. Phys.* **76**, 215 (2004).
- [26] B. Blank and M. Ploszajczak, *Rept. Prog. Phys.* **71**, 046301 (2008).
- [27] P. Delheij, L. Blomeley, M. Froese, G. Gwinner, V. Ryjkov, M. Smith, and J. Dilling, *Hyp. Int.* **173**, 123 (2006).
- [28] M. Mukherjee, D. Beck, K. Blaum, G. Bollen, J. Dilling, S. George, F. Herfurth, A. Herlert, A. Kellerbauer, H.-J. Kluge, et al., *Eur. Phys. J. A* **35**, 1 (2008).
- [29] B. Schlitt, K. Beckert, T. Beha, H. Eickhoff, B. Franzke, H. Geissel, H. Irnich, H. C. Jung, T. F. Kersch, O. Klepper, et al., *Hyp. Int.* **99**, 117 (1996).
- [30] M. W. Kirson, *Phys. Lett. B* **646**, 246 (2007).
- [31] H. Frisk, *Z. Phys. A* **330**, 241 (1988).
- [32] A. Gorgen, E. Clement, E. Bouchez, A. Chatillon, W. Korten, Y. Le Coz, C. Theisen, C. Andreoiu, F. Becker, B. Blank, et al., *Acta Phys. Pol. B* **36**, 1281 (2005).
- [33] M. Ionescu-Bujor, A. Iordachescu, N. Marginean, C. Ur, D. Bucurescu, G. Suliman, D. Balabanski, F. Brandolini, S. Chmel, P. Detistov, et al., *Phys. Lett. B* **650**, 141 (2007).
- [34] K.-H. Schmidt, S. Steinhuser, C. Bockstiegel, A. Grewe, A. Heinz, A. R. Junghans, J. Benlliure, H.-G. Clerc, M. de Jong, J. Muller, et al., *Nucl. Phys.* **A661**, 221 (2000).
- [35] M. A. Caprio (2005), Ph.D. Thesis, nucl-ex/0502004.
- [36] D. Ackermann, *Nucl. Phys.* **A787**, 353 (2007).
- [37] D. Lacroix, "Introduction - Strong interaction in the nuclear medium : new trends", *Lectures given at Joliot Curie Summer School : Strong interaction in the nuclear medium : new trends, Lacanau, France, 27 Sept.-03 Oct., arXiv :1001.5001* (2009).
- [38] P. Moller, J. R. Nix, W. D. Myers, and W. J. Swiatecki, *At. Data Nucl. Data. Tables* **59**, 185 (2002).
- [39] G. Royer and C. Gautier, *Phys. Rev.* **C73**, 067302 (2006).
- [40] J. L. Friar, G. L. Payne, V. G. J. Stoks, and J. J. de Swart, *Phys. Lett. B* **311**, 4 (1988).
- [41] W. Glockle and H. Kamada, *Phys. Rev. Lett.* **71**, 971 (1993).
- [42] A. Nogga, D. Huber, K. Hamada, and W. Glockle, *Phys. Lett. B* **A409**, 19 (1997).
- [43] B. S. Pudliner, V. R. Pandharipande, J. Carlson, S. C. Pieper, and R. B. Wiringa, *Phys. Rev. C* **56**, 1720 (1997).
- [44] R. B. Wiringa, *Nucl. Phys.* **A631**, 70 (1998).
- [45] R. B. Wiringa, S. C. Pieper, J. Carlson, and V. R. Pandharipande, *Phys. Rev. C* **62**, 014001 (2000).
- [46] K. Varga, Y. Suzuki, K. Arai, and Y. Ogawa, *Nucl. Phys.* **A696**, 383 (1998).
- [47] Y. Suzuki, K. Varga, and J. Usukura, *Nucl. Phys.* **A631**, 91 (1999).
- [48] C. Ordonez, K. Arai, Y. Suzuki, and K. Varga, *Nucl. Phys.* **A673**, 122 (2001).

- [49] P. Navrátil and B. R. Barrett, Phys. Rev. C **54**, 2986 (1996).
- [50] P. Navrátil and B. R. Barrett, Phys. Rev. C **57**, 562 (1998).
- [51] P. Navrátil and B. R. Barrett, Phys. Rev. C **57**, 3119 (1998).
- [52] P. Navrátil, G. P. Kamuntavicius, and B. R. Barrett, Phys. Rev. C **61**, 044001 (2000).
- [53] K. Kowalski, D. J. Dean, M. Hjorth-Jensen, T. Papenbrock, and P. Piecuch, Phys. Rev. Lett. **92**, 132501 (2004).
- [54] D. J. Dean and Hjorth-Jensen, Phys. Rev. C **69**, 054320 (2004).
- [55] G. Hagen, D. J. Dean, M. Hjorth-Jensen, and T. Papenbrock, Phys. Lett. B **656**, 169 (2007).
- [56] G. Hagen, T. Papenbrock, D. J. Dean, A. Schwenk, A. Nogga, M. Wloch, and P. Piecuch, Phys. Rev. C **76**, 034302 (2007).
- [57] G. Hagen, D. J. Dean, M. Hjorth-Jensen, T. Papenbrock, and A. Schwenk, Phys. Rev. C **76**, 044305 (2007).
- [58] G. Hagen, T. Papenbrock, D. J. Dean, and M. Hjorth-Jensen (2010), arXiv :1005.2627.
- [59] W. H. Dickhoff and C. Barbieri, Prog. Part. Nucl. Phys. **52**, 377 (2004).
- [60] C. Barbieri and M. Hjorth-Jensen, Phys. Rev. C **79**, 064313 (2009).
- [61] C. Barbieri, Phys. Rev. Lett. **103**, 202502 (2009).
- [62] E. Caurier, G. Martínez-Pinedo, F. Nowacki, A. Poves, and A. P. Zuker, Rev. Mod. Phys. **77**, 427 (2005).
- [63] D. J. Dean, T. Engeland, M. Hjorth-Jensen, M. Kartamyshev, and E. Osnes, Prog. Part. Nucl. Phys. **53**, 419 (2004).
- [64] D. J. Dean, T. Engeland, M. Hjorth-Jensen, M. Kartamyshev, and E. Osnes, Prog. Part. Nucl. Phys. **53**, 419 (2004).
- [65] B. A. Brown and W. A. Richter, Phys. Rev. C **74**, 034315 (2006).
- [66] A. P. Zuker, Phys. Rev. Lett. **90**, 042502 (2003).
- [67] T. Otsuka, T. Suzuki, J. D. Holt, A. Schwenk, and Y. Akaishi (2009).
- [68] M. Bender, P.-H. Heenen, and P.-G. Reinhard, Rev. Mod. Phys. **75**, 121 (2003).
- [69] M. Grasso, “*Effective interactions and energy functionals : applications to nuclear systems*”, *Lectures given at Joliot Curie Summer School : Strong interaction in the nuclear medium : new trends, Lacanau, France, 27 Sept.-03 Oct.* (2009).
- [70] V. Rotival and T. Duguet, Phys. Rev. C **79**, 054308 (2009).
- [71] E. Chabanat, P. Bonche, P. Haensel, J. Meyer, and R. Schaeffer, Nucl. Phys. **A635**, 231 (1998).
- [72] V. Rotival, K. Bennaceur, and T. Duguet, Phys. Rev. C **79**, 054309 (2009).
- [73] F. Tondeur, M. Brack, M. Farine, and J. M. Pearson, Nucl. Phys. **A420**, 297 (1984).
- [74] S. Köhler, Nucl. Phys. **A258**, 301 (1976).
- [75] T. Lesinski, M. Bender, K. Bennaceur, T. Duguet, and J. Meyer, Phys. Rev. C **76**, 014312 (2007).
- [76] M. Beiner, H. Flocard, N. Giai, and P. Quentin, Nucl. Phys. **A238**, 29 (1975).
- [77] R. Machleidt, F. Sammarruca, and Y. Song, Phys. Rev. C **53**, 1483 (1996).
- [78] R. Machleidt, Phys. Rev. C **63**, 024001 (2001).
- [79] V. G. J. Stoks, R. A. M. Klomp, C. P. F. Terheggen, and J. J. de Swart, Phys. Rev. C **49**, 2950 (1994).
- [80] E. Epelbaum, “*Nuclear forces from chiral effective field theory : a primer*”, *Lectures given at Joliot Curie Summer School : Strong interaction in the nuclear medium : new trends, Lacanau, France, 27 Sept.-03 Oct.*, arXiv :1001.3229 (2009).
- [81] M. Walzl, U.-G. Meißner, and E. Epelbaum, Nucl. Phys. **A693**, 663 (2001).
- [82] E. Epelbaum, U.-G. Meißner, and W. Glöckle, Nucl. Phys. **A714**, 535 (2003).
- [83] E. Epelbaum, W. Glöckle, and U.-G. Meißner, Nucl. Phys. **A747**, 362 (2005).
- [84] E. Epelbaum, Prog. Part. Nucl. Phys. **57**, 654 (2006).
- [85] B. Borasoy, E. Epelbaum, H. Krebs, D. Lee, and U.-G. Meißner, Eur. Phys. J. A **31**, 105 (2007).
- [86] B. Borasoy, E. Epelbaum, H. Krebs, D. Lee, and U.-G. Meißner, Eur. Phys. J. A **35**, 343 (2008).

- [87] S. K. Bogner, A. Schwenk, R. J. Furnstahl, and A. Nogga, Nucl. Phys. A **763**, 59 (2005).
- [88] S. K. Bogner, R. J. Furnstahl, A. Nogga, and A. Schwenk (2009), arXiv :0903.3366.
- [89] K. Hebeler and A. Schwenk (2009), arXiv :0911.0483.
- [90] S. K. Bogner, R. J. Furnstahl, and A. Schwenk (2009), arXiv :0912.3688.
- [91] G. P. Lepage, “*How to Renormalize the Schrödinger Equation*”, *Lectures given at 9th Jorge Andre Swieca Summer School : Particles and Fields, Sao Paulo, Brazil, February, nucl-th/9706029* (1997).
- [92] P. F. Bedaque and U. van Kolck, Ann. Rev. Nucl. Part. Sci. **52**, 339 (2002).
- [93] S. K. Bogner, T. T. S. Kuo, and A. Schwenk, Phys. Rept. **386**, 1 (2003).
- [94] E. Epelbaum, H.-W. Hammer, and U.-G. Meissner, Rev. Mod. Phys. **81**, 1773 (2009).
- [95] S. Ramanan, S. K. Bogner, and R. J. Furnstahl, Nucl. Phys. **A797**, 81 (2007).
- [96] S. K. Bogner, T. T. S. Kuo, A. Schwenk, D. R. Entem, and R. Machleidt, Phys. Lett. B **576**, 265 (2003).
- [97] F. Coester, S. Cohen, B. Day, and C. M. Vincent, Phys. Rev. C **1**, 769 (1970).
- [98] M. I. Haftel and F. Tabakin, Phys. Rev. C **3**, 921 (1971).
- [99] H. A. Bethe, Ann. Rev. Nucl. Part. Sci. **21**, 93 (1971).
- [100] E. Epelbaum, W. Glockle, and U.-G. Meissner, Nucl. Phys. **A747**, 362 (2005).
- [101] S. C. Pieper, Nucl. Phys. A **751**, 516 (2005).
- [102] S. Quaglioni and P. Navratil, Few Body Syst. **44**, 337 (2008).
- [103] G. Hagen, T. Papenbrock, D. J. Dean, and M. Hjorth-Jensen, Phys. Rev. Lett. **101**, 092502 (2008).
- [104] P. Hohenberg and W. Kohn, Phys. Rev. **136**, B864 (1964).
- [105] W. Kohn and L. J. Sham, Phys. Rev. **140**, A1133 (1965).
- [106] W. Kohn, Rev. Mod. Phys. **71**, 1253 (1998).
- [107] A. Nagy, Phys. Rep. **298**, 1 (1998).
- [108] R. M. Dreizler and E. K. U. Gross, *Density Functional Theory : An Approach to the Quantum Many-Body Problem* (Springer-Verlag, Berlin, 1990).
- [109] R. G. Parr and W. Yang, *Density-Functional Theory of Atoms and Molecules* (Clarendon, Oxford, 1989).
- [110] C. Fiolhais, F. Nogueira, and M. Marques, eds., *A Primer in Density Functional Theory*, vol. 620 of *Lecture Notes in Physics* (Springer, Berlin and Heidelberg, 2003).
- [111] W. Koch and M. C. Holthausen, *A Chemist’s Guide to Density Functional Theory* (Wiley-VCH, Weinheim, 2001).
- [112] M. Beiner and R. J. Lombard, Ann. Phys. (NY) **86**, 262 (1974).
- [113] I. Z. Petkov and M. V. Stoitsov, *Nuclear Density Functional Theory* (Clarendon, Oxford, 1989).
- [114] S. A. Fayans, S. V. Tolokonnikov, E. L. Trykov, and D. Zawischa, Nucl. Phys. **A676**, 49 (2000).
- [115] G. A. Lalazissis, P. Ring, and D. Vretenar, eds., *Extended Density Functionals in Nuclear Physics*, vol. 641 of *Lecture Notes in Physics* (Springer, Berlin and Heidelberg, 2004).
- [116] Y. Yu and A. Bulgac, Phys. Rev. Lett. **90**, 222501 (2003).
- [117] R. J. Furnstahl, J. Phys. **G31**, S1357 (2005).
- [118] J. Engel, Phys. Rev. C **75**, 014306 (2007).
- [119] J. Messud, M. Bender, and E. Suraud, Phys. Rev. **C80**, 054314 (2009).
- [120] D. Lacroix, T. Duguet, and M. Bender, Phys. Rev. **C79**, 044318 (2009).
- [121] T. Duguet and J. Sadoudi, J. Phys. G : Nucl. Part. Phys. **37**, 064009 (2010), arXiv :1001.0673.
- [122] B. G. Giraud, Phys. Rev. C **77**, 014311 (2008).
- [123] B. G. Giraud, B. K. Jennings, and B. R. Barrett, Phys. Rev. **A78**, 032507 (2008).
- [124] T. Lesinski, K. Bennaceur, T. Duguet, and J. Meyer, Phys. Rev. C **74**, 044315 (2006).
- [125] M. Kortelainen, J. Dobaczewski, K. Mizuyama, and J. Toivanen, Phys. Rev. **C77**, 064307 (2008).
- [126] M. Bender, K. Bennaceur, T. Duguet, P.-H. Heenen, T. Lesinski, and J. Meyer, Phys. Rev. **C80**, 064302 (2009).
- [127] J. Margueron, H. Sagawa, and K. Hagino, Phys. Rev. **C77**, 054309 (2008).

- [128] T. Niksic, D. Vretenar, and P. Ring, Phys. Rev. **C78**, 034318 (2008).
- [129] B. G. Carlsson, J. Dobaczewski, and M. Kortelainen, Phys. Rev. **C78**, 044326 (2008).
- [130] S. Goriely, S. Hilaire, M. Girod, and S. Peru, Phys. Rev. Lett. **102**, 242501 (2009).
- [131] M. Kortelainen, T. Lesinski, J. More, W. Nazarewicz, J. Sarich, N. Schunck, M. V. Stoitsov, and S. Wild (2010), arXiv :1005.5145.
- [132] H. A. Fertig and W. Kohn, Phys. Rev. **A62**, 052511 (2000).
- [133] E. K. U. Gross, L. N. Oliveira, and W. Kohn, Phys. Rev. **A37**, 2809 (1988).
- [134] A. Gorling, Phys. Rev. **A47**, 2783 (1993).
- [135] J. E. Drut, R. J. Furnstahl, and L. Platter, Prog. Part. Nucl. Phys. **64**, 120 (2010).
- [136] G. Hagen, J. Holt, T. Lesinski, and T. Papenbrock (2010), private communication.
- [137] R. Roth, P. Papakonstantinou, N. Paar, H. Hergert, T. Neff, and H. Feldmeier, Phys. Rev. **C73**, 044312 (2006).
- [138] A. Gunther, R. Roth, H. Hergert, and S. Reinhardt (2010), arXiv :1005.1599.
- [139] K. A. Brueckner, Phys. Rev. **100**, 36 (1955).
- [140] J. Goldstone, Proc. Roy. Soc. (London) **A239**, 267 (1957).
- [141] T. Lesinski, T. Duguet, K. Bennaceur, and J. Meyer, Eur. Phys. J. **A40**, 121 (2009).
- [142] T. Duguet and T. Lesinski, AIP Conf. Proc. **1165**, 243 (2009), arXiv :0907.1043.
- [143] J. W. Negele and D. Vautherin, Phys. Rev. **C5**, 1472 (1972).
- [144] J. Dobaczewski, “*Interactions, symmetry breaking, and effective fields from quarks to nuclei. (A primer in nuclear theory)*”, *Lectures given at the 2002 Joliot Curie Summer School : Les noyaux exotiques : un autre regard sur la structure nucléaire, Maubuisson, France, nucl-th/0301069* (2002).
- [145] N. Kaiser, S. Fritsch, and W. Weise, Nucl. Phys. **A724**, 47 (2003).
- [146] N. Kaiser, Phys. Rev. **C68**, 014323 (2003).
- [147] S. K. Bogner, R. J. Furnstahl, and L. Platter, Eur. Phys. J. **A39**, 219 (2009).
- [148] N. Kaiser and W. Weise, Nucl. Phys. **A836**, 256 (2010).
- [149] B. Gebremariam, T. Duguet, and S. K. Bogner (2009), arXiv :0910.4979.
- [150] B. Gebremariam, S. K. Bogner, and T. Duguet, Comput. Phys. Commun. **181**, 1167 (2010).
- [151] B. Gebremariam, T. Duguet, and S. K. Bogner, Comput. Phys. Commun. **181**, 1136 (2010).
- [152] B. Gebremariam, S. K. Bogner, and T. Duguet (2010), arXiv :1003.5210.
- [153] J. Dobaczewski, B. G. Carlsson, and M. Kortelainen (2010), arXiv :1002.3646.
- [154] B. G. Carlsson and J. Dobaczewski (2010), arXiv :1003.2543.
- [155] D. Vautherin and D. M. Brink, Phys. Rev. **C 5**, 626 (1972).
- [156] M. Anguiano, J. L. Egido, and L. M. Robledo, Nucl. Phys. **A696**, 467 (2001).
- [157] J. Dobaczewski, M. V. Stoitsov, W. Nazarewicz, and P. G. Reinhard, Phys. Rev. **C76**, 054315 (2007).
- [158] M. Bender, T. Duguet, and D. Lacroix, Phys. Rev. **C79**, 044319 (2009).
- [159] T. Duguet, M. Bender, K. Bennaceur, D. Lacroix, and T. Lesinski, Phys. Rev. **C79**, 044320 (2009).
- [160] C. Simenel, B. Avez, and D. Lacroix, “*Microscopic approaches for nuclear Many-Body dynamics : applications to nuclear reactions*”, *Lectures given at Joliot Curie Summer School : Les réactions nucléaires comme sondes de la structure, Maubuisson, France, 17 Sept.-22 Sept., arXiv :0806.2714* (2007).
- [161] H. Goutte, J. F. Berger, P. Casoli, and D. Gogny, Phys. Rev. **C71**, 024316 (2005).
- [162] T. Duguet and T. Lesinski, Eur. Phys. J. **ST 156**, 207 (2008), arXiv :0711.4386.
- [163] K. Hebeler, T. Duguet, T. Lesinski, and A. Schwenk, Phys. Rev. **C80**, 044321 (2009).
- [164] S. Baroni, A. O. Macchiavelli, and A. Schwenk (2009), arXiv :0912.0697.
- [165] T. Duguet, T. Lesinski, K. Hebeler, and A. Schwenk (2010), arXiv :1004.2358.
- [166] J. Dobaczewski, H. Flocard, and J. Treiner, Nucl. Phys. **A422**, 103 (1984).
- [167] E. Perlinska, S. G. Rohozinski, J. Dobaczewski, and W. Nazarewicz, Phys. Rev. **C 69**, 014316 (2004).
- [168] M. Bender, H. Flocard, and P.-H. Heenen, Phys. Rev. **C 68**, 044321 (2003).

- [169] S. G. Rohozinski, J. Dobaczewski, and W. Nazarewicz (2010), arXiv :1001.4478.
- [170] J. Dobaczewski and J. Dudek, *Comput. Phys. Commun.* **102**, 166 (1997).
- [171] E. Chabanat, P. Bonche, P. Haensel, J. Meyer, and R. Schaeffer, *Nucl. Phys.* **A627**, 710 (1997).
- [172] J. Dobaczewski, W. Nazarewicz, T. Werner, J.-F. Berger, C. Chinn, and J. Dechargé, *Phys. Rev.* **C53**, 2809 (1996).
- [173] P. J. Borycki, J. Dobaczewski, W. Nazarewicz, and M. V. Stoitsov, *Phys. Rev. C* **73**, 044319 (2006).
- [174] H. Esbensen, G. F. Bertsch, and K. Hencken, *Phys. Rev. C* **56**, 3054 (1997).
- [175] T. Papenbrock and G. F. Bertsch, *Phys. Rev. C* **59**, 2052 (1999).
- [176] G. Bruun, Y. Castin, R. Dum, and K. Burnett, *Eur. Phys. J. D* **7**, 433 (1999).
- [177] A. Bulgac (1999), nucl-th/9907088.
- [178] A. Bulgac and Y. Yu (2001), nucl-th/0109083.
- [179] V. Rotival, Ph.D. thesis, Commissariat à l’Energie Atomique, Saclay, 91191 Gif sur Yvette Cedex, France (2008), <http://tel.archives-ouvertes.fr/tel-00409482/fr/>.
- [180] M. Bender, G. F. Bertsch, and P. H. Heenen, *Phys. Rev.* **C73**, 034322 (2006).
- [181] H. J. Lipkin, *Ann. Phys. (NY)* **9**, 272 (1960).
- [182] J. Dobaczewski, *J. Phys.* **G36**, 105105 (2009).
- [183] A. Valor, J. L. Egido, and L. M. Robledo, *Phys. Rev.* **C53**, 172 (1996).
- [184] A. Kamlah, *Z. Phys.* **216**, 52 (1968).
- [185] R. R. Rodriguez-Guzman and K. W. Schmid, *Eur. Phys. J.* **A19**, 45 (2004).
- [186] M. Bender, P. Bonche, T. Duguet, and P.-H. Heenen, *Phys. Rev. C* **69**, 064303 (2004).
- [187] M. Bender and T. Duguet, *Int. J. Mod. Phys.* **E16**, 222 (2007).
- [188] G. F. Bertsch, B. Sabbey, and M. Uusnakki, *Phys. Rev. C* **71**, 054311 (2005).
- [189] J. Sadoudi and T. Duguet (2010), unpublished.
- [190] M. Yamagami, Y. R. Shimizu, and T. Nakatsukasa, *Phys. Rev.* **C80**, 064301 (2009).
- [191] B. A. Brown, T. Duguet, T. Otsuka, D. Abe, and T. Suzuki, *Phys. Rev. C* **74**, 061303(R) (2006).
- [192] M. Zalewski, J. Dobaczewski, W. Satula, and T. R. Werner, *Phys. Rev. C* **77**, 024316 (2008).
- [193] C. L. Bai et al. (2010), arXiv :1005.2445.
- [194] L.-G. Cao, G. Colo, and H. Sagawa, *Phys. Rev.* **C81**, 044302 (2010).
- [195] P. G. Reinhard et al., *Phys. Rev.* **C60**, 014316 (1999).
- [196] D. R. Entem and R. Machleidt, *Phys. Rev. C* **68**, 041001 (2003).
- [197] S. K. Bogner, R. J. Furnstahl, R. J. Perry, and A. Schwenk, *Phys. Lett.* **B649**, 488 (2007).
- [198] S. K. Bogner, T. T. S. Kuo, A. Schwenk, D. R. Entem, and R. Machleidt, *Phys. Lett. B* **576**, 265 (2003).
- [199] E. Epelbaum, *Prog. Part. Nucl. Phys.* **57**, 654 (2006).
- [200] R. Machleidt, “*Nuclear Forces from Chiral Effective Field Theory*”, *Lectures given at Workshop on Physics and Astrophysics of Hadrons and Hadronic Matter, Shantiniketan, India, arXiv :0704.0807* (2006).
- [201] G. P. Lepage, “*What is Renormalization ?*”, *Lectures given at TASI’89 Summer School : From Actions to Answers, Boulder, CO, USA, nucl-th/0506330* (1999).
- [202] S. Y. Lee and K. Suzuki, *Phys. Lett.* **B91**, 173 (1980).
- [203] K. Suzuki and S. Y. Lee, *Prog. Theor. Phys.* **64**, 2091 (1980).
- [204] V. G. J. Stoks, R. A. M. Kompl, M. C. M. Rentmeester, and J. J. de Swart, *Phys. Rev. C* **48**, 792, doi = (1993).
- [205] R. Machleidt, *Phys. Rev.* **C63**, 024001 (2001).
- [206] S. K. Bogner, T. T. S. Kuo, and A. Schwenk, *Phys. Rept.* **386**, 1 (2003).
- [207] S. K. Bogner.
- [208] K. A. Brueckner and C. A. Levinson, *Phys. Rev.* **97**, 1344 (1954).
- [209] B. D. Day, *Rev. Mod. Phys.* **39**, 719 (1967).

- [210] B. D. Day, *Rev. Mod. Phys.* **50**, 495 (1978).
- [211] B. D. Day, *Phys. Rev. C* **24**, 1203 (1981).
- [212] A. Schwenk, *J. Phys.* **G31**, S1273 (2005).
- [213] P. Navratil, G. P. Kamuntavicius, and B. R. Barrett, *Phys. Rev.* **C61**, 044001 (2000).
- [214] S. K. Bogner et al., *Nucl. Phys.* **A801**, 21 (2008).
- [215] S. K. Bogner, R. J. Furnstahl, and R. J. Perry, *Annals Phys.* **323**, 1478 (2008).
- [216] E. D. Jurgenson, P. Navratil, and R. J. Furnstahl, *Phys. Rev. Lett.* **103**, 082501 (2009).
- [217] L. P. Gorkov, *Sov. Phys. JETP* **34**, 505 (1958).
- [218] M. Gell-Mann and F. E. Low, *Phys. Rev.* **84**, 350 (1951).
- [219] K. A. Brueckner, C. A. Levinson, and H. M. Mahmoud, *Phys. Rev.* **95**, 217 (1954).
- [220] P. Nozieres, *Theory of interacting Fermi systems* (Westview Press, Boulder, CO, 1964).
- [221] R. Roth, P. Papakonstantinou, N. Paar, H. Hergert, T. Neff, and H. Feldmeier, *Phys. Rev. C* **73**, 044312 (2006).
- [222] E. Engel, *Lecture Notes in Physics 620, A primer in Density Functional Theory* (Springer, Berlin, 2003).
- [223] B. Gebremariam, S. K. Bogner, and T. Duguet (2010), unpublished.
- [224] V. Rotival, T. Duguet, S. K. Bogner, and R. J. Furnstahl, unpublished.
- [225] J. W. Negele and D. Vautherin, *Phys. Rev.* **11**, 1031 (1975).
- [226] X. Campi and A. Bouyssy, *Phys. Lett.* **73B**, 263 (1973).
- [227] J. Meyer, J. Bartel, M. Barack, P. Quentin, and S. Aicher, *Phys. Lett. B* **172**, 122 (1986).
- [228] V. B. Soubbotin and X. Vinas, *nucl-th/9902039*.
- [229] M. Stoitsov, M. Kortelainen, S. K. Bogner, T. Duguet, R. J. Furnstahl, B. Gebremariam, T. Lesinski, and N. Schunck (2010), unpublished.